University of Southern Queensland

Faculty of Engineering and Surveying

High Impedance Earth Fault Modelling

A dissertation submitted by

Robert Walter Coggan

In fulfilment of the requirements of

Courses ENG4111 and 4112 Research Project

towards the degree of

Bachelor of Engineering (Electrical and Electronic)

Submitted: October 2010

ABSTRACT

Single Wire Earth Return (S.W.E.R) Distribution networks were installed by Electrical Distribution entities to distribute power to customers who are remote from Zone Substations and have a low energy demand. As is common with typical distribution systems, S.W.E.R. systems are being subjected to an array of appliances with higher energy demands than were ever anticipated. An increase in load without an increase in the available fault current highlights the benefits of non traditional fault detection techniques. Detection of faults historically relied on the use of fundamental power system signals to distinguish between normal operation and fault conditions. Recent introduction of microprocessor based protection relays allows monitoring of low level signals generated by power system faults to increase the protection coverage. The project has deconstructed a typical SWER power system and validated models for each power system component. COMTRADE files have been produced that can be replayed to protection relays attempting to detect arching and high impedance faults.

.

University of Southern Queensland

Faculty of Engineering and Surveying

<div style="border: 1px solid black; padding: 10px;">

ENG4111 & ENG4112 Research Project

</div>

Limitations of Use

The Council of the University of Southern Queensland, its Faculty of Engineering and Surveying, and the staff of the University of Southern Queensland, do not accept ant responsibility for the truth, accuracy or completeness of the material contained within or associated with this dissertation.

Persons using all or any part of this material do so at their own risk, and not at the risk of the Council of the University of Southern Queensland, its Faculty of Engineering and Surveying or the Staff of the University of Southern Queensland.

This dissertation reports an educational exercise and has no purpose of validity beyond this exercise. The sole purpose of the course pair entitled "Research Project" is to contribute to the overall education within the student's chosen degree program. This document, the associated hardware, software, drawings, and other material set out in the associated appendices should not be used for any other purpose: if they are so used, it is entirely at the risk of the user.

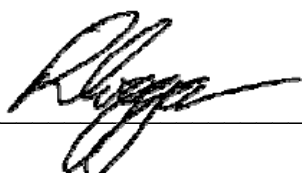**Prof Frank Bullen**
Dean
Faculty of Engineering and Surveying

Certification

I certify that the ideas, designs and experimental work, analyses and conclusions set out in this dissertation are entirely my own effort, except where otherwise indicated and acknowledged.

I further certify that the work is original and has not been previously submitted for assessment in any other course or institution, except where specifically stated.

Robert Walter Coggan

Student Number: 0050066392

_____

Signature

____27th OCTOBER__2010

Date

Acknowledgements

This research was carried out under the principal supervision of Dr Tony Ahfock.

Table of Contents

List of Figures

List of Tables

Chapter 1

Introduction

1.1 What is a High Impedance Fault?

High impedance faults in the context of a power system are short circuits between energised parts of the power system that are beyond the detection capabilities of traditional protection relays. The short circuit may be between two or more phases alternatively it may be between one or more phases and earth. The fault impedance may be such that it approximates the impedance of a load.

Traditional protection schemes are those based on overcurrent detection. When determining the operational parameters for a protection scheme the user will identify the minimum fault level, maximum fault level and maximum prospective load.

The maximum fault level is used to determining the co-ordination between devices. The aim of the project is to detect low level faults so the maximum fault will not be discussed in great detail. The minimum fault level and load are the two aspects that approach one another as a distribution network gets further from a strong source of supply.

1.2 System Overview

The systems considered specifically for this project were Single Wire Earth Return SWER Networks. SWER Networks typically are located at the end of the historical electricity supply chain. For the purpose of this section a historical or traditional system is one that has no distributed generation at the customer premises and the power flow is from a market generator to the end user.

Historically the electricity was generated at power stations at voltages in the order of 10-15kV. The electricity was transformed from the generated voltage up to a high voltage for transmission. The transmission of electricity was and is carried out at voltages from 132kV to 500kV in Australia. Transmission networks deliver energy to large load centres. At these load centres the voltage was transformed to either a subtransmission voltage or a distribution voltage level. Subtransmisson systems deliver energy to minor load centres where it is further transformed to distribution voltages. Typically subtransmission voltages range from 33kV to 132kV.

Distribution systems are local networks that deliver power to customer's premises. Distribution systems are those most obvious in urban environments where power lines transmit energy at voltages between 6.6 and 33kV.

In the above description all voltages are nominal and it is up to the respective utility to determine exactly what is a subtransmission system and what is Distribution. Similarly the lines may be blurred between transmission and subtransmission depending on the line configuration, the route and the type or types of customers connected. As an example Ergon Energy uses 33kV lines for subtransmission in some areas and Distribution in others. This voltage selection is based on the practices of the legacy electricity boards that were merged to form Ergon Energy as it is today.

Generally the systems described above are a three phase three wire system from generation to distribution. However once the overhead distribution line leaves the substation the topology may take either a three phase line, single phase line (two wires) or unisolated SWER. All other connections to the distribution system are made through transformers and are typically considered a separate network of the power system.

unisolated SWER is a legacy practice where a single wire was connected to a normal three wire system. This wire was run from the point of connection to a customer premises. The customer was connected through a single phase transformer with the second terminal of the high voltage winding connected to earth. The primary system current return path was to the zone substation transformer neutral.

In areas where this practice is common high neutral currents may exist if the loads are not balanced throughout the entire load cycle. This creates an earth current that can reduce the sensitivity of applied traditional earthfault protections. Unisolated SWER is not a current practice and programs are in place to install isolation transformers on these unisolated SWER systems. Unisolated SWER systems have been excluded from this study for this reason.

Figure 1.1 below shows the connections made to a distribution network. On the left hand side is the secondary winding of a transformer that would be typical for a subtransmission to distribution step down transformer. Typically for subtransmission this would be a delta star transformer. Other transformers are used when stepping down directly from a transmission voltage (e.g. 132kV) to a distribution voltage. When stepping down from transmission voltage levels a star winding is preferred on the Transmission side to minimise the cost of insulation. Star windings allow the insulation to be rated at a lower voltage level at the neutral end, provided that the neutral end of

the power transformer is solidly earthed. In these cases a delta distribution winding and earthing transformer may be employed. This connection is irrelevant in the course of this work and is only shown for interest.

The three connections leaving the transformer are assumed to be the overhead line leaving the substation. A relay and CT connection are shown in red. The relay has been connected so that it will only respond to earth faults. The connection is termed a residual connection or Holmgreen connection. The connections are shown for typical three phase distribution transformer and a SWER isolating transformer.

Of interest in Figure 1.1 is that fact that the devices are connected to the power system between two or more phases. When connecting loads like this the protection relay employing a residual connection can be set somewhat independently of load. The relay is set so that the inaccuracies in the current transformers and line configurations do not cause operation. Settings for sensitive earth fault relays connected in such a manner are in the order of 4A to 8A with a time delay set such that it is stable for power system transients.
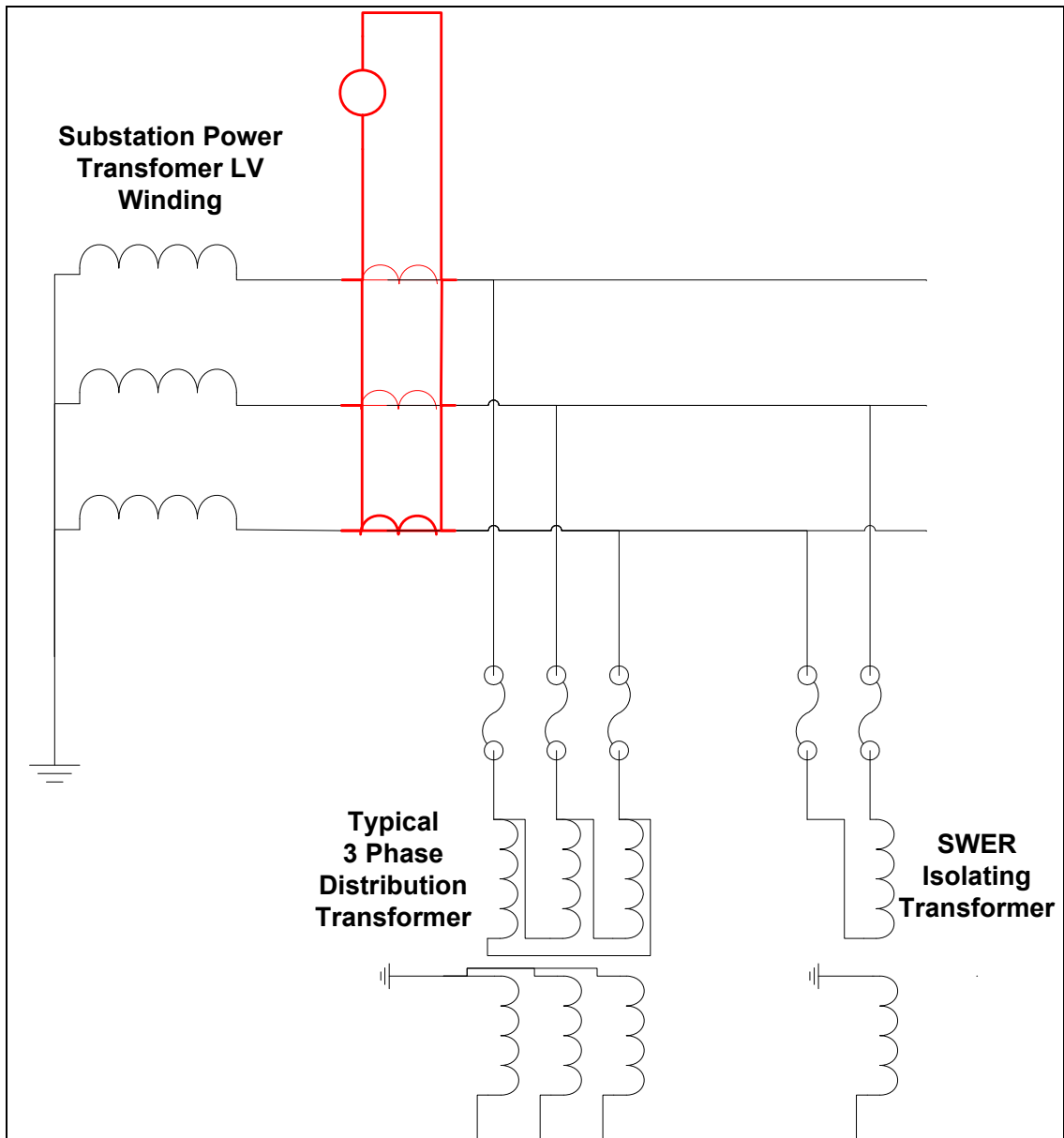
Figure 1.1 - Distribution Network Connections - Schematic

On the right hand side of Figure 1.1 a SWER isolating transformer is shown. This is the point on the electrical network where a single phase (two wire) connection is transformed to Single Wire Earth Return (SWER). Figure 1.2 shows the protection arrangement for the start of a SWER system. In Figure 1.2 two primary side fuses are shown. They are intended to protect the SWER transformer and section of network between the SWER isolating transformer and the downstream overcurrent protection device (single phase recloser). The fuses also provide limited backup protection for faults beyond the recloser.

In contrast to the earthfault protection that was shown in Figure 1.1 the earthfault protection in Figure 1.2 will respond to system earth faults as well as overloading. It is impossible to set the earth fault protection independently load. The load and fault current loop involve the SWER isolating transformer, recloser, high voltage line, and the earth. The only difference is the load passes through the customer's equipment whereas the fault current bypasses the customer's equipment.
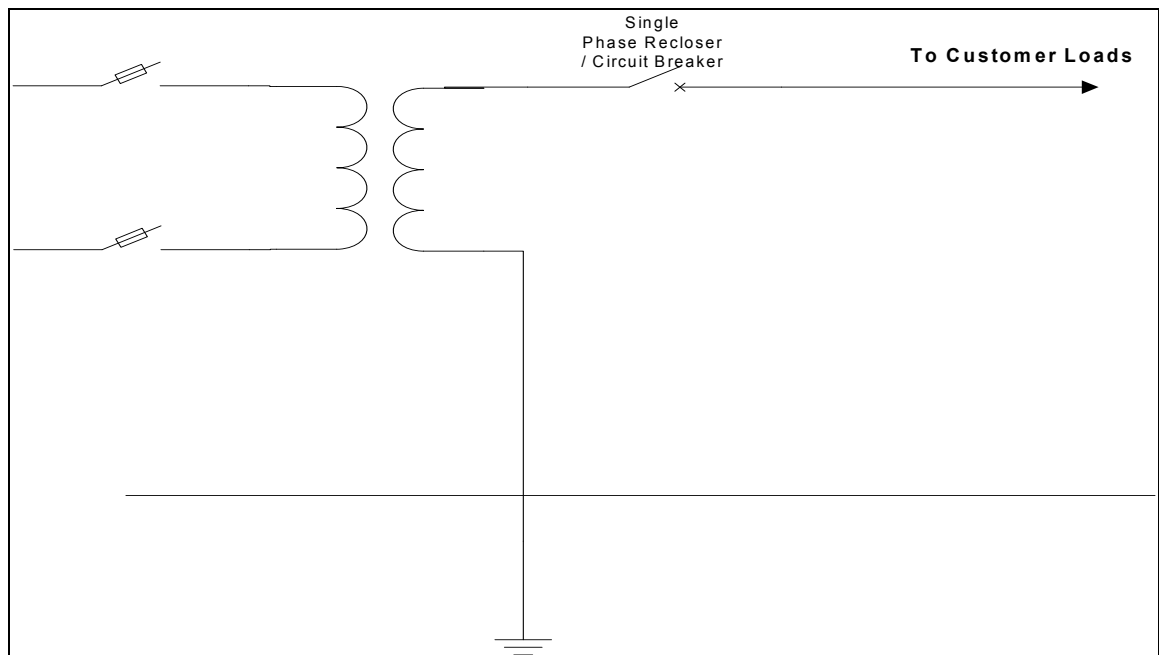
Figure 1.2 - SWER Isolator Protection Scheme

1.3   Protection Systems for SWER Networks

Protection systems for SWER networks involve measuring the current at the single phase reclosers at the SWER Isolator. The protection element is an overcurrent element that responds to the fundamental component of the measured waveform. Once this overcurrent element threshold has been exceeded the device will begin to time. Once the programmed time has elapsed the device will open the reclosers and disconnect the downstream network.

The overcurrent threshold is programmed to be immune for system loading conditions and operate only for short circuits. Take for example an ideal case where an infinite source exists upstream of a 200kVA 3.3% impedance SWER isolator with a 19.1kV SWER winding. The transformer full load is calculated as:

$$I_{FULL\_LOAD} \quad = \quad \frac{S_{NOM}}{V_{NOM}}$$

$$= \quad \frac{200000}{19100}$$

$$= \quad 10.5\text{A}$$

The maximum transformer fault current is calculated by using the reciprocal of the transformer impedance times the full load current:

$$I_{FAULT} \quad = \quad \frac{1}{X_{PU}} \times I_{FULL\_LOAD}$$

$$= \quad \frac{1}{0.033} \times 10.5$$

$$= \quad 318\text{A}$$

The fault current that is used for calculating protection coverage is that of the system impedance plus additional 50Ω for fault resistance. 50Ω fault resistance is used in Ergon Energy as the earthing systems for line hardware is tested to have a maximum resistance of 30Ω when isolated from other earths. An additional 20 Ohms is allowed for seasonal variation of the earth in which the system is installed.

$$I_{FAULT} \quad = \quad \frac{V_{NOM}}{Z}$$

$$= \quad \left| \frac{19100}{50 + 60j} \right|$$

$$= \quad 162\text{A}$$

Allowing a 20% margin above full load for security of supply we have the criteria

$$\frac{I_{FULL\_LOAD}}{0.8} \langle I_{SETTING} \langle \frac{I_{FAULT}}{2}$$

$$\frac{10.5}{0.8} \langle I_{SETTING} \langle \frac{162}{2}$$

$$14A \langle I_{SETTING} \langle 81A$$

For this ideal scenario the protection setting would be set between 14 and 81A to provide adequate protection to this system. This system has neglected to consider the

upstream source impedance and the line impedance beyond the isolator. Both of these impedances further reduce the upper boundary and in some cases conflicts begin to occur between a safe setting above load and a reliable setting below the minimum prospective fault current.

It is not common to have faults at the maximum transformer let through current as derived above. More often than not fault currents are in the range 18 to 100A. This is due to a combination of the network impedance up to the SWER Isolating transformer, the isolating transformer impedance, the impedance beyond the isolator up to the fault location and some fault impedance. Faults at the lower end of the stated range is where problems begin to occur for protection setting staff as the fault current and the load current are not diverse enough to allow typical safety margins.

By investigating the use of technology specifically designed to detect high impedance faults (those beyond the reach of short circuit protection) it may be possible in the future to set the overcurrent protection to detect solid short circuits leaving the arcing / high impedance faults to specialist algorithms. This technology would ideally allow the protection settings used to detect high impedance faults to be configured independently of load.

1.4 Project Background

1.4.1 Aims

Single Wire Earth Return (SWER) distribution networks aim to deliver cost effective grid connected electricity supply to remote customers. The system uses a single wire to deliver power to customers with the return path being the general mass of the earth. To ensure that the electrical network is protected an overcurrent protection device is commonly employed at the point of connection to the distribution network.

The thresholds for overcurrent protection systems employed on these networks are determined by the use of modelling software that takes into account the anticipated maximum demand and the minimum prospective fault current. With ever expanding electrical networks and increasing consumer demand the margin between maximum load and minimum fault currents is approaching the limit where security of supply and network performance may begin to be impacted.

This project aims to investigate the application of non fundamental base fault detection technology (commonly known as high impedance fault detection) to SWER networks to determine if the technology can alleviate some of the conflicting requirements between consumer loads and protection system design.

1.4.2 Rationale

It is recognised that there are limitations of protection schemes presently used for fault detection in distribution networks. These limitations are commonly identified when trying to correctly detect what are known as high impedance faults. Faults that are beyond the sensitivity of traditional protection schemes are deemed to be high impedance in nature. New technology is commercially available in some relays which may be utilised to improve the protection scheme coverage to detect high impedance faults. An assessment of this technology is the intent of this project.

SWER systems are of particular interest in this project as we presently do not have the ability to set earth fault protection independent of system load. With increasing load currents on Ergon Energy's network in general, increased overcurrent settings are being required to ensure that conflicts do not occur between load current and fault currents (load encroachment). Increasing setting current that is used to discriminate between loads and faults desensitises the protective scheme reducing the fault coverage provided.

One of the highlighted major drawbacks for SWER systems outlined in Ergon Energy's SWER taskforce report was "difficulties in ensuring adequate fault levels to operate protection if the SWER line comes down in a storm". It is believed that it may be possible to increase sensitivity by utilising this technology.

1.5 Protection Testing Philosophies

1.5.1 Overview

Protection relays are safety devices that are used to detect and clear power system faults. Protection relays are one component that comprises a protection scheme. Protection testing involves verification that the protection scheme operates as designed. Protection testing typically breaks down the protection scheme into relays, wiring, instrument transformers, circuit breakers and communication systems. Each component of the system is tested independently to ensure that is functioning within prescribed limits. Once each of the components has been verified functional tests are carried out with multiple elements of the scheme interacting with one another to ensure that the entire protection scheme is functioning.

For the purposes of this project testing of protection relay will be concentrated on. The interaction of the protection relay with the remaining elements of the power system is not intended to be atypical and standard tests will remain valid.

Protection relays are typically categorised as:

- Electromechanical

- Static

- Numerical

The reason for testing each of the three types of relays is somewhat different.

Electromechanical relays are mechanical in nature and operate by generating a magnetic flux that is used to turn an induction disc or attract a relay armature. Electromechanical relays by design have moving parts as such they are subject to deterioration with age. Testing of electromechanical relays is used to ensure that the relay is operating within its calibration at the desired settings.

Static relays are the first generation relays to use microcontrollers, discrete components, comparators with the only moving parts being the output contacts themselves. Depending on the relay design the characteristic may be subject to drift with age. Testing of static relays is used to ensure that the relay is operating within its calibration at the desired settings. However the characteristic is generally tested to ensure correct operation.

Numerical protection relays are microprocessor based relays that have analogue to digital converters at the relays measuring inputs. The functionality of a numerical relay

is controlled by software typically referred to as firmware. Firmware is created by the relay manufacturer and is not accessible to the end user. Firmware is where the mathematical algorithms that govern relay performance reside. Numerical relays are continuously monitored by watchdog timers. These watchdog timers are used to highlight a problem to a power system operator. Testing of protection elements is carried out to ensure that the desired settings have taken effect in the protection relay.

With all of the protection relay types mentioned above testing is carried out routinely to ensure that they are still operative and fit for purpose. Prior to this maintenance testing and in some cases prior to procurement the protection is evaluated by the end user. This user type testing is undertaken to determine if the functionality and performance of the relay or element thereof is appropriate for the application identified by the user. This project is aimed at determining if a user type test can be determined so that a manufacturer independent evaluation can be carried out.

1.6 Project Methodology

As it is impossible to conduct a large number of site specific trials without incurring large cost. A modelling and model validation process has been undertaken. The project will break the network down into the elements that are in the path of the signal that is intended to be measured. The identified elements are power transformers, overhead lines, current transformers and the arc model itself. Each of these elements where possible will be modelled and compared against actual test data or against mathematical validation techniques.

Each of the modelled components will then be collated into a model that can be used to generate waveforms for relay performance. The end result is expected to be a series of recordings that will be able to be replayed to protection relays that employ arc detection techniques. These waveforms will be used to assess the protection relays prior to procurement. These waveforms can also be used by commissioning staff to validate the alarms and indications that the protection relay provide.

Chapter 2

Literature Review

2.1   Transformers

Hasman (1987) investigates the effect of a power transformer as the terminating device on a power line subjected to a travelling wave. This paper provides a model that can be used to determine the winding self impedance and the leakage inductance between the coupled windings. The paper is very general and looks at the frequency response of a 200kVA single phase transformer. The frequency of interest for Hasman (1987) is assumed to be >500Hz from the graphs that have been provided. Adimaik (2010) suggests an upper limit for the harmonic monitoring of the 25th harmonic. This upper limit provides only a slight overlap in the frequencies of interest. The impedance plots in Hasman (1987) are open to interpretation at the low end of the scale. For this reason analysis of the impacts of frequency on the transformer leakage inductance, stray capacitance, hysteresis loss and eddy current loss will be verified from testing carried out on transformer that are used on SWER networks.

2.2   Transmission Line Modelling

Marti (1993) suggests that sufficient accuracy of the model will be achieved provided that the line resistance is much less than the modal (Surge) impedance of the transmission line. The approximate surge impedance for raisin conductor is of the order of 634 Ohms and has a resistance in the order of 1.6 Ohms / km. Modelling of the proposed SWER configuration from 10 to 200km is proposed and would most likely impinges on the requirement that R << Zc. A comparison of the distributed parameter line and frequency dependent line will be carried out to see if the impact is significant.

2.3   Instrument Transformer Modelling

Samesima et al. (1991) identifies that the transformation ratio and angular displacement of the input to output current is relatively constant from the nominal frequency up to values in the order of 50kHz. The equivalent circuit of a CT with bar primary (the type

that would be proposed for use on the SWER system) is shown below in Figure 2.1. Samesima (1991) connects a 15VA burden to the CT under test and experiences no discernable effect of the capacitance C2. Using numerical relays that have a low burden for example 0.2VA for the GE F60 (GE Industrial Systems 2008), the voltage behind the winding resistance is kept relatively low, reducing the effect of the secondary winding stray capacitance.

The current transformers selected for this application are expected to be class PL under the previous Australian standard AS1675-1986 or class PX under the current version AS60044.1-2007. CT's with this designation have windings spaced evenly around the toroidal core in an attempt to minimise the leakage flux. Minimising the leakage inductance will minimise the voltage expressed across the winding stray capacitance which will aide in minimising the effect of C2 as shown in Figure 2.1.

Modelling of current transformers is explained in detail by Kezunovic (1994) and Folkers (1999). Both papers focus on the use of C Class CT's. C Class Ct's are defined under the ANSI/IEEE standard C57.13-2008. Class C CT's are a specified by the knee point voltage available to drive 20 times full load current into a standard burden, with a limit of 10% ratio error at 20 times full load current.

The C Class CT is specified to have a low leakage reactance similar to the PL and PX used in Australia. To allow simplification of transient models through the exclusion of the leakage reactance a class PL or PX CT would be selected for this application.

 The use of a saturable transformer in ATP-EMTP allows the inclusion of both primary and secondary inductances and resistances along with the current flux relationship of the magnetising characteristic. The saturation routine available in ATP-EMTP is able to be used to determine the input parameters from data obtained through standard commissioning tests.
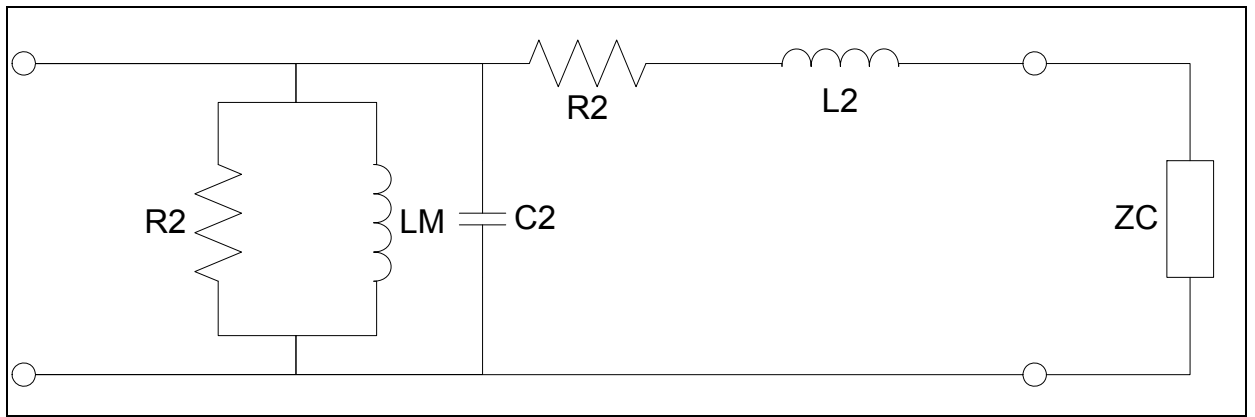
Figure 2.1 - Current Transformer Equivalent Circuit

2.4   ARC Model

High impedance faults of interest are those involving earth. While detection of high impedance faults as defined by Tending (1996) would involve two or more phases it is believed that the risk to the general public from these types of faults is low. Further when focussing on SWER systems only single phase to ground conditions can exist. The "earthfault only" direction simplifies the requirements placed on a manufacturer while satisfying the aims of this investigation.

Schweitzer Engineering Laboratories (SEL) have provided a waveform that is believed to be the one from Hou (2007). Waveforms that have been supplied by SEL have been done so in confidence. For this reason they have not been reproduced in this report. The waveforms appear to be from power system arrangements that are not common in Ergon Energy. The waveforms generally have a prefault neutral current flowing. This neutral current is indicative of a 4 wire power system that is not a system arrangement employed by Ergon.

In Ergon Energy three wire distribution systems are employed. Residual current that is measured is present under abnormal system operating conditions and faults.

Hou (2007) and Adimaik (2010) look at the input current to the protection relay with a slightly different approach. Hou (2010) looks for a "sum of difference current" by

24

comparing the sampled data to a corresponding point on the waveform that occurred in the past. The primary quantities that Adimaik (2010) searches for is sustained energy in specific sets of harmonics (odd, even or none), a parallel algorithm runs searching for an increase in one of the measured harmonics, followed by erratic behaviour afterwards. Both manufacturers have highlighted the erratic nature of the signal being monitored as a key for fault detection. Modelling as described by Goldberg (1989) has not shown a pronounced deviation from cycle to cycle in initial simulations. The results from site tests as conducted by Taylor (1987) are shown in Figure 2.3. Randomness that is expected by Hou (2007) and Adimaik (2010) is not evident when analysing this visually. Keeping in mind this is only a limited window of data and it is not possible to numerically analyse this care should be taken with these results.
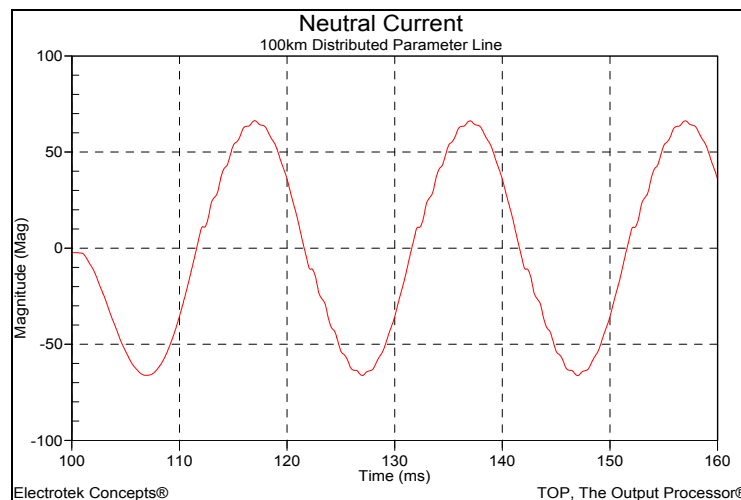
Figure 2.2 - Neutral Current due to Simple Arc Model

Goldberg et al (1989) presents a method of modelling an arc during single phase operation of a transmission line. Single phase operation of a network as described by Goldberg was the final state of a single pole trip (on a three phase network). Once the faulted phase was isolated from its direct source of energy the arc moved from what was deemed a primary arc to a secondary arc. The energy used to sustain the secondary arc is obtained from the interphase coupling from the two phases that remain energised. Goldberg's study focused on the time after a single pole trip that must elapse before a reclose can be successfully attempted.

25

In the act of isolating a section of a distribution network we operate all three phases of a circuit breaker. Similarly for SWER systems we generally intend to operate the circuit breaker that is supplying all of the energy to the network eliminating the need to consider the secondary arc.

Further to this Goldberg (1989) was not interested in detecting the fault through the characteristic of the primary arc. On Extremely High Voltage (EHV) networks sufficient energy is available from the source along with sophisticated communication schemes that allow tradition protection schemes to detect and clear faults.

Figure 2.3 and Figure 2.4 show the result of tests staged by the Taylor (1987). The voltage at the point of the fault is shown in Figure 2.4 and is similar to that modelled in Golberg (1989). The voltage at the fault point is somewhat clamped and no longer able to follow the natural sinusoidal shape that would be found on an unfaulted power system that is free from harmonics.

A simple arc conduction circuit similar to that introduced by Golberg (1989) is shown in Figure 2.5. The main part of the circuit consists of two diodes and two voltage sources. The Alternative Transients Program (ATP) proposed for this study includes a modelling system that allows for transient modelling (Analysis) of control systems (TACS). TACS is a Fortran based modelling tool that includes general mathematical operator along with various filters. With this facility the Transient Analysis of Control System (TACS) voltage sources can set the clamping voltage. The circuit including the TACS sources is shown in Figure 2.5.

The arc clamping voltage is calculated by

$$V_P \quad = \quad 75 \times I_P^{-0.4}$$

Where Vp is the ceiling voltage and Ip is the prospective short circuit current for a solid phase to ground fault.
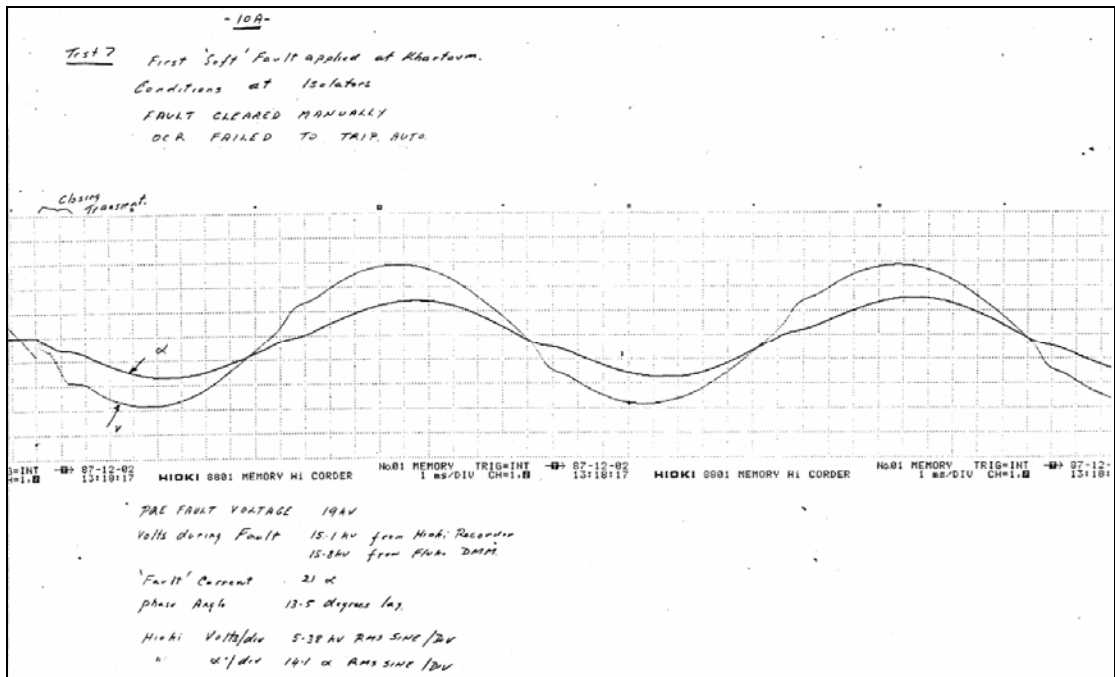
Figure 2.3 - Voltage and Current at SWER Isolator (Taylor (1987))
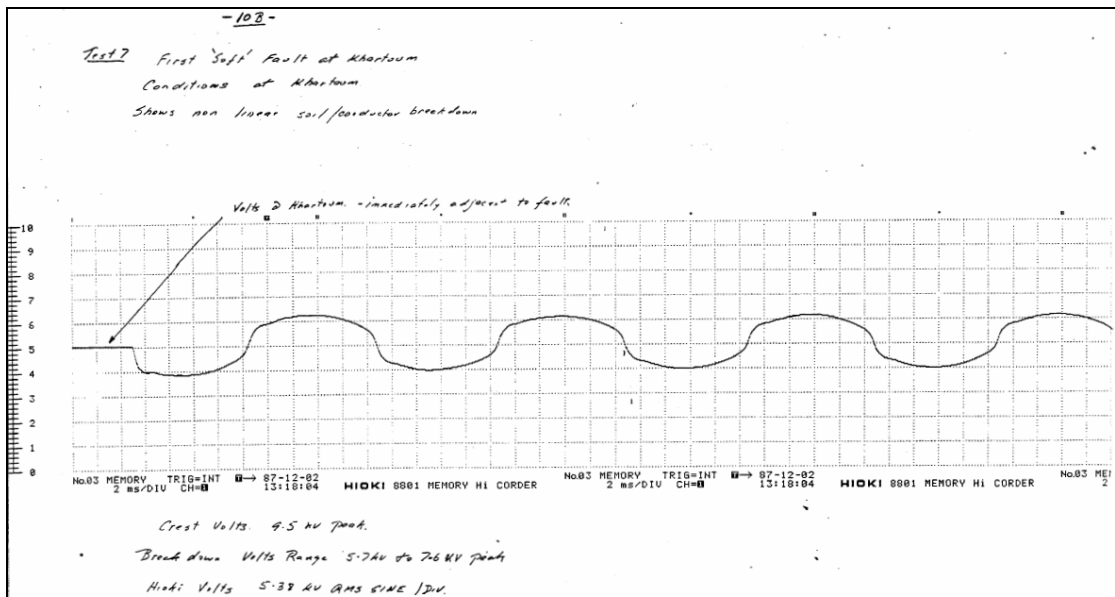
Figure 2.4 - Voltage Adjacent to Fault (Taylor (1987))
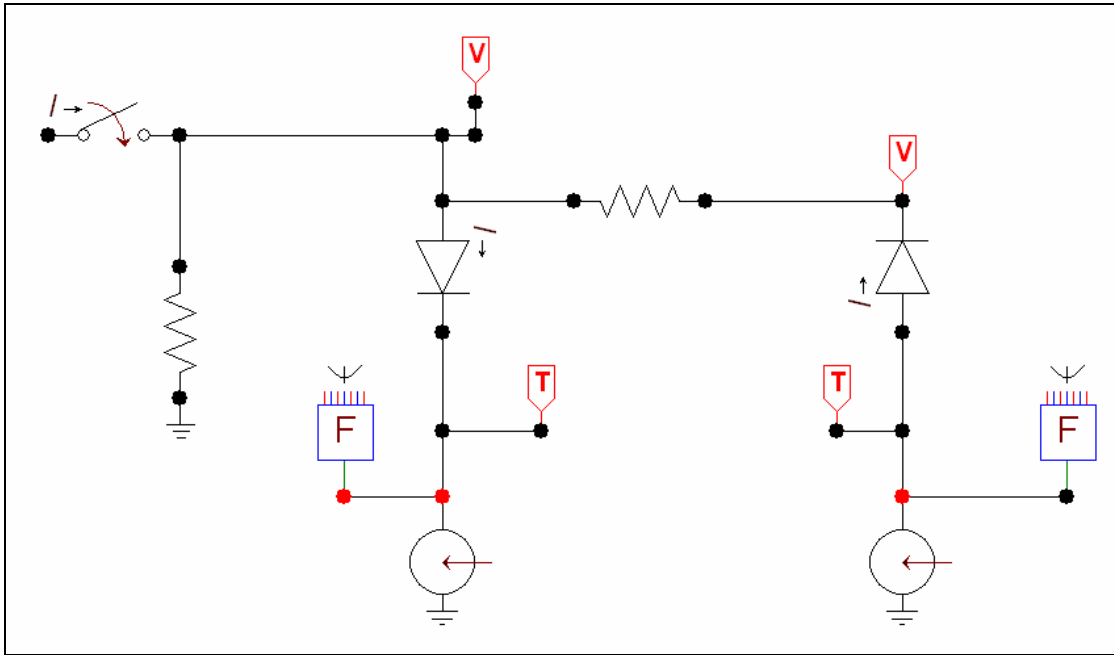
Figure 2.5 - Simple ARC Model

Should Goldberg's technique not be suitable to facilitate relay operation two extensions are possible. Rogers (n.d.) documents a technique to model free air arcs using a non linear resistor. The output of simple model using arbitrary parameters is show to approximate that measured near the fault location as shown in Figure 2.6.
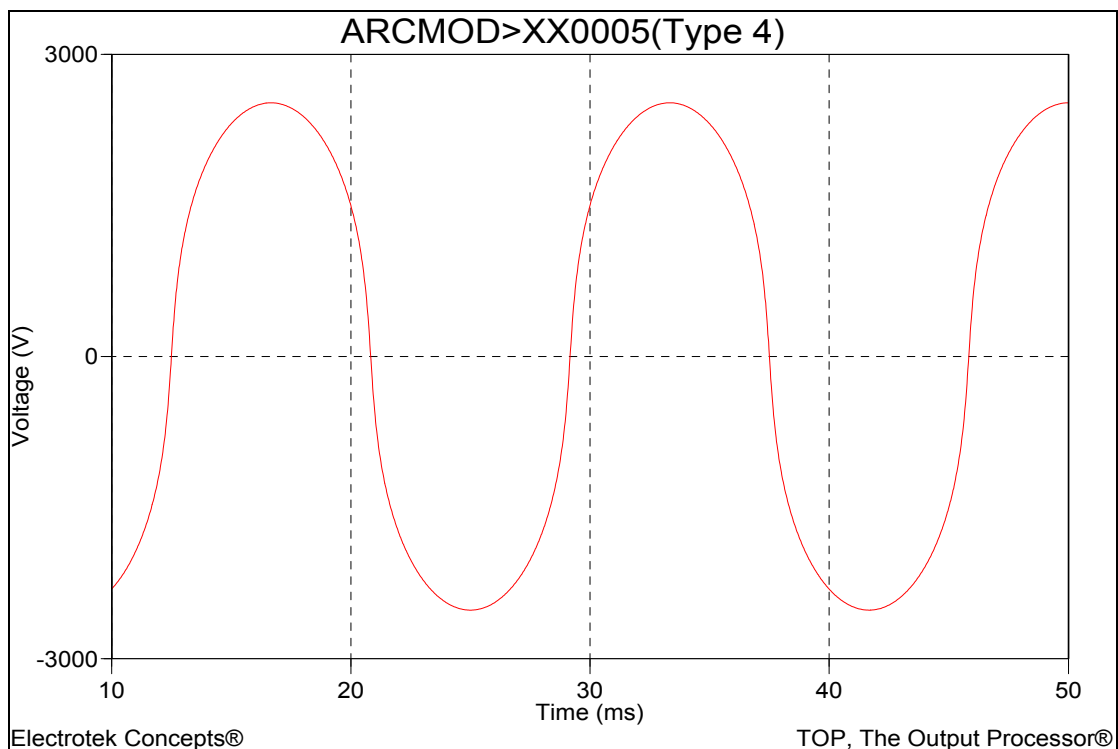
Figure 2.6 - ARC Voltage Model Using Rogers Technique

Secondly it is possible with this simple model to control the breakdown voltages to emulate variability of the material under test. This method is expected to allow the definition of limits as to what the relays under test define as random. Controlled high voltage testing would be required to determine the black box characteristics of the material under test.

An investigation into the arc model and the power system equipment that it impacts on is undertaken in the following sections.

Chapter 3

ARC Model

3.1 Overview

One of the key aspects of a power system model for simulating arcing faults is indeed the model of the arc at the fault location. This arc model initiates the signal that will be presented to the connected power system components. In an attempt to validate the arc model two data sources were used.

Power system testing carried out by Taylor (1987) have provide examples of what signals are present when a line makes contact with the ground. These signals have been used for validation of he selected arc model.

Secondly an electric arc welder was used to initiate an arc event in the power engineering research laboratory at the University of Southern Queensland. Both the voltage across the arc and the supplied current were recorded.

3.2 Historical Results

Testing by Taylor (1987) resulted in non sinusoidal fault voltages (at the fault location) as shown in Figure 2.4. Taylor's report into Mistake Creek North uses the term 'soft fault' for faults that are beyond the sensitivity of traditional protection schemes on the network. The results were captured with a paper chart recorder and have only a few cycles of information available. For these two reasons it was not possible to replay the waveforms back to the protection relay.

The voltage at the fault point shows a slight rounding of the expected sinusoidal peak. For the same fault the current at the start of the SWER Network is measured and shown in Figure 2.3. In this diagram the sending voltage at the S.W.E.R. isolating transformer and the total S.W.E.R. current is shown. The author of the Mistake Creek Report identifies that the irregularity of the current waveform (α) may be a source of information to detect high impedance faults.

3.3 Laboratory Testing

3.3.1 Overview

Testing was carried out in the Power Engineering Research Laboratory at the University of Southern Queensland. This testing was designed to simulate a power arc and to further verify the power system model.

3.3.2 Test Methodology

The testing was intended to simulate a power arc that has a high current. In an ideal situation both a high arc current and high system voltage would be available. It is believed that this would have provided a better result as larger arc lengths may have been sustainable.

The tests were carried out using a typical older generation arc welder. The welder selected for testing was without any power electronic control. The only adjustment was via selection of the desired voltage tapping on the welders control panel. The circuit used for laboratory testing is shown below in Figure 3.1.
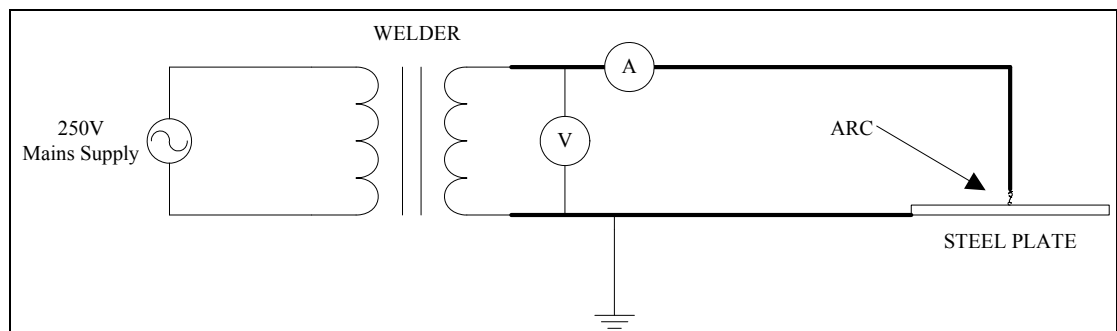
Figure 3.1 - High Current ARC Testing

3.3.3 Test Results

A qualitative analysis of the results was undertaken to identify the action of the user and the impact on the results. Figure 3.1 shows voltage and current measured on the output side of the welder scaled so that the instrument transformer outputs are in primary terms.
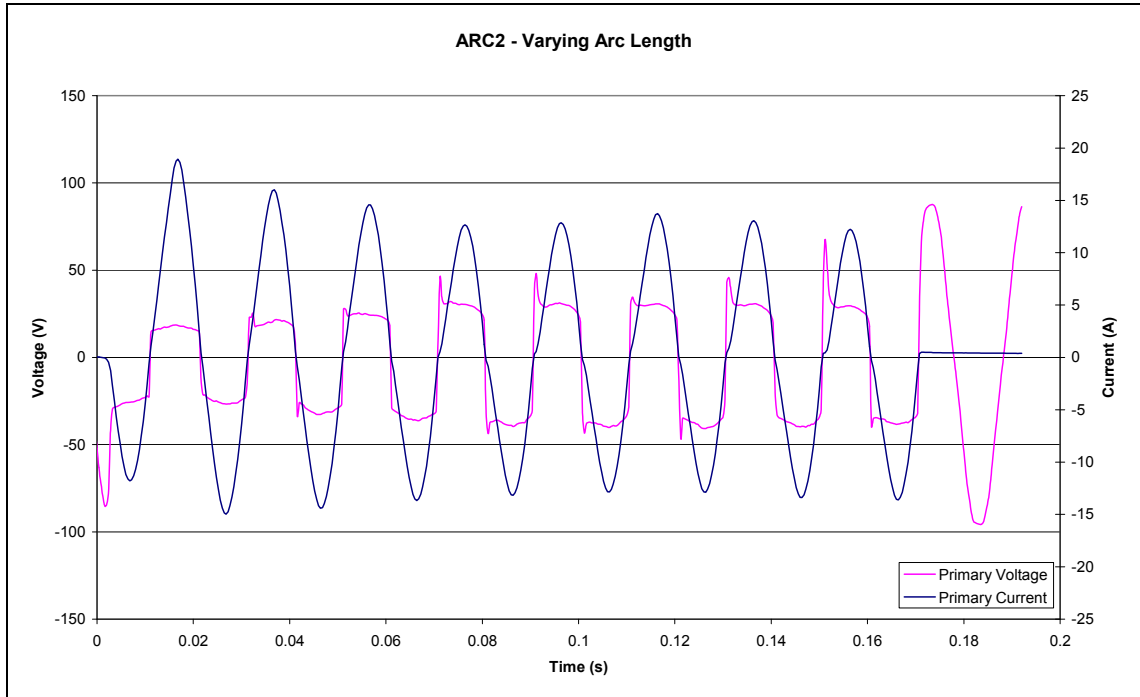
Figure 3.2 - Arc Measurement Varying Arc Length

Figure 3.2 shows one of the results obtained during an arc test with the welder. By inspection we can see that their is a DC offset in the applied current. The DC offset decays rapidly over the first cycle. At time 0.055 seconds the current waveform zero crossing distortion becomes evident. This zero crossing distortion occurs each half cycle for the remainder of the recording. Corresponding to the zero crossing distortion that is evident in the current waveform is a leading edge peak or overshoot in the applied voltage. This voltage peak is a result of the welder operator and is representative of one of the variables of an arc. As the user strikes an arc we expect, and do see waveforms similar to that shown in Figure 3.2 up to approximately time 30ms. Beyond that the welder operator is moving the electrode away from the earth plane creating an air gap. The further the operator moves the electrode from earth the higher the voltage peak relative to that of the waveform at $\sin(\omega t + 90)$ becomes. This is termed flashover voltage.

Figure 3.3 shows a few cycles of data before the arc was extinguished at 78ms. Figure 3.3 has a wave shape that tends to that measured adjacent to the fault location at Mistake Creek (shown in Figure 2.4). The most obvious difference is the small flashover voltage. The second difference between the two waveforms is the waveform distortion particularly evident in Figure 3.3 at time 0.06 seconds. This is expected to be

due to the method of measurement of the fault adjacent to the arc location. For the tests in the laboratory the measurements were taken with a differential voltage probe connected directly to the system being studied. In the case of the Mistake Creek North SWER test a voltage transformer close to the fault location was used. It is expected that the use of the transformer has removed some of the high frequency data.
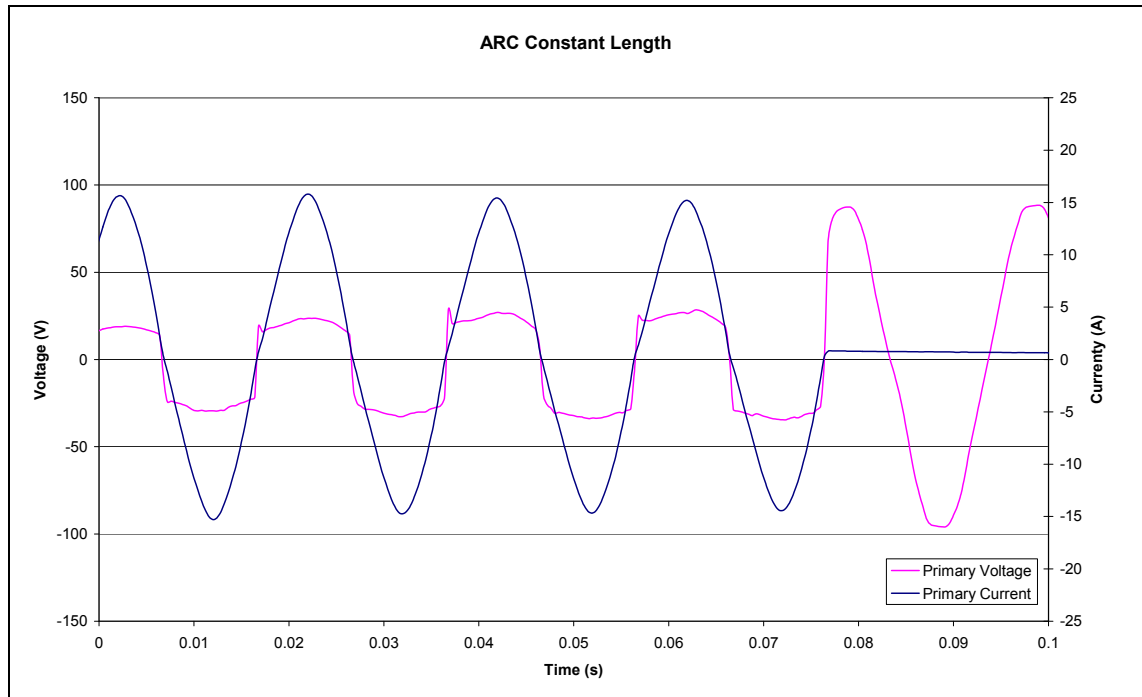
Figure 3.3- Arc Measurement Constant Arc Length

3.4   ARC Model Development

Three arc models have been developed and trialled as part of this project each with increasing degrees of complexity. The models trialled were a simple arc model with a flashover voltage equal to the arc voltage, a voltage clamp with constant flashover voltage and finally a model that has the ability to vary the flashover voltage each cycle in order to create a stochastic model.

The voltage selected for the arc voltage is that of the transition point shown in the waveforms recorded in Taylor (1987). These waveforms transition at approximately 3.00kV. This is the starting point for crest voltage selection.

3.4.1 Simple Model

The Simple Model is shown in Figure 3.4 below. The model is connected to a power system section using the floating node as shown. The right hand leg and left hand leg of the circuit are used to control the positive and negative half cycle of the applied system voltage as required. Each leg consists of an ideal diode and a TACS (Transient Analysis of Control System) Voltage Source. The TACS voltage source is set by the FORTRAN statement block labelled F. In addition to the elements that control the circuit a TACS measurement probe labelled T and a Voltage Probe labelled V are included so the response of the system can be monitored.

The circuit operates by monitoring the voltage from the power system that is applied to the arc model. During a positive half cycle the voltage increases in magnitude with respect to time. Once the voltage exceeds the value set in the FORTRAN statement the circuit is allowed to conduct. In this case the ignition voltage or forward voltage drop of the diode has been set to 0V to create an ideal diode.
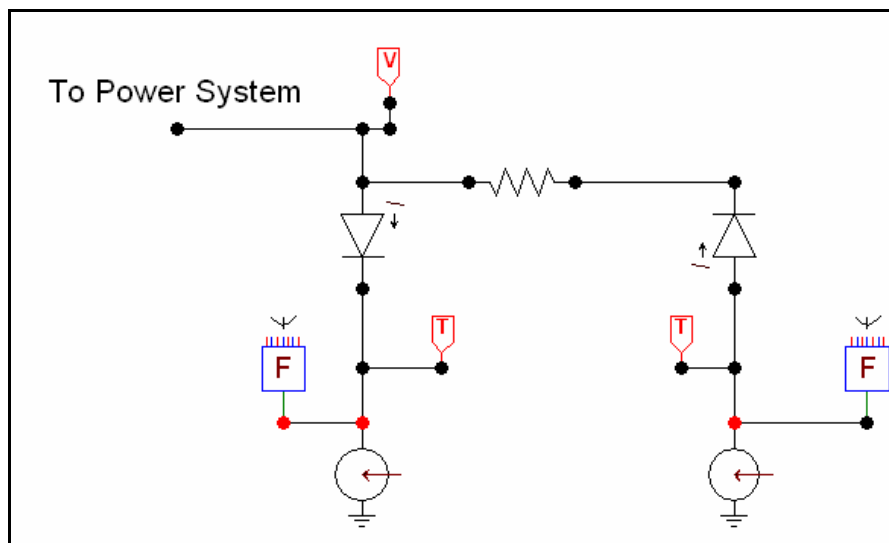
Figure 3.4 - Simple Model (Voltage Clamp)

Two outputs from the simple model are shown in Figure 3.5 and Figure 3.6 below. The model is supplied by a single phase transformer with no source impedance behind it. Figure 3.5 shows the natural result with high voltage peaks at the point where the diode is about to conduct. These high voltage peaks are the result of the calculation of the diode forward voltage drop. The diode is only able to conduct when the evaluated forward voltage exceeds the configured ignition voltage. In order to overcome the effect of the numerical overshoot two approaches are available, either minimise the time step

(DELTAT) or reduce the time step and take limited points of the calculated data for analysis. Reducing the time step does not stop the effect, it does however reduce the magnitude of the voltage peaks. Alternatively only returning every 100th sample in a system that is calculated every 1µs provides results sampled at 1kHz and a result that is adequate for the simulation.
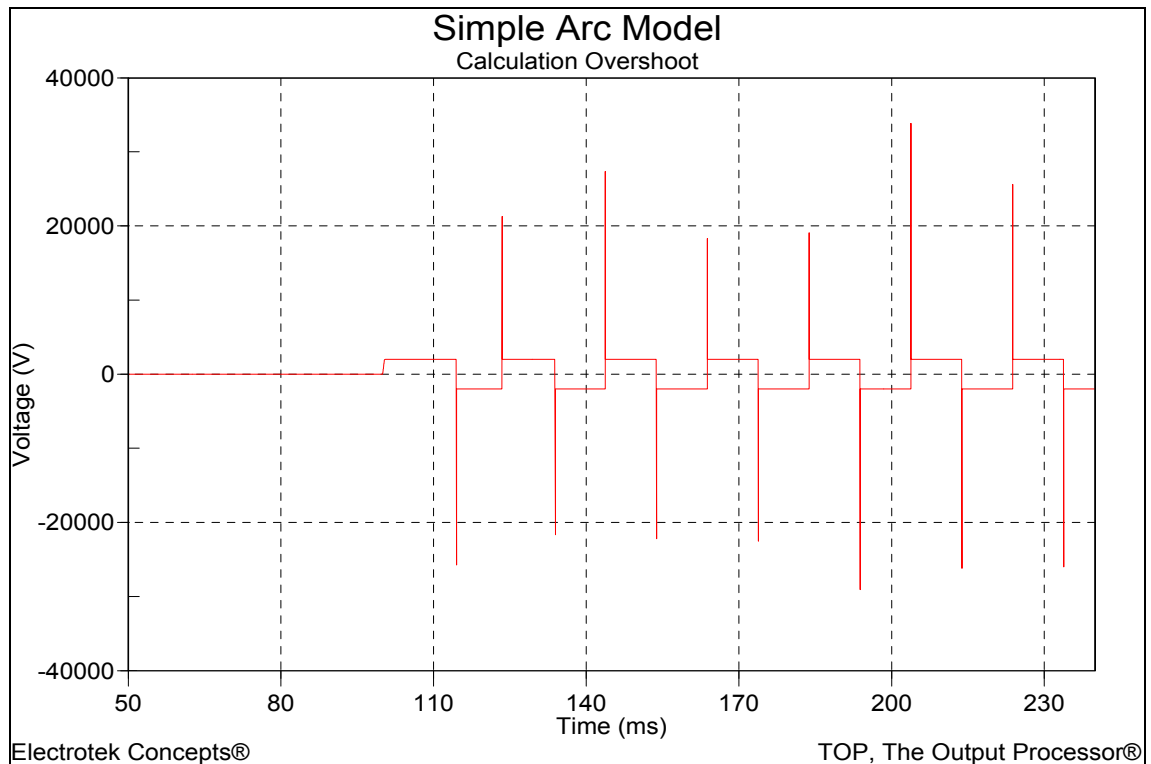
Figure 3.5 - Simple Arc Model Result - Numerical Overshoot
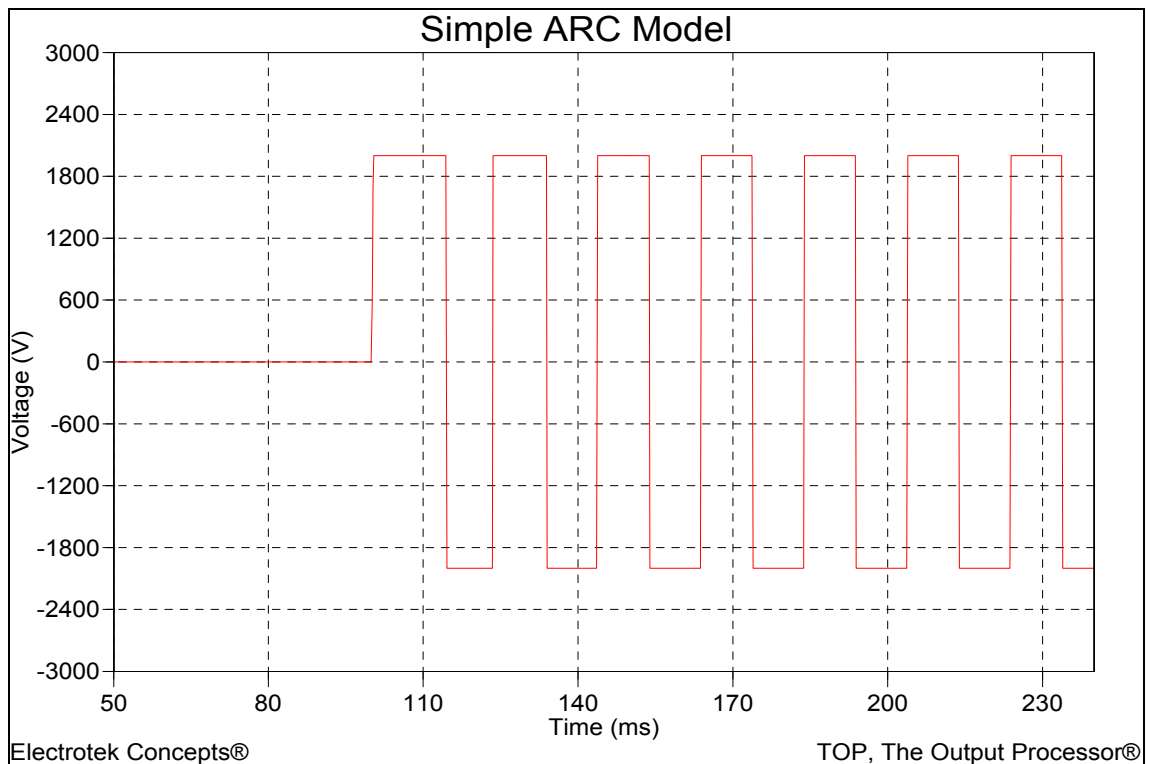
Figure 3.6 - Simple Arc Model Result – Filtered

3.4.2   Model with Voltage Flashover

To allow the user to control the voltage at which the system conducts a modified version of the Simple Arc Model has been created. This modified logic is shown in Figure 3.7. The model created is similar in operation to that of Figure 3.4 with the following inclusions and refinements.

The Arc Voltage control has been modified so that the user only needs to enter a single value and it is applied to both the positive and negative half cycle controls. A series resistance has been included between the TACS sources and the ideal diode. This was intended to allow the user to include additional arc resistance. A three terminal device has been connected between the power system and the ideal diode. This device is a user defined voltage flashover switch and will be elaborated on below. The flashover switch logic is controlled by a FORTRAN statement labelled Flash Control Voltage. This flash voltage control defines the voltage above the user controlled arc voltage that must be exceeded by the power system for the switch to close.

36
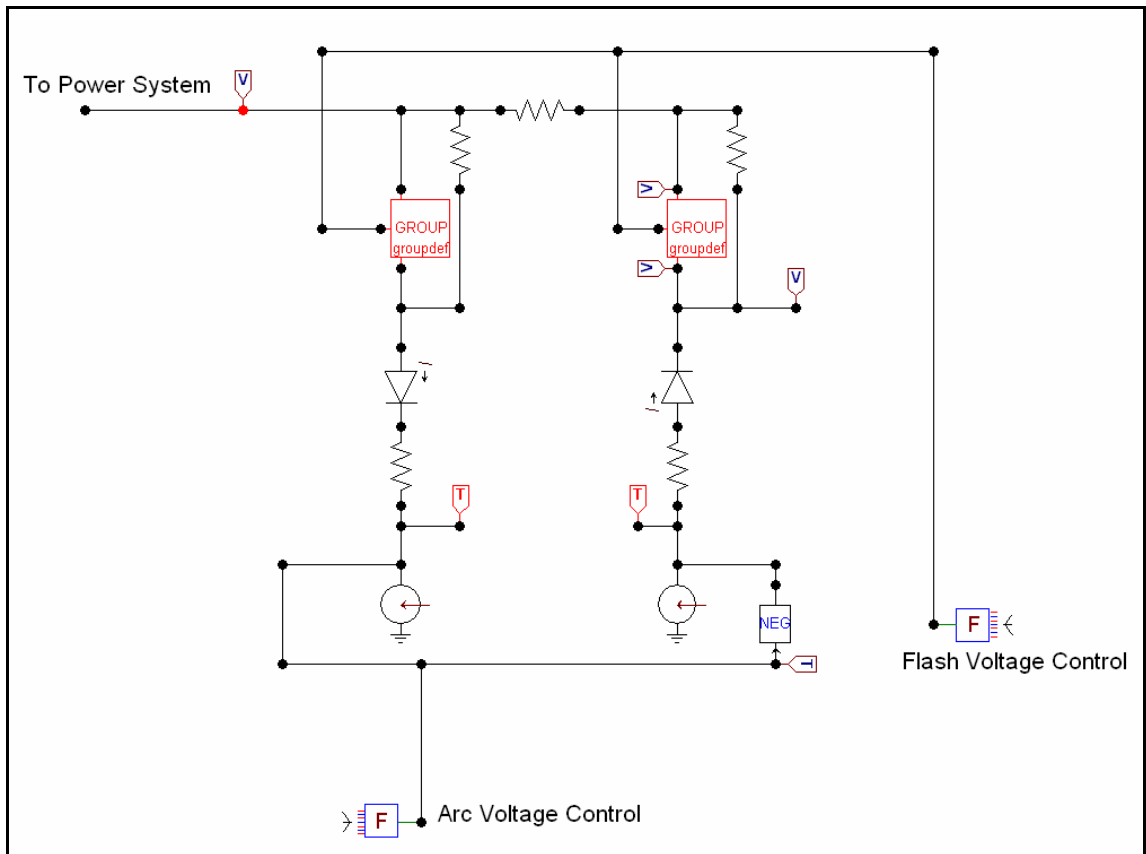
Figure 3.7 - Modified Arc Model with Flashover Control

The variable voltage flashover switch is a TACS controlled switch that has been designed to measure the voltage across the open contacts using a summing junction. The output of the summing junction is fed into an IF statement block and compared with the user defined Flash Control Voltage. If the voltage measured across the open switch is in excess of the user controlled flash voltage a logic 1 will be applied to the TACS switch control via an OR gate. The second input to the OR gate is from a current measuring element. To avoid the TACS switch from closing and shorting out the measured voltage then opening on the next simulation iteration (a process that will continue while the power system voltage is above the flash voltage) a current 'seal in' circuit has been employed. Once the switch has closed a current will tend to flow through the TACS switch for the remainder of the half cycle that initiated the switch close. This current will only cease once the supply voltage has changed polarity and the system current attempts to flow in the opposite direction allowed by the diode in Figure 3.7.

37
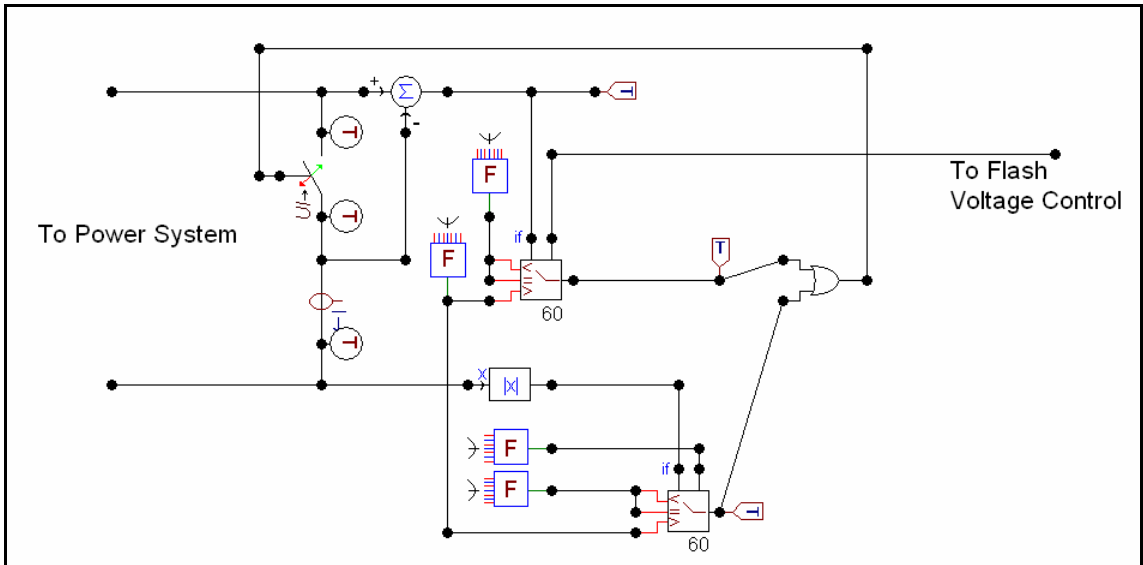
Figure 3.8 - Controllable Flashover Voltage Switch with Series Seal in Circuit

The arc voltage output is shown in Figure 3.9. The user has the ability to control the voltage that occurs in the middle of each half cycle of the arcing event as well as the peak of the voltage that can be expected.
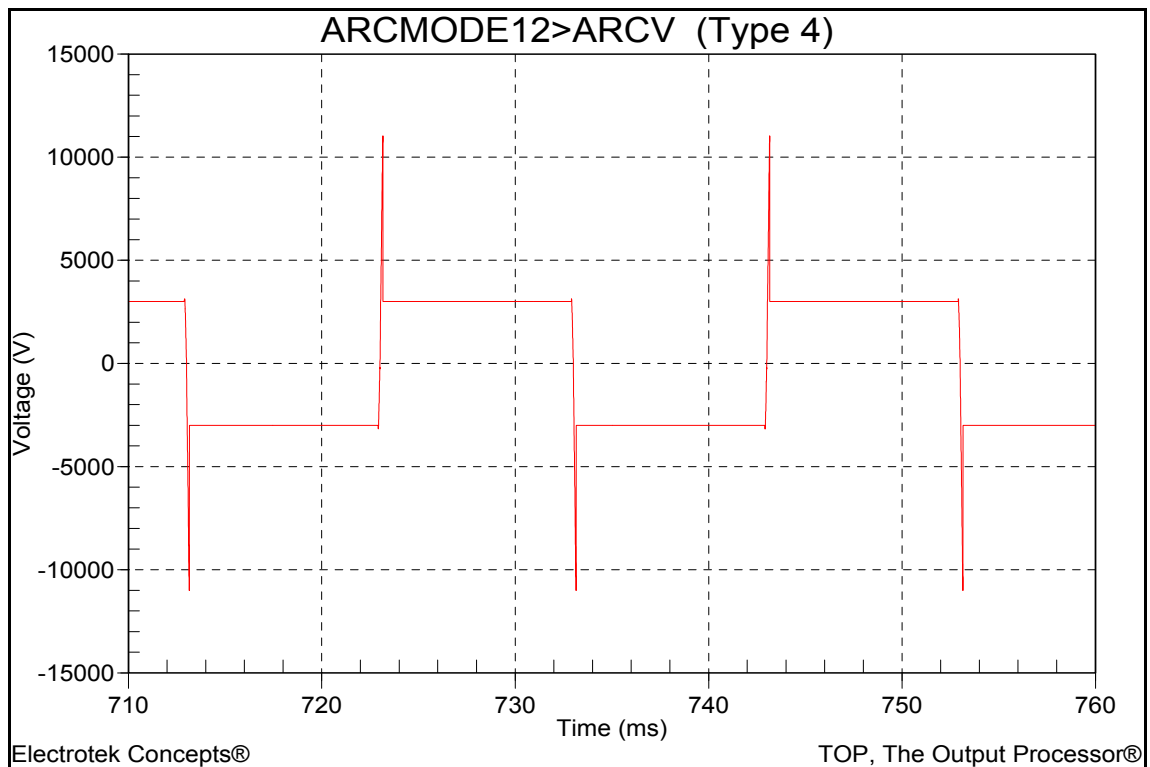
Figure 3.9 - ARC Voltage with Controlled Flashover

3.4.3 Model with Variable Voltage Flashover

The GE Multilin Relay being considered in this project will be discussed in a later section. However to explain the reason for the next ATP model evolution it should be mentioned here that the relay manual [9] discusses the general theory of operation for the high impedance algorithm. The relay has 24 arc detection algorithms running concurrently in order to determine an arcing event. The specific element that are considered for this model are the Energy Algorithm and the Randomness Algorithm. Both of these algorithms monitor the odd, even and non or inter harmonics. The algorithms look for sustained and sudden increases of the harmonics to trigger an event to the expert arcing detection algorithm.

To provide a cycle by cycle "randomness" the Flash voltage control randomly calculated (within user defined limits) every 20ms in an attempt to provide relay operation. The logic in Figure 3.10 has been included in the model to allow the voltage to be varied every cycle.
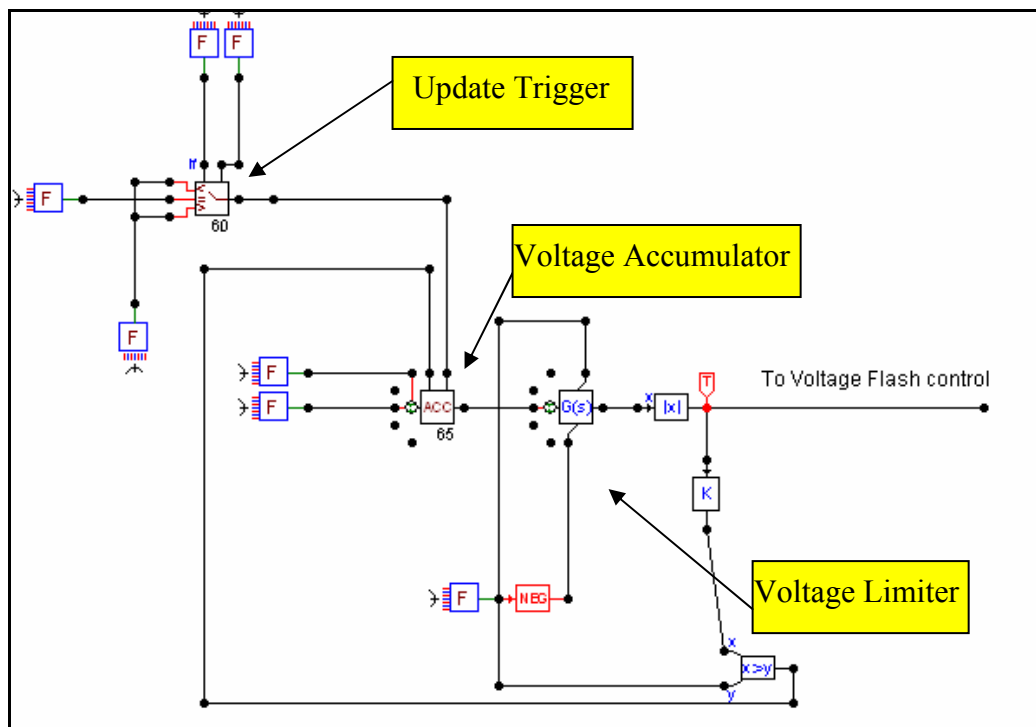
Figure 3.10 - Variable Flashover Control Logic

The IF statement located in the top left hand corner of Figure 3.10 is used to trigger an update of the flash voltage accumulator. The two FORTRAN statements calculate the product of the iteration step and the step size for each scan of the simulation. One of the

FORTRAN statements (the change counter) truncates the result to give the integer value for the last step. Each time the integer value is equal to the free running value one cycle has elapsed. This is a trigger to the accumulator for an update. The output of the iteration control is shown in Figure 3.11.

The voltage accumulator summates two FORTRAN inputs. The FORTRAN inputs are –RAN(1)*K and RAN(1)*K. These inputs are random number generators scaled by a constant K. Each cycle the accumulator is allowed to move up or down in value by the sum of both of the accumulator inputs. The value K controls how large a step change in voltage can be between cycles. A large K value will cause large variations in flashover voltage per cycle.

The output of the accumulator is fed into a control block that is used to limit the flashover voltage to a value determined by the user. This is a safety feature to ensure that the flashover voltage does not exceed the difference between the system peak voltage and the arc voltage.
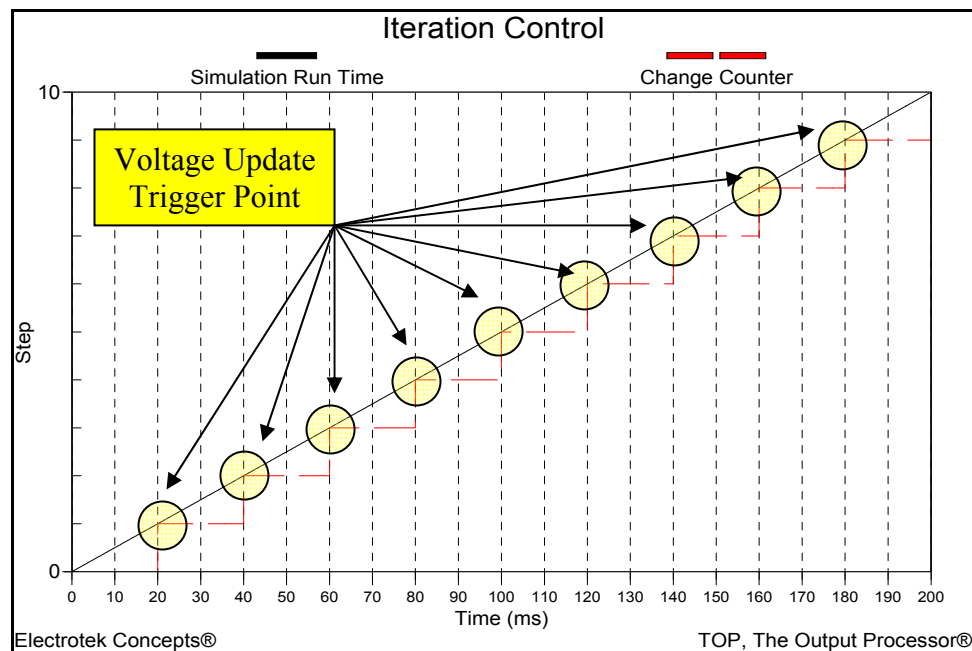
Figure 3.11 - Variable ARC Voltage Iteration Control

Below in Figure 3.12 is an arc voltage plot from 400ms to 1000ms. It can be seen that each cycle has a differing magnitude between the arc voltage and the peak flashover voltage.
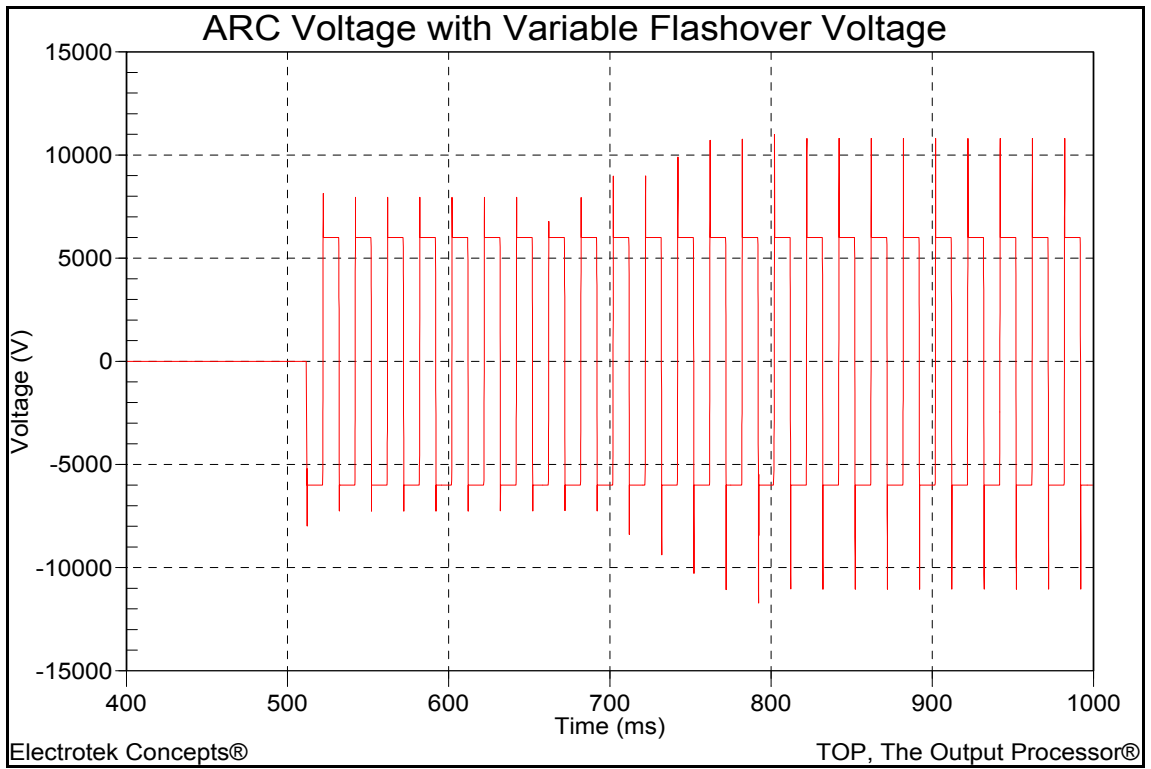
Figure 3.12 - Variable Flashover Voltage Control Enabled

3.4.4 ARC Model Output

The output for the constant voltage flashover has been included below in figure 3.13. This waveform has been selected for discussion as it is static and the discussion can be extrapolated to the variable flashover voltage as required. It also presents information due to a switching event that occurs after the voltage zero crossing as controlled by the variability in the flashover point. The waveform in this static form has a distorted zero crossing similar to that in the waveforms measured in the arc welder tests. The waveform also has the distortion at the same point as that measured in the Mistake Creek Tests.
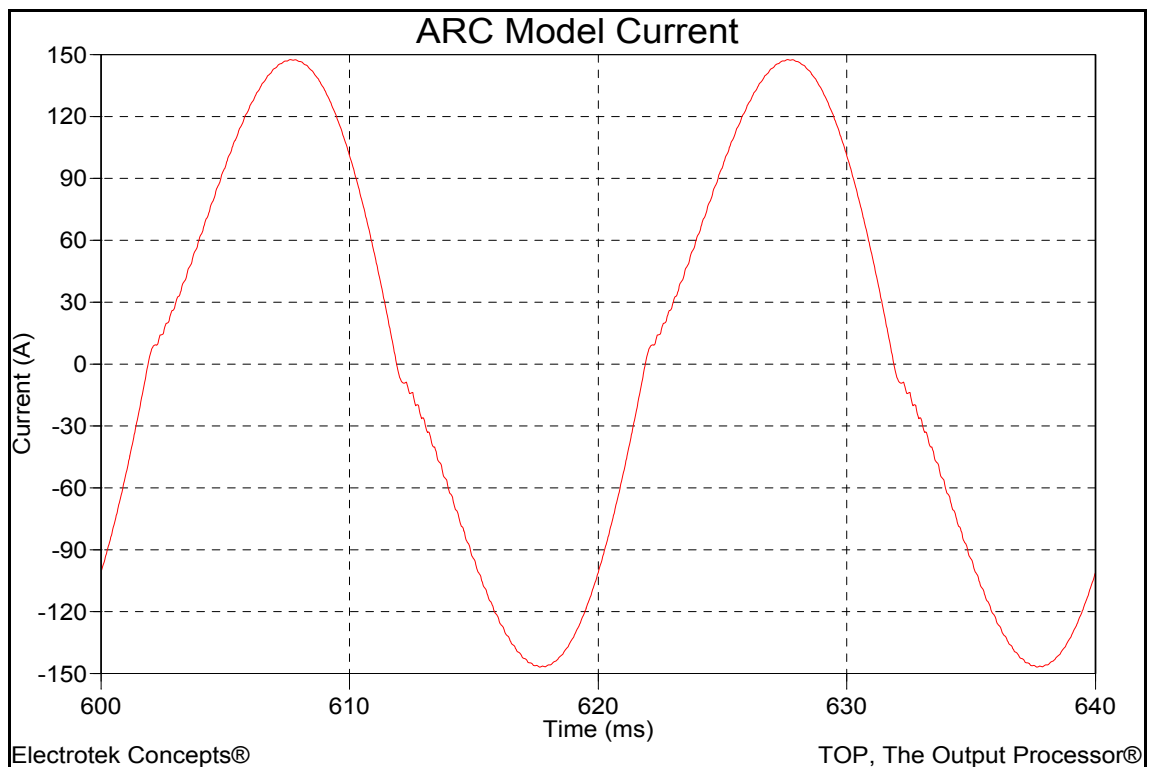
Figure 3.13 - ATP System Current

Chapter 4

Instrument Transformers

4.1   Overview

Instrument Transformers are applied to a power system to provide isolation and conditioning of high voltage and high current signals from relatively delicate measuring instruments that are used for monitoring and control.

Instrument Transformers commonly used on power systems are:

- Current Transformers – Metering and Protection Grade
- Voltage Transformers – Electromagnetically or Capacitively Coupled

Instrument transformers are expected to faithfully transform signals that are not able to be directly measured by instruments or protective systems. The instrument transformers used on Ergon Energy's protection systems are typically designed for 50Hz operation.

4.2   Available Protective Current Transformers

Current Transformers used in Australia are currently covered by Standard AS60044.1-2007; historically the governing standard was AS1675-1986.

Protection current transformers according to AS1675-1986 had classification of P, PS and PL, of these P and PL are typically found on Ergon Energy's network. Class PL CT's (Figure 4.1) are CT's that are defined in terms of knee-point voltage(Uk), maximum exciting current at the knee-point voltage (Ie), secondary resistance (Rs) and turns ratio. Class P CT's (Figure 4.2) define the composite error at the accuracy limit factor, the rated secondary reference voltage and the rated accuracy limit factor.
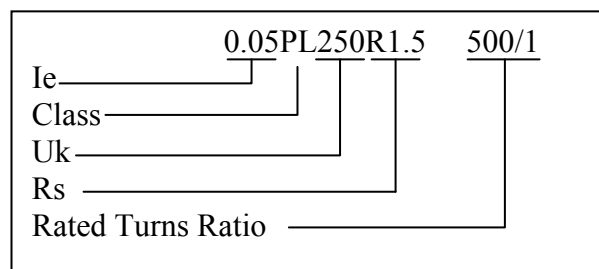
Figure 4.1- Class PL Designation Example

```
                    5P 250 F20 500/1
Rated Composite Error┘    │   │    │
Class ────────────────────┘   │    │
Rated Secondary Voltage ───┘   │    │
Accuracy Limit Factor ─────────┘    │
Rated Turns Ratio ──────────────────┘
```
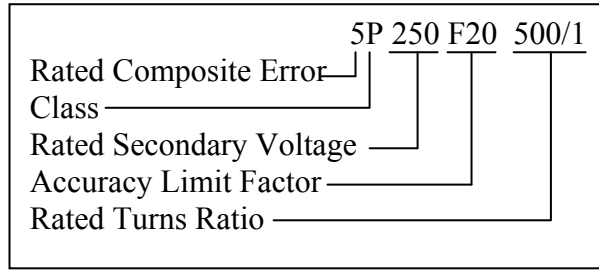
Figure 4.2 - Class P Designation (AS1675)

Care must be taken with class P CT's as they were concurrently defined under an equivalent IEC standard (Figure 4.3). Under the IEC standard class P CT's were defined by the rated output (in VA), the composite error at the accuracy limit factor and the accuracy limit factor. Nomograms and methods for converting between the two standards were included in AS1675-1986.

```
                    15VA 5P F20 500/1
Rated Burden ────────────┘   │    │    │
Rated Composite Error ───────┘   │    │
Class ───────────────────────────┘    │
Accuracy Limit Factor ───────────────┘    │
Rated Turns Ratio ────────────────────────┘
```
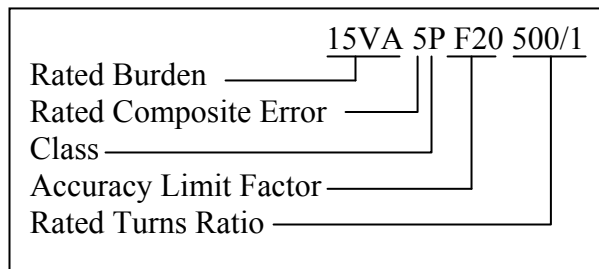
Figure 4.3 - Class P Designation (IEC and AS60044.1)

The current Australian standard AS60044.1-2007 defines class P, PR and PX. Class P CT's are defined in the same manner that the IEC standard that operated in parallel with the obsolescent Australian standard dictated. Class P CT's are now specified in terms of the rated output (in VA), the composite error at the accuracy limit factor and the accuracy limit factor. Class PX CT's are similar in specification and performance to class PL under AS1675-1986.

Class PL, PX and P as defined by both legacy and current Australian standards will be explored in terms of the parameters that can be determined either from nameplate data or commissioning tests so that a transient model can be established.

4.3   Routine Testing of Protection Current Transformers

Testing of current transformers on site usually comprises of functional testing to verify that the current transformer is fit for service. Without the aid of special test equipment that is used to verify overall accuracy in revenue metering applications testing is limited to:

- Ratio Testing

- Excitation Characteristic Testing

- Secondary Resistance Measurement
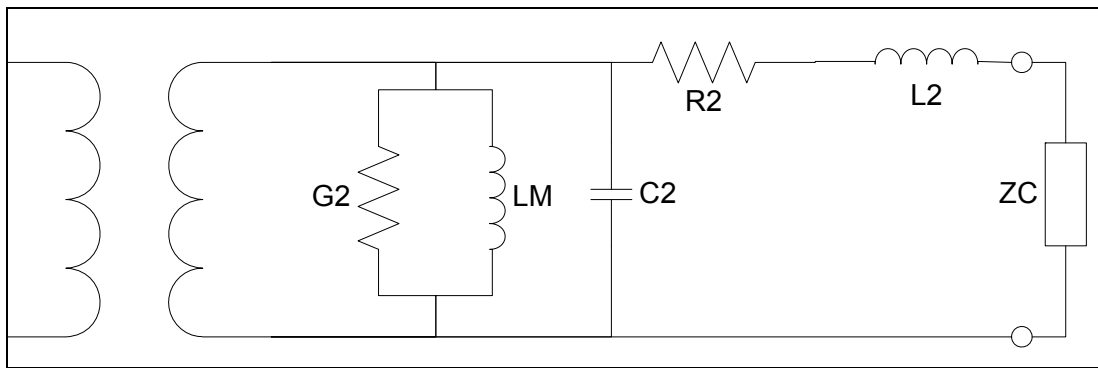
Figure 4.4 - Current Transformer Equivalent Circuit

4.3.1   Ratio Testing

Ratio testing in the field is carried out by one of two methods current ratio method or voltage ratio method. When determining the ratio through current injection a current is injected into the primary winding with the CT secondary shorted. The magnitude of the current in the current transformer secondary is measured. The ratio, N of the current transformer is determined through division of the injected primary current into the measured secondary.

$$ N \quad = \quad \frac{I_{PRIMARY}}{I_{SECONDARY}} $$

Voltage ratio method uses an injected secondary voltage with the primary winding open circuit. The voltage of the primary circuit is measured. The ratio, N of the current transformer is determined through division of the injected secondary voltage into the measured primary.

$$N = \frac{V_{SECONDARY}}{V_{PRIMARY}}$$

Testing CT's using a simple current injection or voltage injection does not accurately identify the CT ratio and provides an indication that the ratio approximates that specified on the nameplate.

4.3.2 Excitation Characteristic Testing

Excitation characteristic testing is used to define the characteristic of the non linear magnetising impedance. An injection is made into the secondary terminals of the current transformer with all other tapings and primary terminals open circuited. A measurement of the RMS excitation current is made and plotted against the RMS excitation voltage. This measurement allows a characteristic to be determined that approximates the magnetising characteristic. Figure 4.5 shows an open circuit test at a voltage approaching the CT's kneepoint. The voltage and current are close to being in phase, indicating most of the exciting current is due to power loss in the CT.
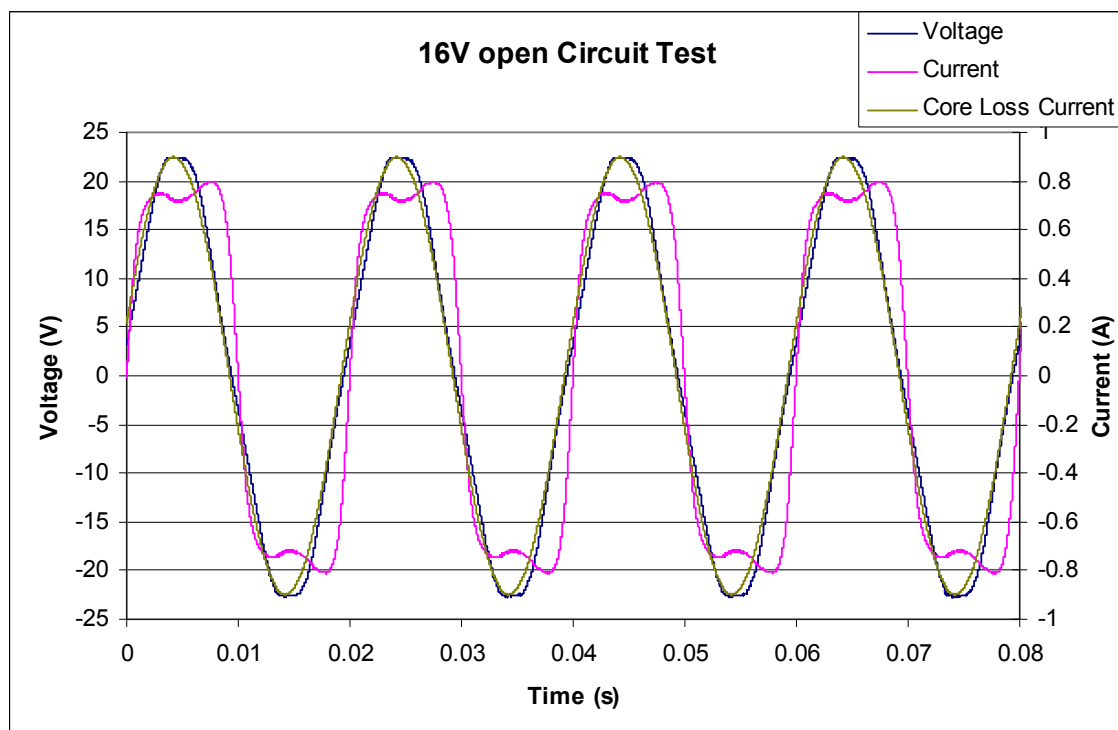
Figure 4.5 - Sample Open Circuit Test Class 5P17.5 F20 at 50/5

In Figure 4.5 the measured values were 16.12V RMS, 0.6822A RMS and 10.248W. The CT resistance was measured to have a value of 0.15Ω.

The power loss in the CT wiring is calculated to be

$$P_{WINDING} \quad = \quad I^2 R$$

$$= \quad 0.6822^2 \text{ x } 0.15$$

$$= \quad 0.0698W$$

In this case the majority of the power loss in the CT excitation test is due to the hysteretic and eddy current loss that is depicted as G2 in Figure 4.4. The current supplying the G2 branch is calculated below.

$$I_G \quad = \quad \frac{P_{TOTAL} - P_{WINDING}}{V_{RMS}}$$

$$= \quad \frac{10.248 - 0.0698}{16.12}$$

$$= \quad 0.6314A$$
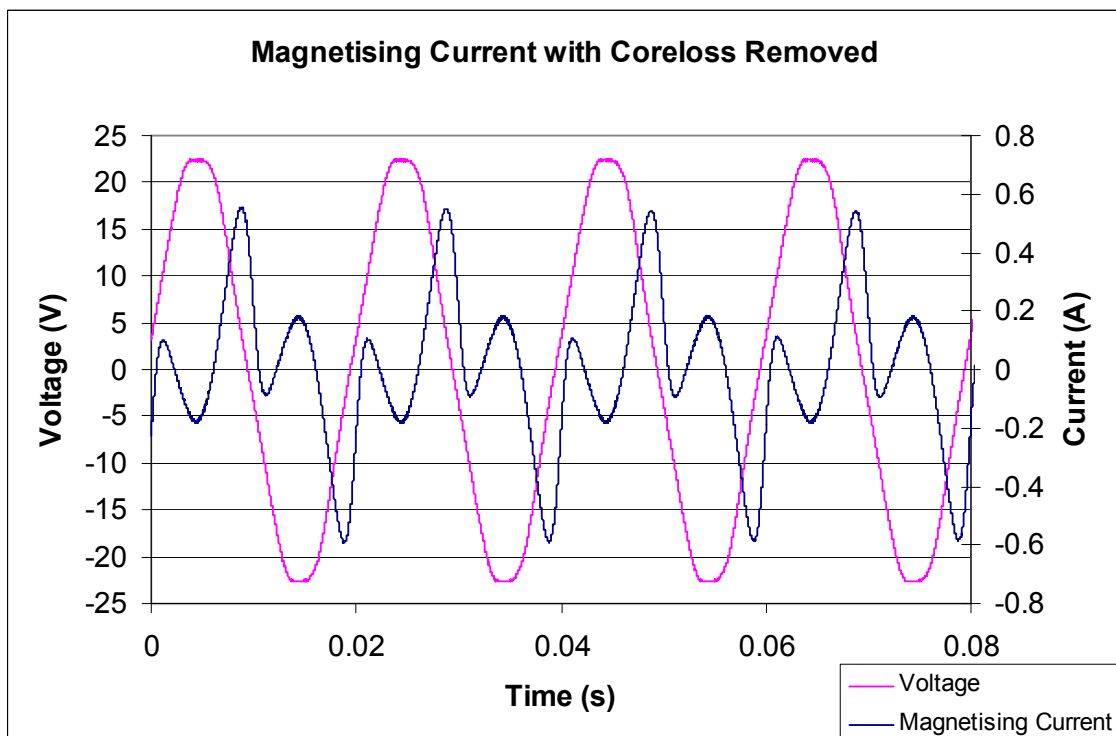
Figure 4.6 - Magnetising current with coreloss removed

The calculated core loss current was removed from the measured values by assuming that the core loss is in phase with the applied excitation voltage. Each sample throughout the range of data was then replotted in Figure 4.6. Figure 4.6 shows that at the end of each half of the voltage cycle the excitation current rapidly increases. This

47

increase in current indicates that the volt time area has begun to exceed the maximum allowable and the CT is saturating.

Figure 4.6 also shows that the assumption that the core loss is linear is untrue. The transitions with direction opposite to the applied voltage waveform starting at 5ms and occurring every 10ms thereafter show that the peak core loss current is an over estimation. This can also be seen to a certain extent in Figure 4.5 where the peak value of the core loss current exceeds the applied test current.

It can be seen from the results above that without specific testing to eliminate the eddy current and hysteretic currents the excitation current test is an approximation for the magnetising current.

4.3.3 Secondary Resistance Measurement

The loop resistance of the CT is measured simply with a calibrated meter. Checks are made to ensure that the value measured on site, once corrected to 75 degrees centigrade are less than the value stamped on the CT name plate.

Class PX and PL Current Transformers

4.3.4 Overview

Class PL and PX CT's have traditionally been employed in protective schemes where direct connection of different CT's sets is required. Typically these types of CT's are found in high impedance bus protection schemes and other schemes where the user requires good transient performance. Class PL and PX CT's are defined by parameters that allow transient performance to be determined through name plate data and simple commissioning or manufacturing tests.

Very little documentation exists regarding the transient simulation of current transformers as defined by Australian standards. Folkers (1999), defines a technique that is used for class C CT's defined under IEEE C37.110-1996. Class C CT's are able to be paralleled with Class PL and PX according to AS1675 and AS60044.1.

4.3.5 Leakage Reactance

According to Australian standard AS1675 (1986) section 3.5.4 Class PL CT's require

- A core that is jointless and wound from an essentially continuous strip.

- Turns for each section of the winding(s) for which performance is specified shall be uniformly distributed

- The primary conductor shall consist of a single conductor through the approximate centre of the core, or of a number of turns distributed approximately evenly over the whole length of the magnetic circuit.

According to Australian standard AS60044.1 (2007) section 2.3.11

"**class PX protective current transformer**: A transformer of low leakage reactance for which knowledge of secondary excitation characteristic, secondary winding resistance, secondary burden and turns ratio is sufficient to asses its performance in relation to the protective relay system with which it is to be used."

Both standards require that the CT's designed reactance is controlled to minimise its impact. The fact that the CT was designed with a low reactance was used by Folker (1999) to avoid the inclusion of the any reactance in the CT model.

When modelling class PX and PL CT's if a reactance value is not available and the CT is not being used at high frequencies the leakage reactance can be ignored.

4.3.6 Turns Ratio

Both PL and PX CT's have a turns ratio that is controlled by the relative governing standard. Class PL CT's have a turns ratio error less than $\pm 0.25\%$ or $\pm 50/N_s$ of the rated transformation ratio where N_s is the number of secondary turns. Class PX CT's have a turns ratio error of less than $\pm 0.25\%$ of the rated transformation ratio.

The clearly defined turns ratio makes the Class PL and PX CT's ideal for transient modelling with the addition of a few simple routine commissioning tests.

4.4   Class P Current Transformers

4.4.1   Overview

Class P CT's do not have strict control over the turns ratio and leakage reactance as do Class PX and PL. Class P CT's allow the manufacturer to apply turns compensation to ensure that the current transformation ratio and composite error are within the limits prescribed by the relevant standard. In manufacture of class PX and PL CT's the turns must be evenly distributed

4.4.2   Leakage Reactance

Class P CT's do not have design requirements of low leakage reactance. Determination of the leakage reactance is beyond the scope of normal commissioning tests. An attempt has been made to define the leakage reactance and resistance of a CT through the inclusion of simple tests that can be included during the commissioning of new plant.

4.4.3   Turns Ratio

The turns ratio of Class P CT's may differ from the reciprocal of the current transformation ratio on the name plate. This is due to the manufacturers latitude to add compensating turns in Class P CT's under the standard.

Simple modelling where no data other than the nameplate and commissioning test data is available will be based on the turns ratio of the current transformer.

4.4.4   Excitation Characteristic

Similar to section 4.3.2 excitation characteristic testing is used to define the characteristic of the non linear magnetising impedance. An injection is made into the secondary terminals of the Current Transformer with all other tapings and primary terminals open circuited. A measurement of the RMS excitation current is made and plotted against the RMS excitation voltage. This measurement allows a characteristic to be determined that approximates the magnetising characteristic

4.5   Current Transformer Testing

4.5.1   Overview

An attempt was made to devise a simple test that allows the parameters required for a transient model to be measured on site as part of a series of commissioning tests. The CT was tested as if it was a power transformer and subjected to a short circuit test.

4.5.2   Current Transformer Impedance Measurement

Determination of the leakage reactance is made by testing the current transformer as if it was a power transformer. Short circuiting the winding with the lowest number of turns (primary winding) and injecting current into the secondary winding give the results in Table 4.1 below. The test arrangement is shown in Figure 4.7.

Table 4.1 - CT Short Circuit Test

Frequency (Hz)	Voltage (V)	Current In (A)	Current Out (A)	Ratio	VA	Power (W)
50	0.790	5.101	47.72	9.36	4.03	3.93

The resulting current transformer impedance determined from the 50 Hz test is $0.151+j0.034\Omega$. This corresponds to a series inductance of 108µH. The resistance at 50Hz is the AC resistance. An attempt to measure the DC resistance with a meter gave a result of 150mΩ.

Figure 4.7 - Current Transformer Bench Testing

4.5.3 Transformer Performance at frequencies >50Hz

A range of frequencies from the nominal frequency of the transformer (50Hz) up to the limit of the Doble secondary injection test set (1000Hz) was carried out and tabulated below.

Table 4.2 - Current Transformer Table of Test Results

Frequency (Hz)	Voltage (V)	Current In (A)	Current Out (A)	Ratio	VA	Power (W)
50	0.790	5.101	47.72	9.36	4.03	3.93
100	0.948	5.249	49.22	9.38	4.97	4.16
200	1.409	5.339	49.72	9.31	7.52	4.37
400	2.521	5.426	50.32	9.27	13.68	4.71
800	4.937	5.553	51.25	9.23	27.42	5.47
1000	6.194	5.616	51.77	9.22	34.79	5.95

The resistance of the current transformer is plotted in Figure 4.8, it can be seen increasing slightly with frequency in the range of 50 to 1000Hz.
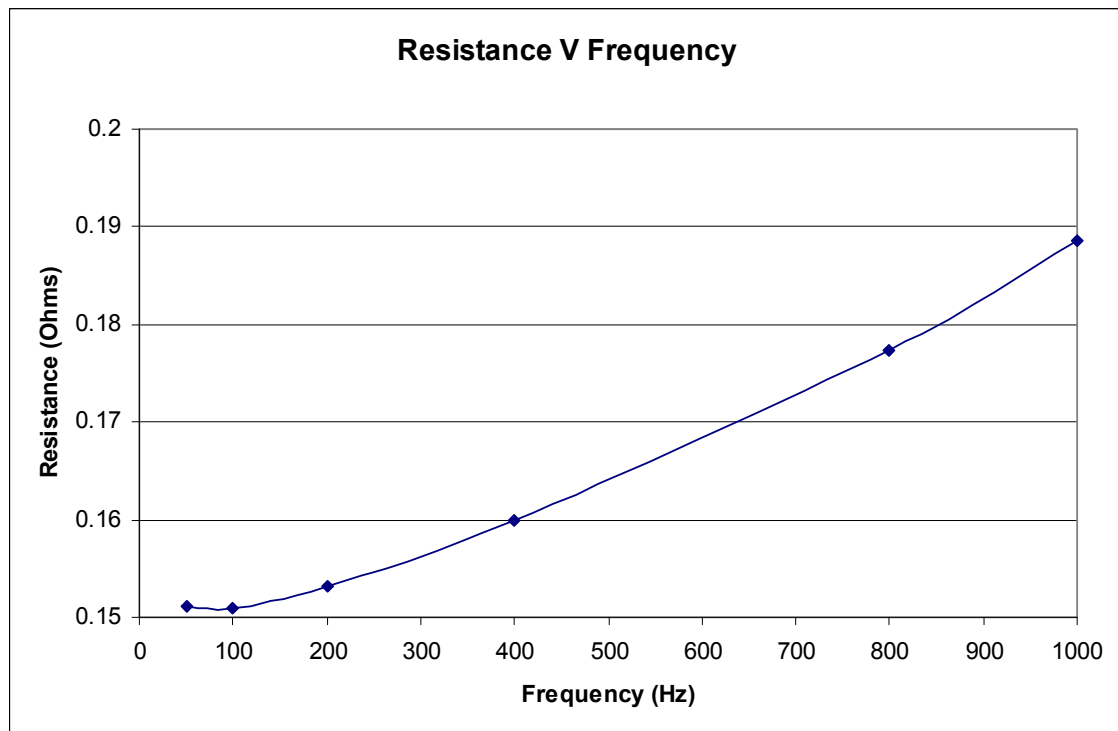
Figure 4.8 - Current Transformer Resistance against Frequency

The reactance of the CT (Figure 4.9) appears to increase proportionally with frequency from 50Hz to 1000Hz. The increase in reactance is linked to a constant inductance.
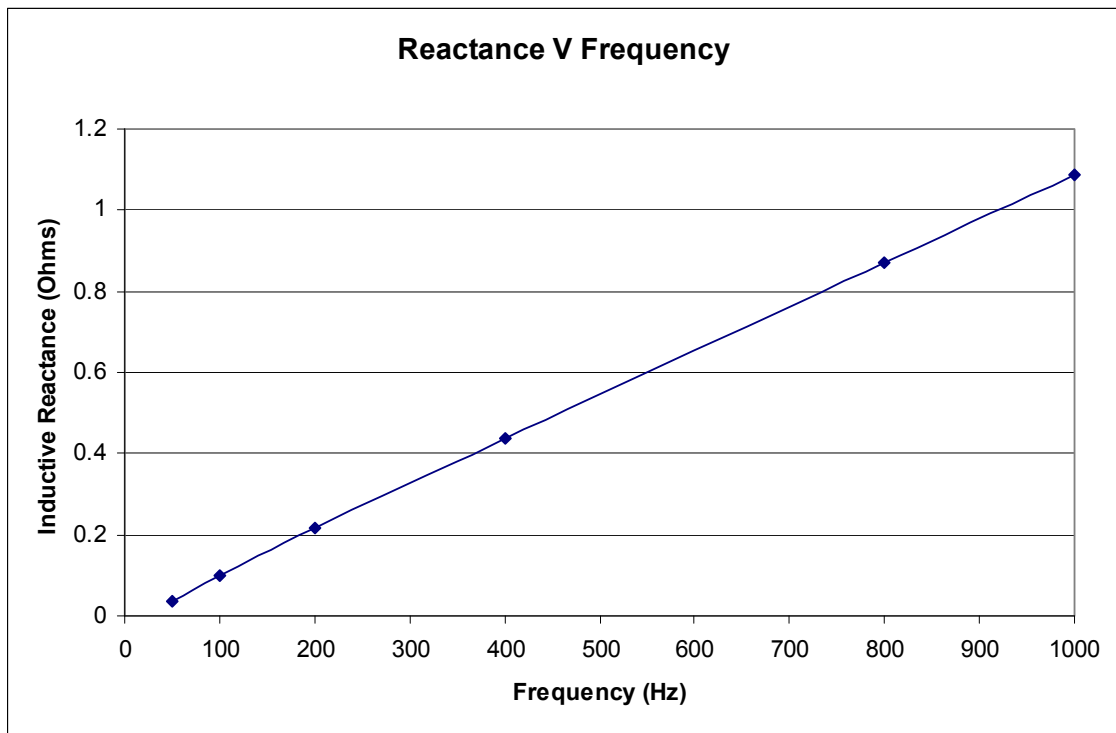
Figure 4.9 - Current Transformer Reactance against Frequency

4.5.4 Excitation Characteristic

Testing was carried out on a general class (Class P) current transformer to define the excitation characteristic. The current transformer was taken into saturation and the RMS voltage an current magnitudes were measured at varying intervals. The values are tabulated below in Table 4.3 and plotted in Figure 4.10.

Table 4.3 - 50/5 10P17.5 CT Excitation Curve

Current (A)	Voltage (V)
0.128	2.012
0.222	4.215
0.282	5.909
0.340	7.715
0.416	10.100
0.478	11.967
0.528	13.252
0.599	14.454
0.611	14.992
0.682	16.124
0.773	17.102
0.906	17.884
2.099	19.127
5.240	19.935

The values from the measured excitation characteristic have been used as an input to the current transformer model.
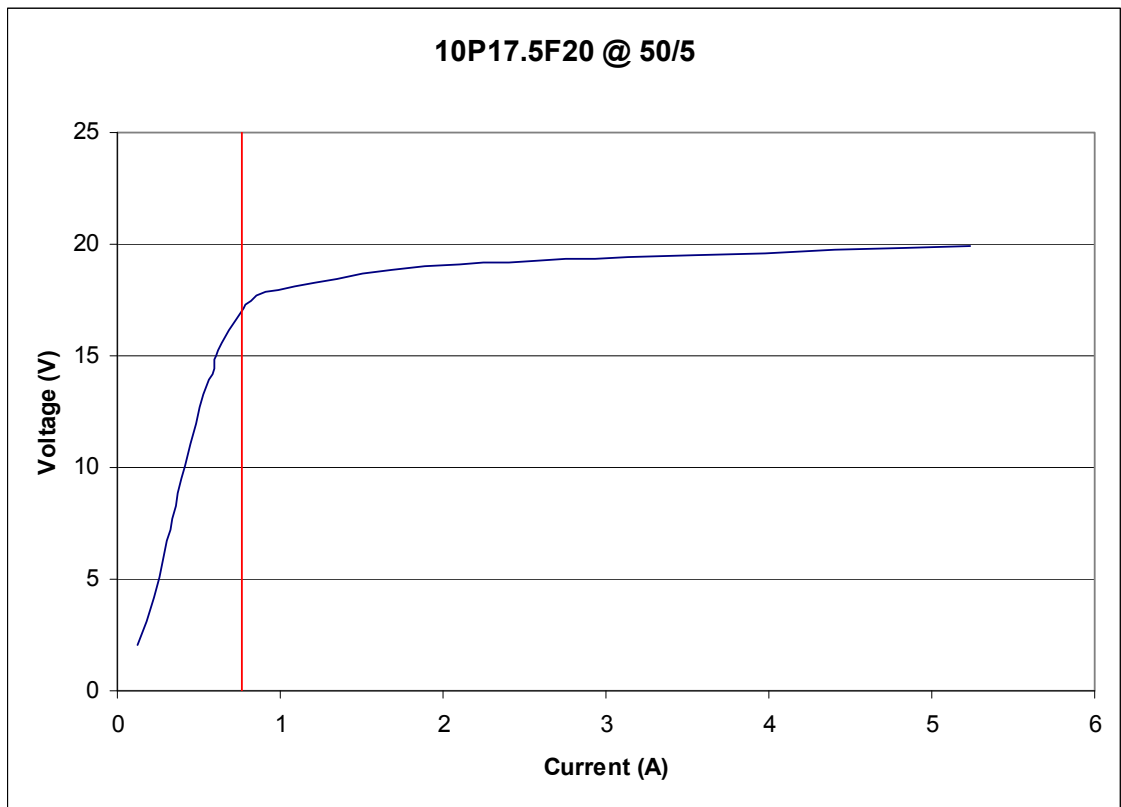
Figure 4.10 - 50/5 10P17.5 CT Magnetising Characteristic

4.6   Current Transformer Model

4.6.1   CT Ratio

A current transformer model was constructed in ATP/EMTP. Figure 4.12 shows the CT under test located in the top left of the diagram. The CT consists of an ideal transformer with the ratio (n) set to the reciprocal of the current transformation ratio. Use of the reciprocal allows the primary winding of the transformer to be connected to the power system and the secondary to the protective relay.

4.6.2   CT Excitation Characteristic

The magnetising branch (Zmag) has been developed using a type 98 Pseudo Non Linear Reactor L(i) and the SATURO routine in ATP. The input data for the SATURO routine was taken directly from the transformer magnetising current testing. The input for the SATURO routine is shown in Appendix C. The output from SATURO is shown in Figure 4.11, the output provides 14 points on the flux, current characteristic that can be used as an input to the CT model.

```
Derived saturation curve gives peak current as a function of flux :
     Row                Current [amp]              Flux [volt-sec]
     -15              -14.7054504373               -0.0897277749
     -14               -5.1804227313               -0.0861040017
     -13               -1.6659251195               -0.0805107866
     -12               -1.2485310096               -0.0769657911
     -11               -1.0561613874               -0.0725542411
     -10               -0.8172136015               -0.0675124698
      -9               -0.9003602422               -0.0650703618
      -8               -0.7409342850               -0.0596347020
      -7               -0.6509532775               -0.0538839315
      -6               -0.5578672552               -0.0454547200
      -5               -0.4513013443               -0.0347409558
      -4               -0.3751555476               -0.0266268551
      -3               -0.2970718932               -0.0189854203
      -2               -0.1809486253               -0.0090594329
       2                0.1809486253                0.0090594329
       3                0.2970718932                0.0189854203
       4                0.3751555476                0.0266268551
       5                0.4513013443                0.0347409558
       6                0.5578672552                0.0454547200
       7                0.6509532775                0.0538839315
       8                0.7409342850                0.0596347020
       9                0.9003602422                0.0650703618
      10                0.8172136015                0.0675124698
      11                1.0561613874                0.0725542411
      12                1.2485310096                0.0769657911
      13                1.6659251195                0.0805107866
      14                5.1804227313                0.0861040017
      15               14.7054504373                0.0897277749
                              9999

Next, check the derived curve by independent reverse computation.
Assuming sinusoidal voltage (flux) at the level of each point,
rms current is found numerically.  This curve should be equal to the
original I-V points inputted.
  Row      Current in P.U.      Voltage in P.U.
    2          0.02559000          0.11500000
    3          0.04449000          0.24100000
    4          0.05649000          0.33800000
    5          0.06806000          0.44100000
    6          0.08315000          0.57700000
    7          0.09561000          0.68400000
    8          0.10567000          0.75700000
    9          0.11980000          0.82600000
   10          0.12220000          0.85700000
   11          0.13644000          0.92100000
   12          0.15467000          0.97700000
   13          0.18213000          1.02200000
   14          0.41957000          1.09300000
   15          1.04798000          1.13900000
```

Figure 4.11 - ATP SATURO Output for 50/5 CT Excitation Curve

The SATURO routine assumes that the testing is carried out using a sinusoidal voltage. The flux current characteristic is determined using a finite difference approximation (ATP Rule Book).

4.6.3   CT Resistance and Reactance

The secondary resistance and reactance values those values calculated in section 4.5.2. The values selected have been based on the 50Hz measurements as these are the ones

that are simpler to obtain from field staff. In addition selection of the 50Hz values gives a lower inductive reactance at the higher frequencies (0.68Ω instead of 1.08Ω). Using the inductance value measured at 1000Hz increases the inductive reactance above the actual value at the nominal frequency of 50Hz (54mΩ instead of 34mΩ). Using the 1000Hz value for the CT's in power frequency studies would place more onerous requirements on the kneepoint of the CT to avoid saturation.

4.6.4   Current Transformer Model Validation

Validation of the model was carried out by injecting voltages into the secondary of the current transformer with the primary winding open circuit. ATP/EMTP will not allow an ideal transformer to be open circuited. In this case a 1e+9Ω resistor was connected to allow model convergence. TACS (Transient Analysis Control System) probes were used to measure the RMS voltage and current for each of the applied voltage steps. The results have been overlayed across the current transformer magnetising characteristic taken in the field. This is shown in Figure 4.13.

Both the measured points on the current transformer magnetising characteristic and the ones simulated in ATP/EMTP are in agreement.
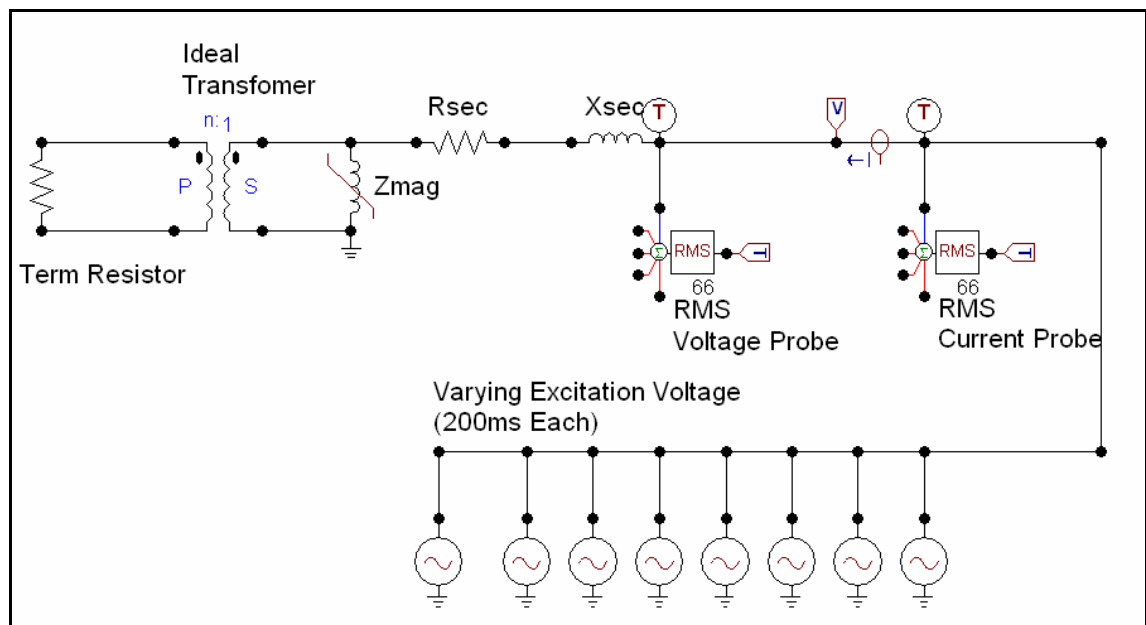
Figure 4.12 - ATP/EMTP Current Transformer Model and Test Circuit

56
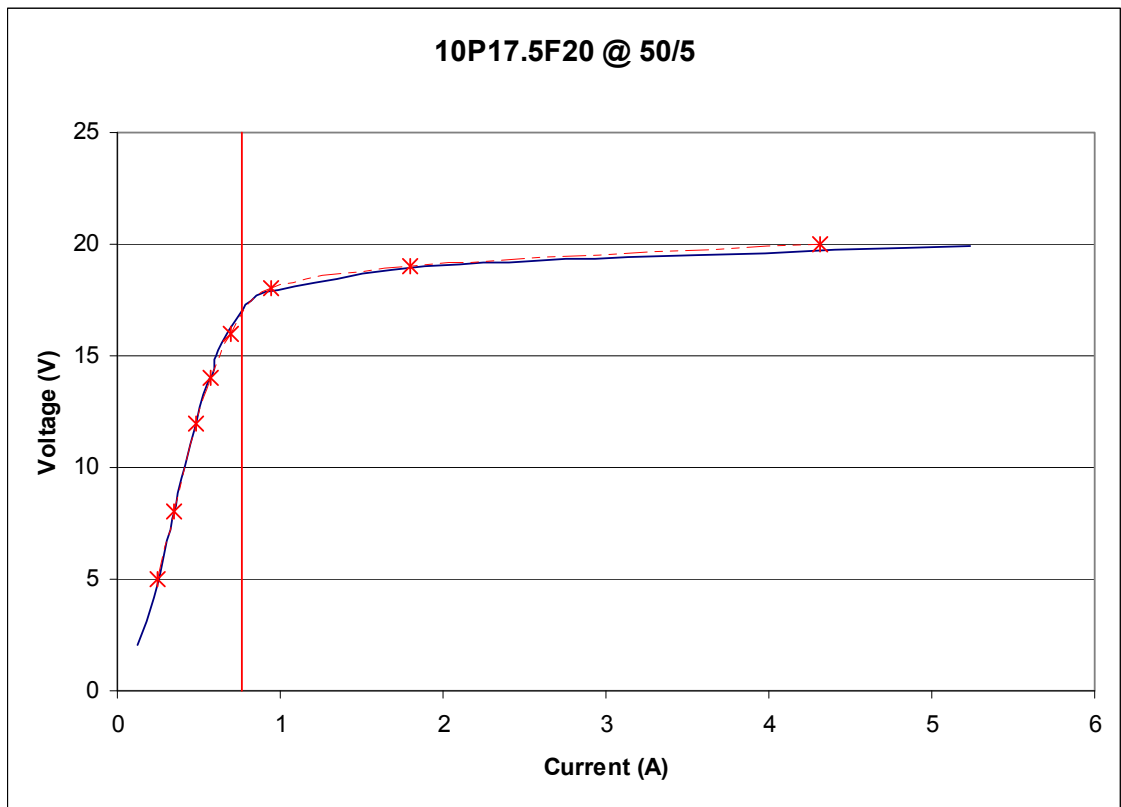
Figure 4.13 - CT Magnetising Characteristic and ATP/EMTP Simulated Results

The CT model was connected into the power system model and a simulation run for 1 second. The last 100ms of the simulation are shown in Figure 4.14. Figure 4.14 depicts the primary current, the secondary current referred through the current transformer ratio and the error between the input and output of the current transformer. The current transformer faithfully represents the power system currents. The error has been calculated and plotted on the same graph (separate axis)

$$\text{Error} \quad = \quad \left(\frac{CT_{PRIM} - n \times CT_{SEC}}{CT_{PRIM}} \right)$$

Large percentage errors are recorded at the zero crossings. This is expected to be non consequential as the magnitude of the currents is low.
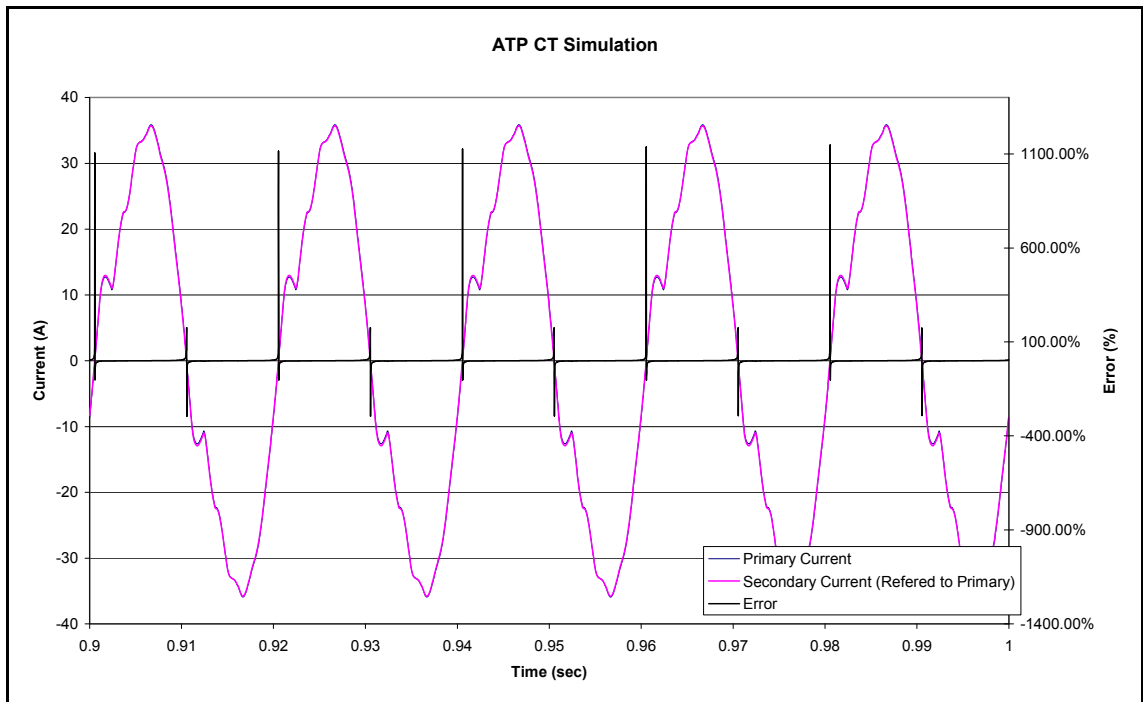
Figure 4.14- CT Performance ATP Model

4.7   Summary

The current transformer can be defined accurately in a transient model by knowing four parameters, the ratio, secondary resistance, secondary inductance and the excitation characteristic. Simple and routine tests exist for obtaining the CT secondary resistance for class P, PL and PX CT's. The ratio of the CT is controlled by governing standards for PL and PX CT's. Class P CT's require additional tests as defined in AS1675 (1986) to determine the ratio. This type of testing is not a common commissioning test and is approximated by primary injection and secondary measurement.

The leakage inductance of the CT's is not a parameter measured in practice. The test methodology proposed in 4.5.2 allows the user to determine the leakage reactance regardless of the CT class. The inductance value calculated from the measured data can be introduced directly into the selected model.

Finally the magnetising characteristic for a CT is approximated from the excitation characteristic tests carried out at site. The measured values are input directly into ATP's SATURO routine, the results are then used in the system model.

Chapter 5

Power Transformer Model

5.1   Overview

The power transformer model is used to couple a typical three phase system to a Single Wire Earth Return (SWER) System. Power transformers are also used at the customer's premises to transform the voltage that is transmitted through an overhead distribution network to a voltage that is safe and practical for a customer to use.

5.2   Application

With regard to a Single Wire Earth Return (SWER) Network the distribution system is typically bounded by transformers at both the supply and load side.

In some instances the source isolation transformer is omitted connecting a single wire system directly creating what is deemed to be "unisolated SWER". A program of installing isolation transformers for unisolated SWER networks is currently underway. Installation of isolation transformers allows these systems to conform to the premise of this research.

5.3   Transformer Testing

Various transformers were tested in an attempt to identify their performance at the nominal frequency and frequencies away from rated for the specified plant. Transformers were tested at different times and locations. It was not possible to carry out all testing all tests for each transformer due to the availability of test equipment at each location.

5.3.1   Manufacturer Testing

The current supplier of distribution transformers to Ergon Energy is ABB. ABB carried out testing of three different types of SWER isolating transformers. The transformers tested were:

- 100kVA 11/12.7kV with 250V auxiliary

- 200kVA 22/19.1kV with 250V auxiliary

- 200kVA 11/19.1kV with 250V auxiliary

The transformers were open circuit tested by injecting into the 250V winding with the Line and SWER windings open circuited. The short circuit testing was carried out by injection through the Line and SWER windings. The results recorded by the manufacturer are detailed below.

The open circuit results for the 200kV 22/19.1kV SWER Isolating Transformer are detailed in Table 5.1. The power loss from the short circuit test (at 200kVA) is 1713W with an impedance of 3.8%.

Table 5.1 - 200kVA 22/19.1kV Open Circuit Test

Voltage Factor	Voltage	Line Current	No Load Loss
0.8	200	1.345	156
0.9	225	1.445	197
1.0	250	1.575	246
1.1	275	2.155	303
1.2	300	6.185	383

The open circuit results for the 200kV 11/19.1kV SWER Isolating Transformer are detailed in Table 5.2. The power loss from the short circuit test (at 200kVA) is 1697W with an impedance of 3.7%.

Table 5.2 - 200kVA 11/19.1kV Open Circuit Test

Voltage Factor	Voltage	Line Current	No Load Loss
0.8	200	0.935	159
0.9	225	1.085	202
1.0	250	1.325	249
1.1	275	2.275	309
1.2	300	7.355	392

The open circuit results for the 100kV 11/12.7kV SWER Isolating Transformer are detailed in Table 5.3. The power loss from the short circuit test (at 100kVA) is 830W with an impedance of 4.2%.

Table 5.3 - 100kVA 11/12.7kV Open Circuit Test

Voltage Factor	Voltage	Line Current	No Load Loss
0.8	200	0.780	123
0.9	225	1.015	156
1.0	250	1.255	188
1.1	275	1.830	235
1.2	300	4.965	301

5.3.2   In House Testing

In house testing was carried out on a 200kVA 33/19.1kV with 250V auxiliary SWER isolating transformer. This testing was an attempt to identify the response of the power transformer to frequencies above the transformer nominal value of 50Hz.

The test was arranged so that the voltage at the highest test frequency corresponded to the maximum available output from the Omicron CMC256 test set. Each time the frequency doubled the voltage was also doubled so as to keep a constant flux density in the magnetising branch of the power transformer.

The injection was made in the SWER (19.1kV) side of the transformer as this was the lowest voltage in the power circuit. The line side (33kV) winding was short circuited for the testing.

One cycle from each of the results from the short circuit test results shown in Figure 5.3 to Figure 5.8 has been analysed to calculate the effect of the high frequency signals on the leakage reactance of the power transformer. The values recorded in Table 5.4 have been calculated from the waveform recordings made at each injection frequency.

Table 5.4 - 200kVA 33/19.1kV Transformer High Frequency Test Results

Frequency (Hz)	Power (W)	Voltage (V)	Current (A)	Impedance (Ω)	Resistance (Ω)	Reactance (Ω)
50	0.991	14.94	0.262	56.95	14.40	55.09
100	1.325	29.85	0.272	109.77	17.92	108.29
200	1.492	59.89	0.274	218.77	19.91	217.86
400	1.848	116.77	0.277	421.90	24.13	421.20
800	3.325	240.91	0.273	881.02	44.48	879.90
1000	4.325	300.92	0.274	1098.91	57.68	1097.40

As can be seen from Figure 5.1 over the range of frequencies studied the reactance is relatively linear indicating that the transformer leakage inductance is a constant value. The characteristic of the resistance (Figure 5.2) however is neither linear nor exponential. The testing carried out at frequencies away from 50Hz has proven problematic due to the low value of injected current that was practical.
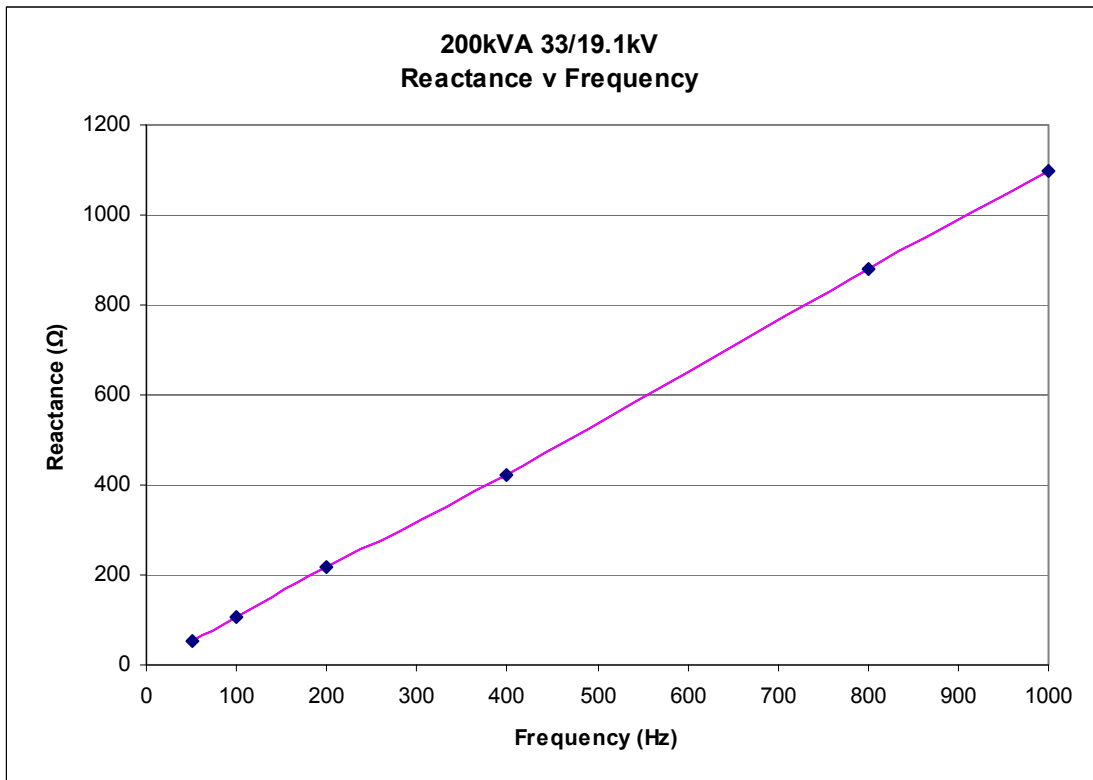
Figure 5.1 - 200kVA 33/11kV SWER Isolating Transformer Reactance V Frequency
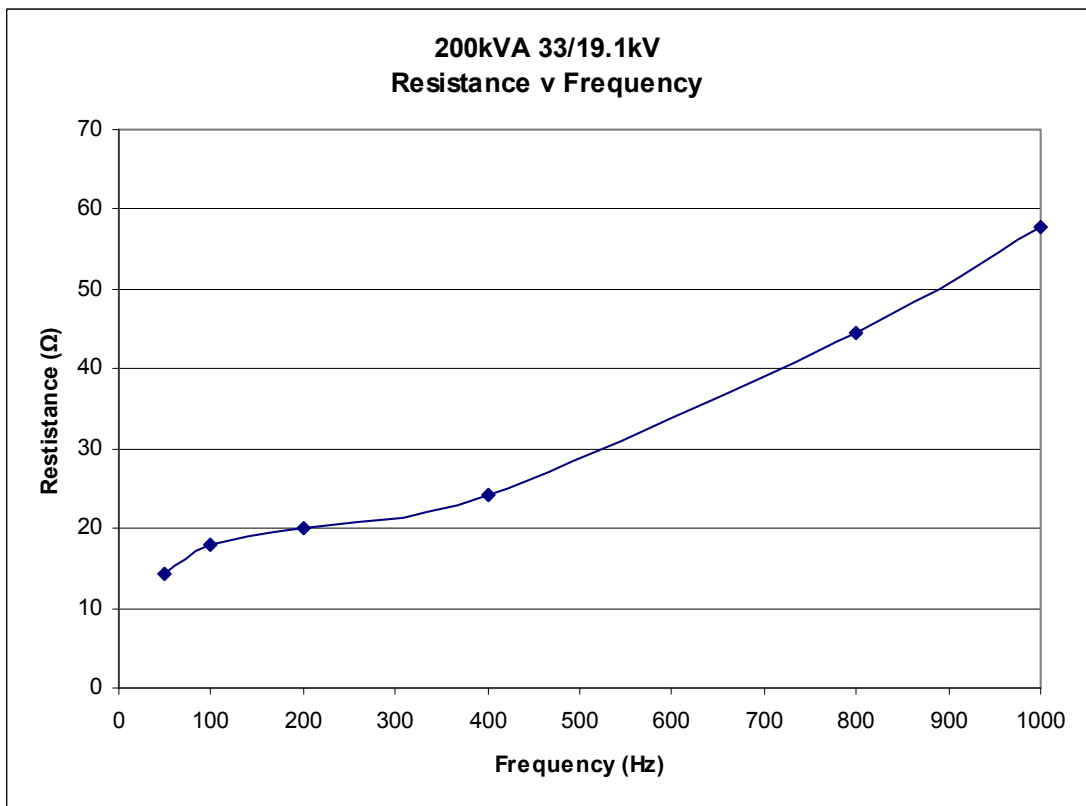
Figure 5.2 - 200kVA 33/11kV SWER Isolating Transformer Resistance V Frequency

The outputs from each of the tests are included in Figure 5.3 to Figure 5.8. The currents measured on the input and output from each test can be seen to remain in phase with one another.
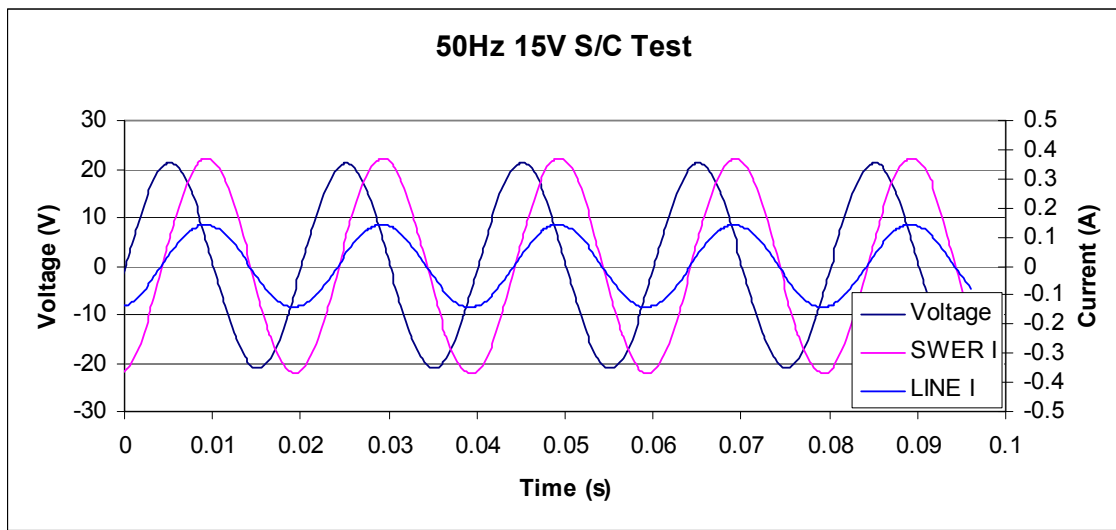
Figure 5.3 - 50Hz S/C Test (200kVA 33/19.1kV)
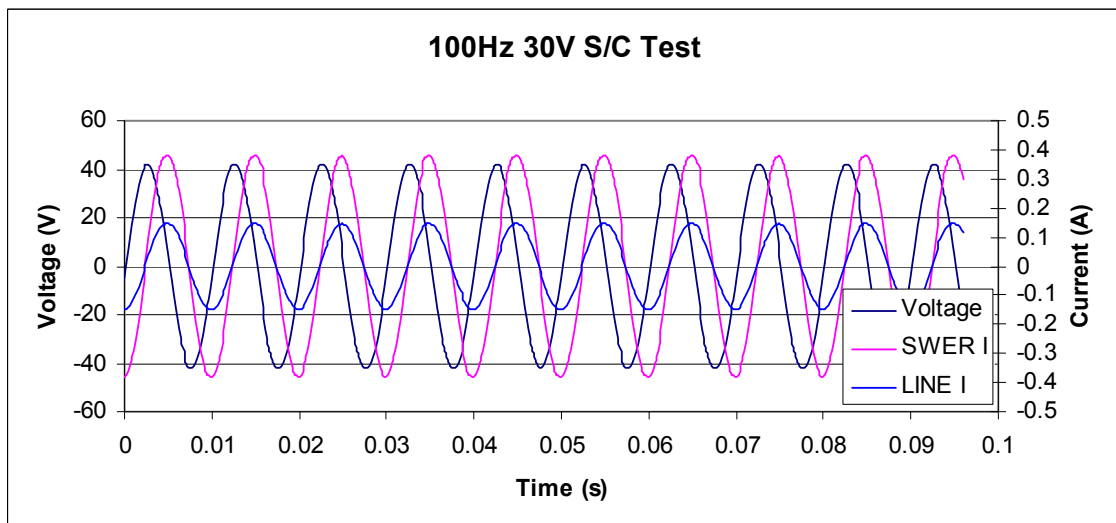
Figure 5.4 - 100Hz S/C Test (200kVA 33/19.1kV)
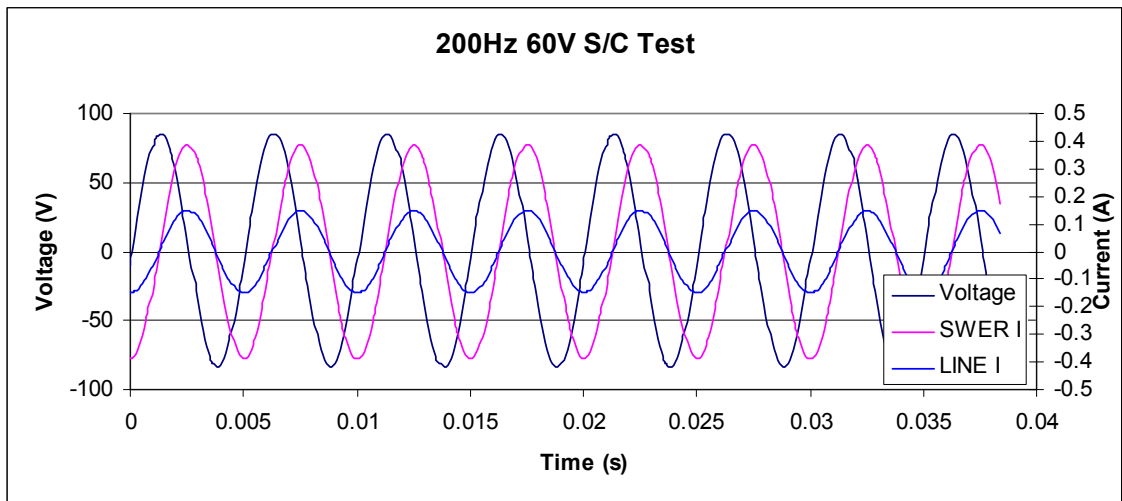
Figure 5.5 - 200Hz S/C Test (200kVA 33/19.1kV)
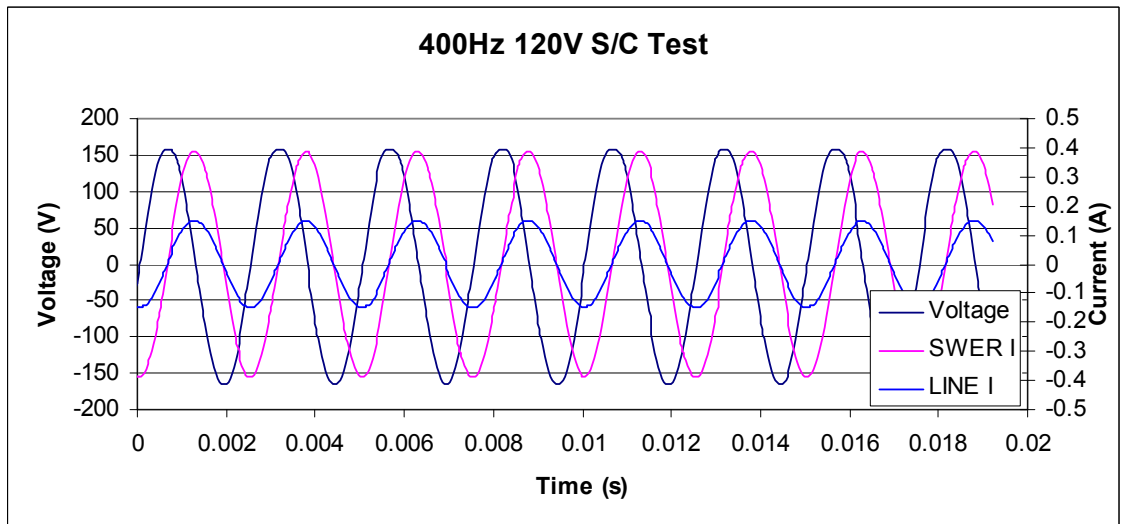
Figure 5.6 - 400Hz S/C Test (200kVA 33/19.1kV)
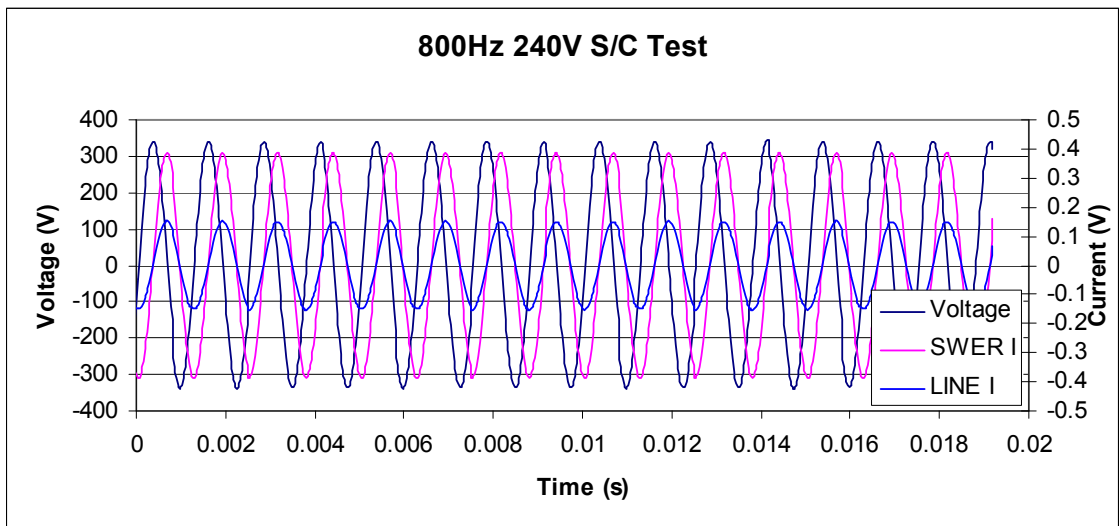
Figure 5.7 - 800Hz S/C Test (200kVA 33/19.1kV)
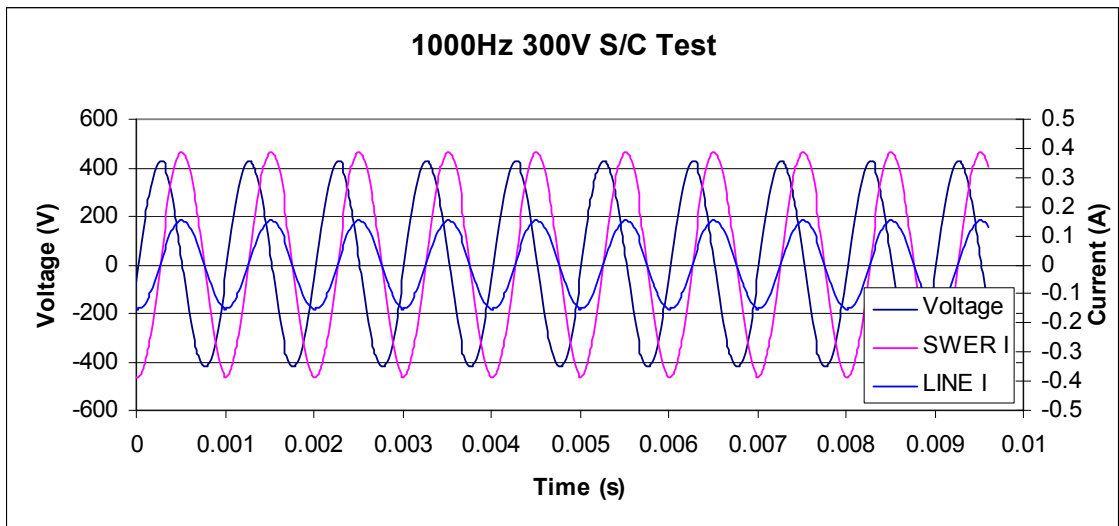
Figure 5.8 - 1000Hz S/C Test (200kVA 33/19.1kV)

5.4   Transformer Testing Summary

Testing at frequencies other than 50Hz proved to be only beneficial as an indication only due to the lack of output capability from the injection test set.

The test results obtained at 50Hz have been used for the power system model. The 50Hz testing was able to drive a sufficient current through the power transformer to comply with current industry practice for short circuit testing.

Chapter 6

Overhead Line Model

6.1   Overview

The overhead line component is the physical connection between the SWER isolating transformer and the customer's distribution transformer. The overhead line component ranges from a few kilometres to many hundreds of kilometres in length.

SWER lines typically are rural remote with relatively low load density. The lines cover long distances and in an effort to economically distribute power to customers overhead line designs have employed conductors with steel reinforcing. The addition of steel reinforcing allows span lengths between poles to be increased minimising the number of poles that are installed.

Typical types of conductor that are used for SWER construction are

- 3/2.75 SCGZ

- 3/2.75 SCAC

- 3/4/2.5 ACSR (Raisin)

- 4/3/3.0 ACSR (Sultana)

- 7/3.0 AAC (Libra)

- 6/1/3.0 ACSR (Apple)

- 6/1/3.75 ACSR (Banana)

Overhead line typically used for SWER is either steel or combinations of steel reinforcing strands and aluminium. Interpretation of the conductor designations above are as follows.

Table 6.1 - Conductor Types

Conductor Designation	Meaning
SCGZ	Steel Conductor Zinc Coated (Galvanised)
SCAC	Steel Conductor Aluminium Coated
ACSR	Aluminium Conductor Steel Reinforced
AAC	All Aluminium Conductor

Where the conductors are not stranded with different conductor types (SCGZ, SCAC and AAC) the preceding numbers reading from left to right are the number of strands and the diameter of the strands in millimetres. For the ACSR conductors the first number is the number of aluminium strands, the second is the number of steel and the third is the conductor diameter.

Figure 6.1 and Figure 6.2 show 3/4/2.5 ACSR (Raisin) and a generic steel (either SCGZ or SCAC) respectively.
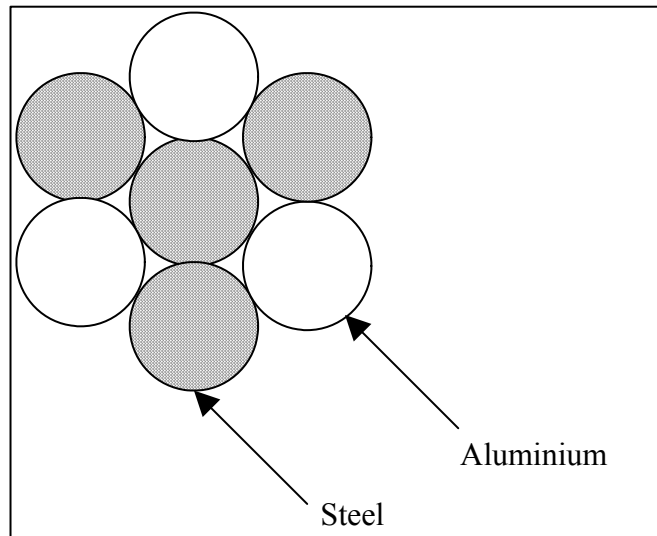
Figure 6.1 - 7 Strand (4 Steel, 3 Aluminium)
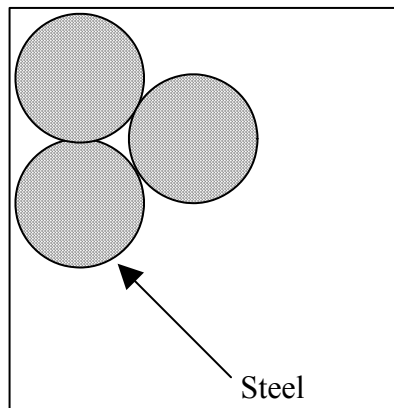
Figure 6.2 - 3 Strand Conductor

6.2   Line Capacitance

6.2.1   Overview

The effect of the steel component on the capacitance of the overhead line has been determined using typical methods available to determine its impact. The line capacitance has been calculated using the method of images, finite element analysis using femlab and finally with EMTP/ATP's line constants program.

All calculations have been based on an average conductor height of 12.7 meters. This height corresponds to an attachment height of 14 meters at the pole and a minimum height at the centre of the span of 12 meters. Due to its steel / aluminium composition and its common use Raisin conductor has been selected for this study.

6.2.2   Method of Images

The method of images assumes that a mirror image of the conductors to be studied exists. The images are created using the earth surface as the plane of reflection. A typical SWER system is shown in Figure 6.3.
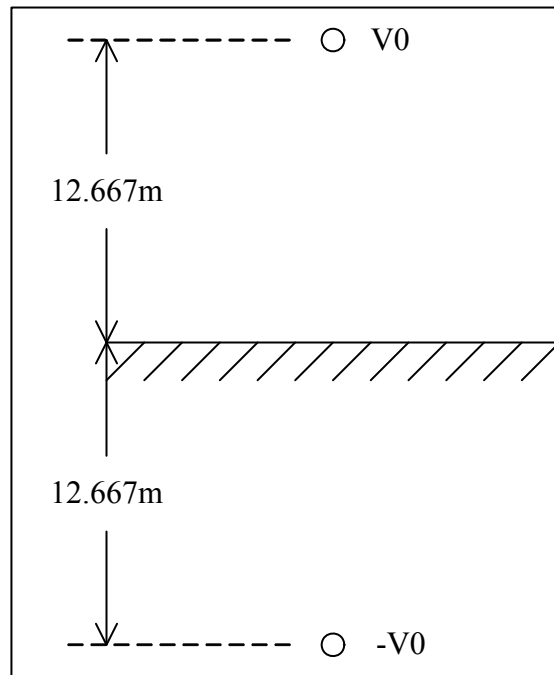
Figure 6.3 - Model for Method of Images

$$C_n = \frac{2\pi k}{\ln\left(\dfrac{D}{r}\right)}$$

Where Cn = line to neutral capacitance

D = distance between two conductors (twice the line to earth distance)

r = radius of the line conductor

k = permittivity of free space (8.85×10^{-12} F/m)

Raisin conductor has an outer diameter of 7.5mm assuming that no compression has taken place.

$$C_n = \frac{2\pi 8.85 \times 10^{-12}}{\ln\left(\dfrac{2 \times 12.667}{0.00375}\right)}$$

$$= \quad 6.306 \times 10^{-12} \text{ F/m}$$

$$= \quad 6.306 \text{ nF/km}$$

6.2.3 Finite Element Analysis

The line data was modelled as two conductors in free air in a similar fashion to the method of images calculation. The resulting electric field is shown in Figure 6.4. The electrical field energy was integrated across the modelled domain.
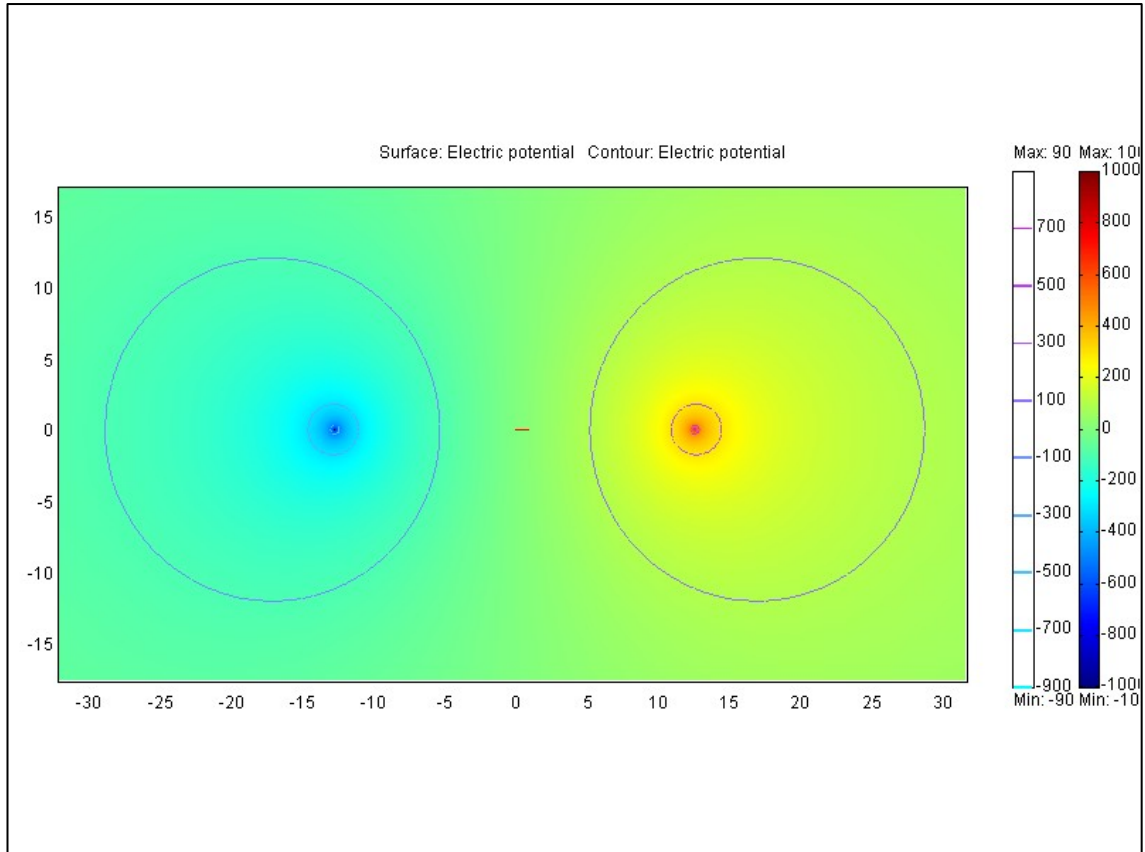
Figure 6.4 - femlab Electric Field Plot

The electric energy density was integrated across the entire domain to calculate the entire energy. The resulting energy inside the domain is 6.33×10^{-4} Joules. The resulting capacitance between the two lines is calculated using

$$U \quad = \quad \frac{1}{2}CV^2$$

Where U = Energy in the modelled domain

C = Capacitance between the two conductors

V = Voltage between the conductors

$$C \quad = \quad \frac{2U}{V^2}$$

$$= \quad \frac{2 \times 6.33 \times 10^{-4}}{20000^2}$$

$$= \quad 3.165\text{x}10^{-12} \text{ F/m}$$

The phase to neutral capacitance is twice that of the calculated.

$$= \quad 6.3309 \text{ nF/km}$$

Both the stranded conductor and the representative single conductor have been modelled using Femlab®. The solid conductor is shown in Figure 6.5, the stranded conductor geometry in Figure 6.6.
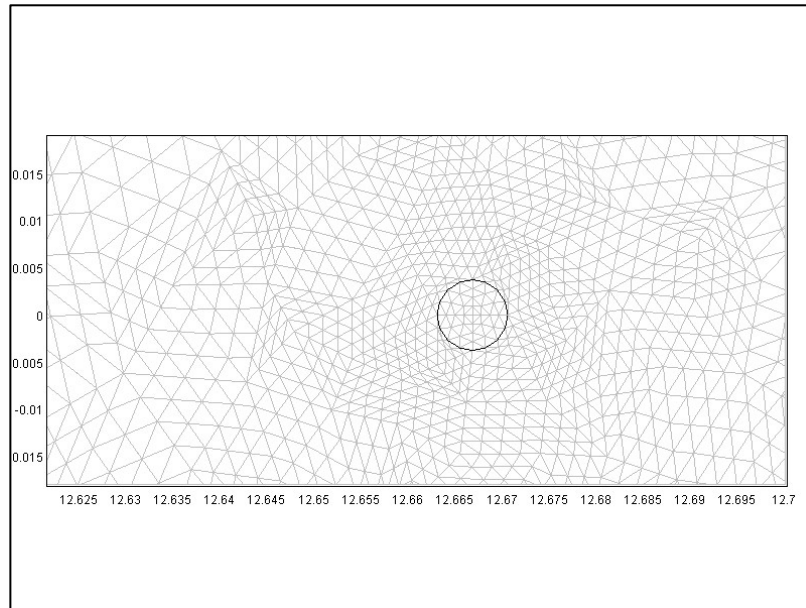
Figure 6.5 - Solid Conductor Geometry
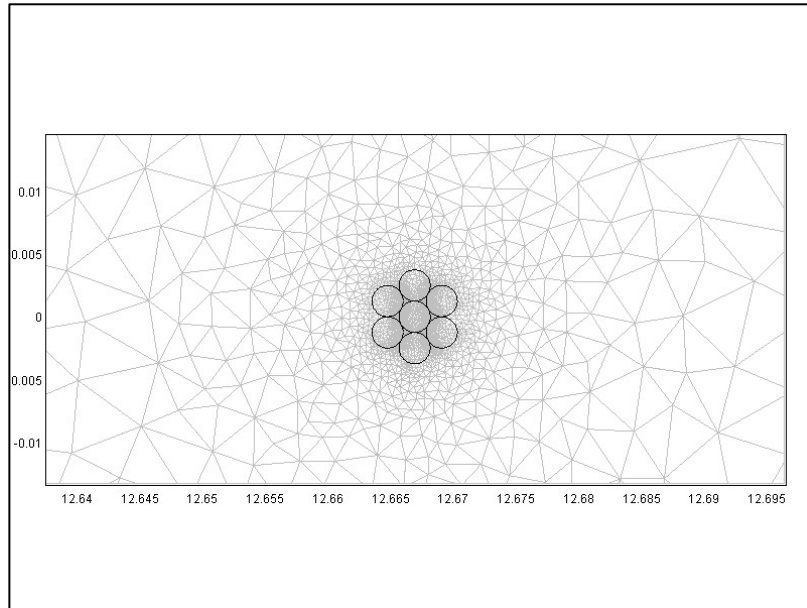
Figure 6.6 - Stranded Conductor Geometry

6.2.4 ATP Line Capacitance Calculation

The Alternative Transients Program was used to ensure that the expected values of capacitance calculated by hand and with Femlab® agreed. Constant voltages with varying frequency were applied to a line that only coupled to earth through its capacitance. The line length was kept to a value that would allow the application to run with a time step that produced a reasonable amount of results. The circuit used for modelling is shown in Figure 6.7.
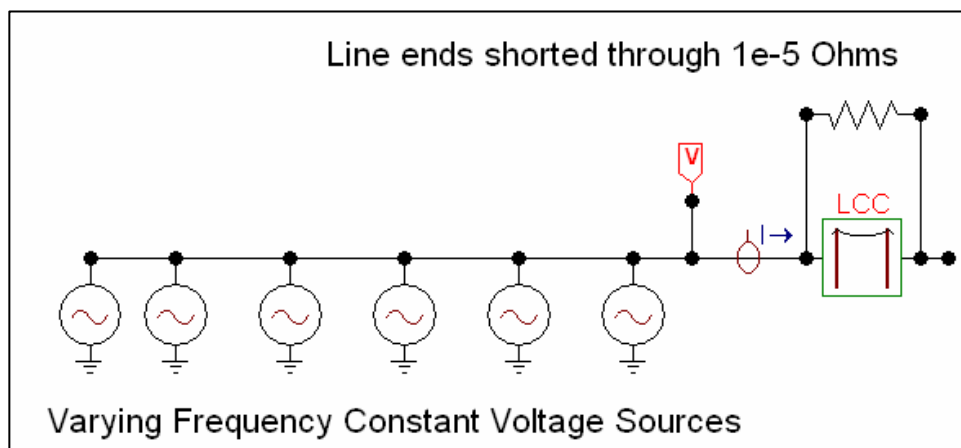
Figure 6.7 - ATP Model for Capacitance Validation
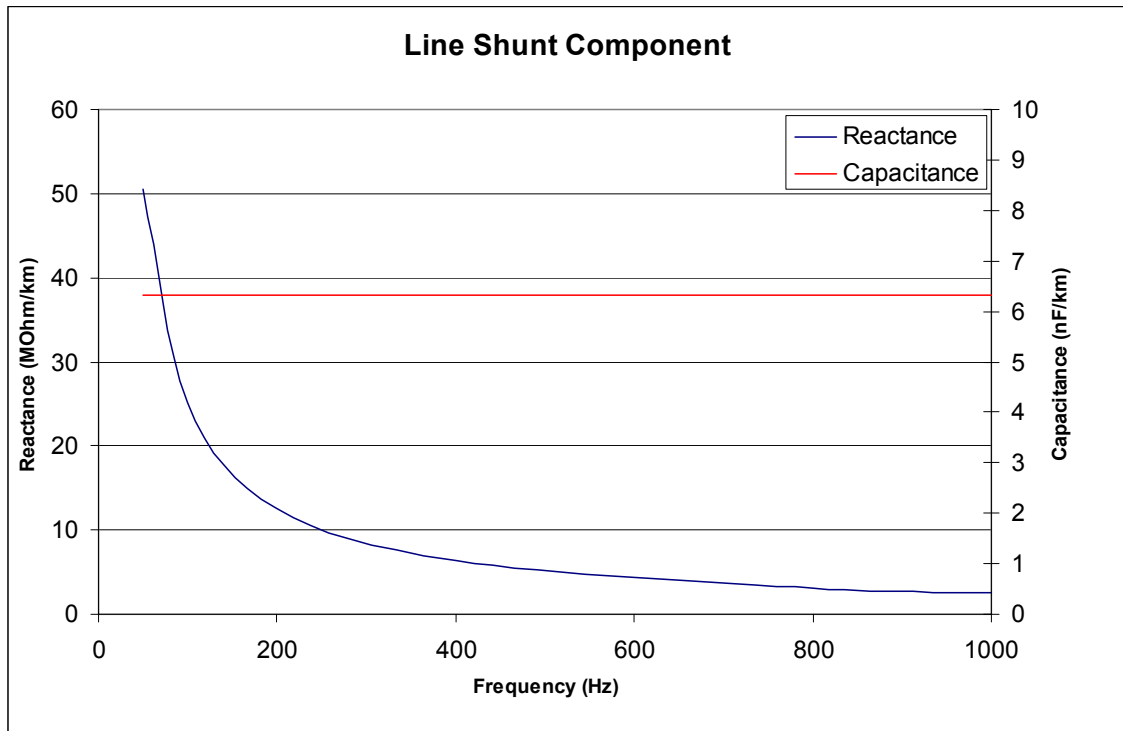
Figure 6.8 - ATP Line Capacitance Test Output

The results from ATP have included a swept frequency analysis (Figure 6.8). The capacitive reactance drops with an increasing frequency. The Line shunt capacitance remains constant through out the range of the test. The calculated capacitance value is in agreement with both the hand calculation and the Femlab® conductor model.

The ATP testing for capacitance has been arranged so that the distributed parameter line model does not affect the calculation of capacitance using measured current and voltage. This has been achieved by making the line section sufficiently small and shorting the line ends together. This technique approximates a lumped parameter model.

6.3   Line Inductance and Resistance

The line Inductance values were calculated three separate ways in order to identify the most suitable line model for the arcing study. Using Carson's equations the line impedance was calculated using MathCAD® for frequencies ranging from 50 to 1000Hz. Secondly the line was modelled in ATP using the Bergeron Line model that is not frequency dependant and uses the values calculated at a used defined frequency. In this case 50Hz was selected as the base frequency. Finally an attempt was made to use a frequency dependant line model. The frequency dependant model selected was the Semlyen option.

73

The comparison of line inductance and resistance has been carried below using a line that has three strands with the reinforcing steel section removed. The conductor is the same geometry as that shown in Figure 4.1.

6.3.1 Carson's Line Equations

Initially the line resistance and reactance values were calculated using the formulas outlined in the ATP Rule Book Line Constants section. The formulas repeated here for convenience are:

$$R = \left(R_{ii} + \Delta R_{ii}\right)$$

Where R_{ii} = DC Resistance

ΔR_{ii} = Correction factor for ground return (Outline in Appendix B)

$$X = \left(2\omega \times 10^{-4} \times \ln\left(\frac{2h}{GMR}\right) + \Delta X_{ii}\right)$$

Where h = Height of Conductor above earth

ΔX_{ii} = Correction factor for ground return (Outline in Appendix B)

The correction factors ΔR_{ii} and ΔX_{ii} were calculated using an expansion of Carson's Equations. ATP uses Carson's equations up to the 20th term for evaluation of the line impedance. The first 8 terms of the series are detailed in the ATP Line Constants Rule Book extension of the equations is carried out to the 20th term. This expansion is outlined in Appendix B.

6.3.2 Bergeron and Semlyen Line Options

Bergeron is the default line model selected when running ATP's LCC device. Bergeron calculates the line parameters at a given frequency. The line parameters are the applied to the entire range of frequencies of the study. Semlyen is a frequency dependent model that is calculated between a user input steady state frequency and a specified dominant frequency matrix. The dominant frequency matrix is selected to be at a point of interest to the user. In this study the dominant matrix has been selected to be the upper limit of the range of considered frequencies (1000Hz).

The test circuit used to model the Bergeron and Semlyen line types is shown Figure 6.9. Multiple constant current sources were connected to a 1km section of line that was shorted to earth through a 0.0001Ω impedance. Each current source was run for 200ms with the voltage across the line and the current through the line being monitored. One cycle of data was exported to Microsoft Office Excel ®. From this data the RMS Voltage, RMS Current, Power, VA, Resistance and Reactance were calculated.
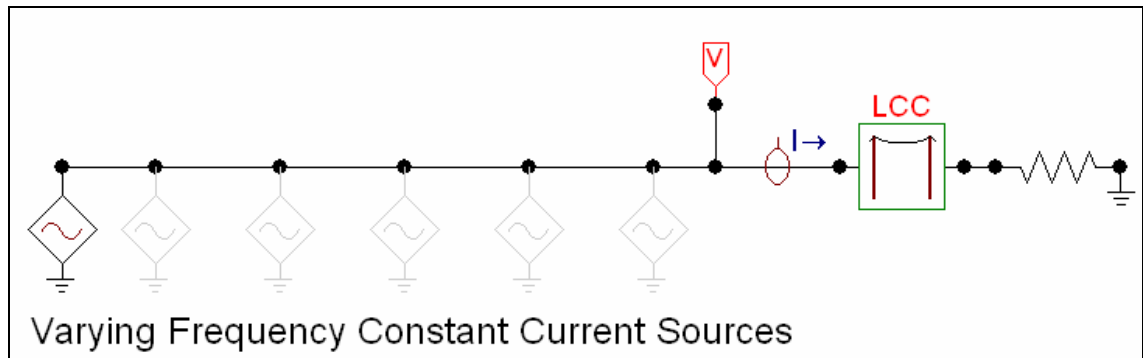
Figure 6.9- ATP Circuit for Line Parameter Testing

Figure 6.10 shows the results for the line reactance for all three calculation methods. Using the reactance calculated with Carson's equations as a reference the Bergeron method can be seen too give an overestimation by about 11.36% of the inductive reactance at 1000Hz. Both the Semlyen and Carson method tend to agree at the higher end of frequencies of this study. The Semylen result is tending closer to the value calculated manually using Carson's equation. Table 6.2 shows the percentage difference from Carson's equation for the considered models.

Table 6.2 - Inductive Reactance Comparison

Frequency Hz	Semylen	Bergeron
50	-32.73%	0.97%
100	-4.20%	-1.64%
200	3.30%	-4.46%
400	3.47%	-7.34%
800	1.51%	-10.36%
1000	0.72%	-11.36%
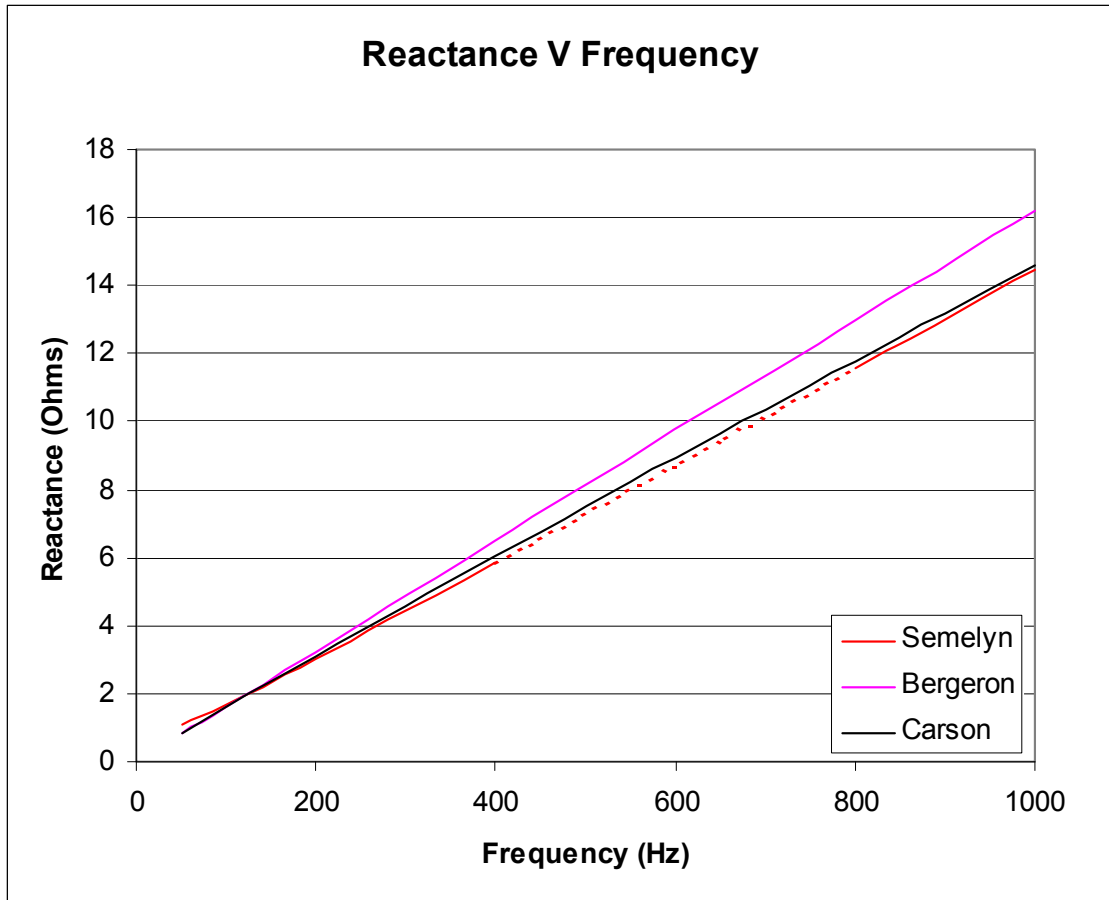
Figure 6.10 - Reactance Calculations (Ohms per km)

The skin depth of aluminium conductor has been plotted against frequency.

$$\delta_S = \sqrt{\frac{2}{2\pi f \times \mu \times \sigma}}$$

Where δ_S = Skin Depth in Meters

μ = Permeability

σ = Conductivity or the Material

Using the permeability of free space ($4\pi x 10^7$) as the conductor type is non magnetic. With a conductivity of $3.44 x 10^7$ Ohm meters the skin depth has been plotted in Figure 6.11. It can be seen that the depth of penetration at the upper frequency limit of 1000Hz is 2.714mm and is greater than the conductor radius of 1.25mm for stranded conductors.

The depth of penetration at frequencies above 500Hz is above the radius of 3.75mm for the solid conductor and we would expect a change in the resistance profile at 500Hz when we start to transition to depths of penetration above the conductor radius.
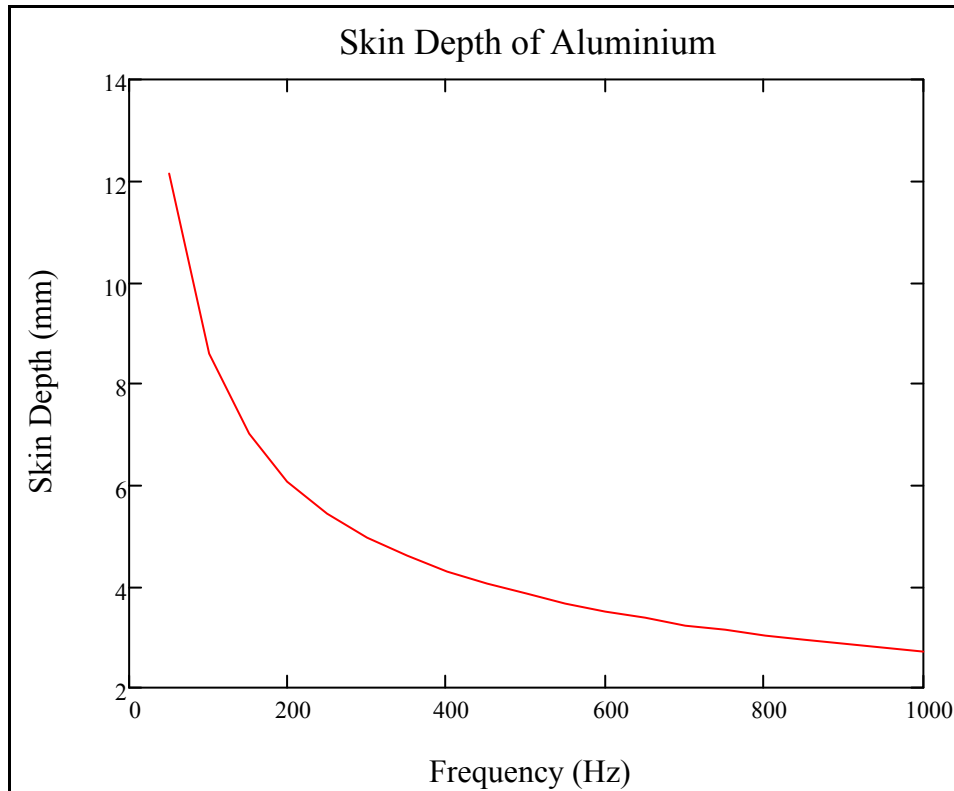
Figure 6.11 - Skin Depth against Frequency for Aluminium

Using the formulae

$$R(f) \quad = \quad \frac{\rho L}{A(f)}$$

Where

$$A(f) \quad = \quad \int_{RADIUS-\delta_s}^{RADIUS} 2\pi r dr$$

The lower boundary of the integral has been kept at zero until the depth of penetration is less than the radius of the conductor. In Figure 6.12 and 6.13 a plot of resistance against frequency for both the 1.25mm and 3.75mm conductors respectively. For the case of the stranded conductor the skin effect is expected to have a negligible effect and would increase at frequencies beyond the range of interest for this study. In the case of the solid conductor the resistance begins to increase at a lower frequency as the depth of penetration is less than the conductor radius at lower frequencies.
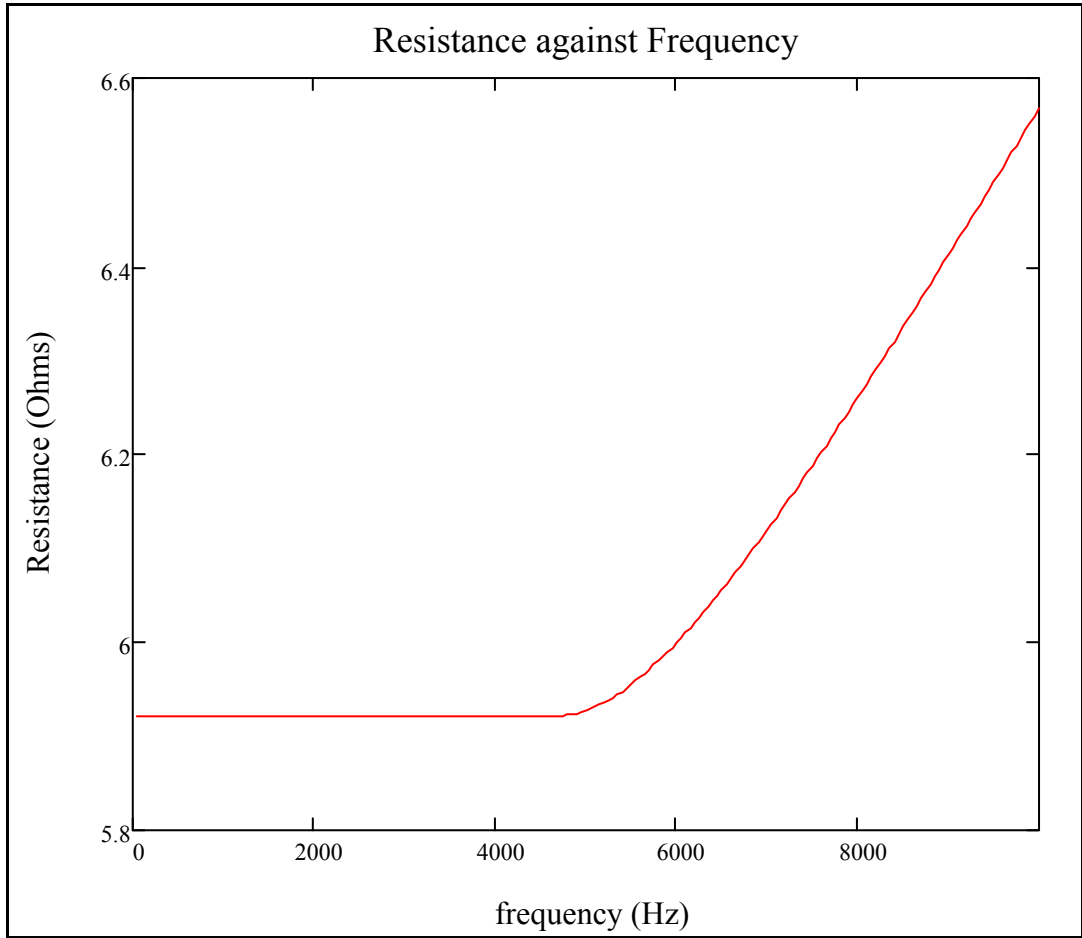
Figure 6.12 – Resistance against Frequency 1.25mm Radius Conductor
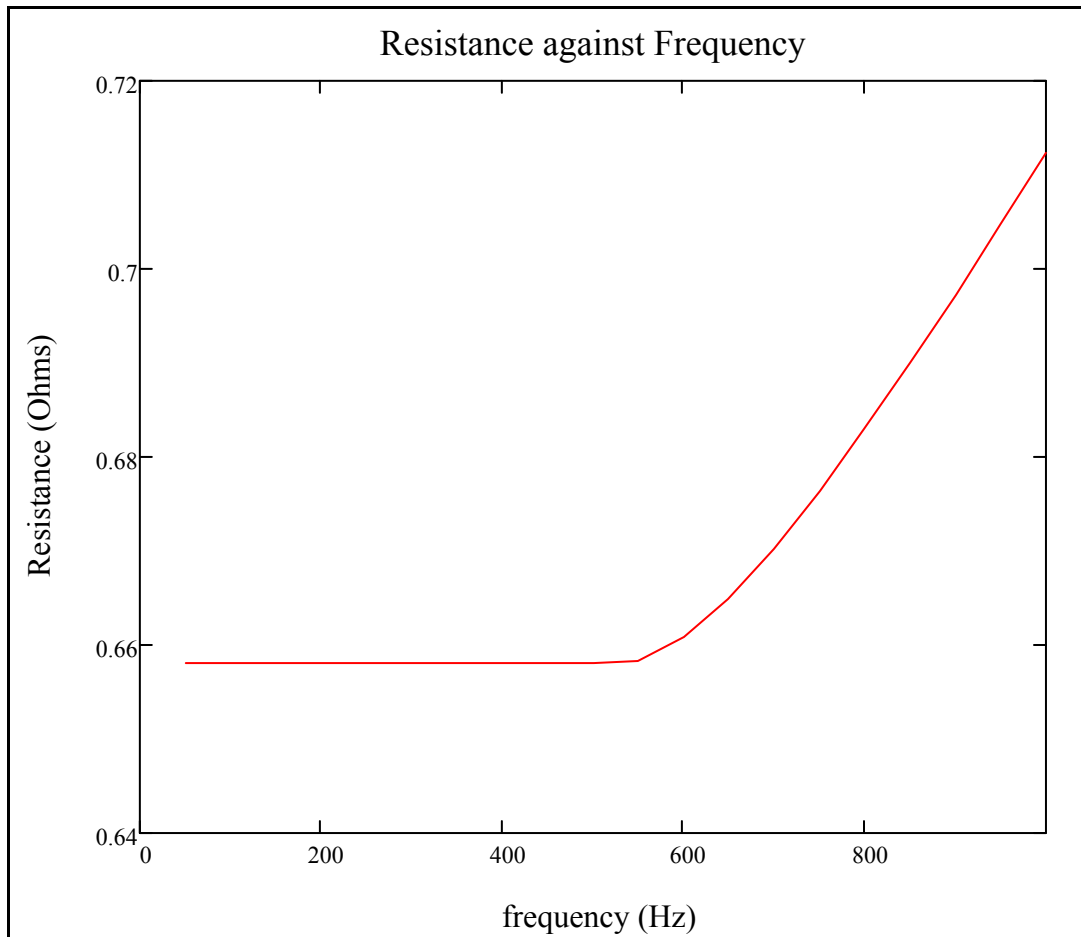
Figure 6.13 – Resistance against Frequency 3.75mm Radius Conductor

The ATP calculated resistance values are shown in Figure 6.14, the manual calculation using Carson's equations is shown in Figure 6.15. The calculated results do not show any consistency between one another. The expected outcome for the resistance component of the line models was:

Bergeron: Constant resistance in addition to a skin effect correction. Increasing slightly at high frequencies.

Semlyen: A resistance that increased as dictated by Carson's Equations in addition to a skin effect correction.

By inspection the Bergeron Model has a resistance value that is increasing as the system frequency is increases. The value appears to be increasing exponentially however the actual increase is only in the order of 800μΩ. This effect is due to the skin effect component. The Semlyen Model however has an increase of 250mΩ across the range of interest. The increase in resistance does not follow the values calculated by Carson's equations as depicted in Figure 6.15.
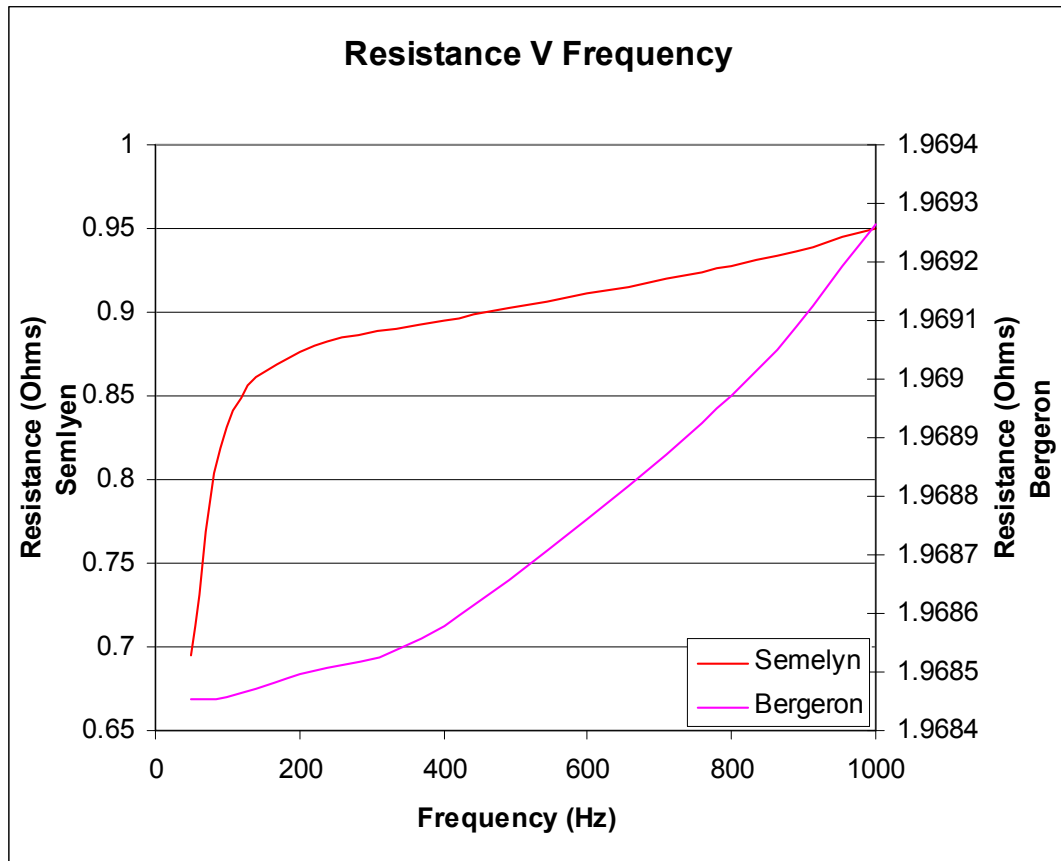
Figure 6.14 - Resistance against Frequency for Bergeron and Semlyen

Both lines approximate the DC resistance starting point. The Bergeron is one third the stranded conductor value. The Semlyen follows the staring point of the solid conductor. In this case the Semlyen model doe not follow the exponential increase as expected in Figure 6.13, for this reason the Bergeron model was selected.
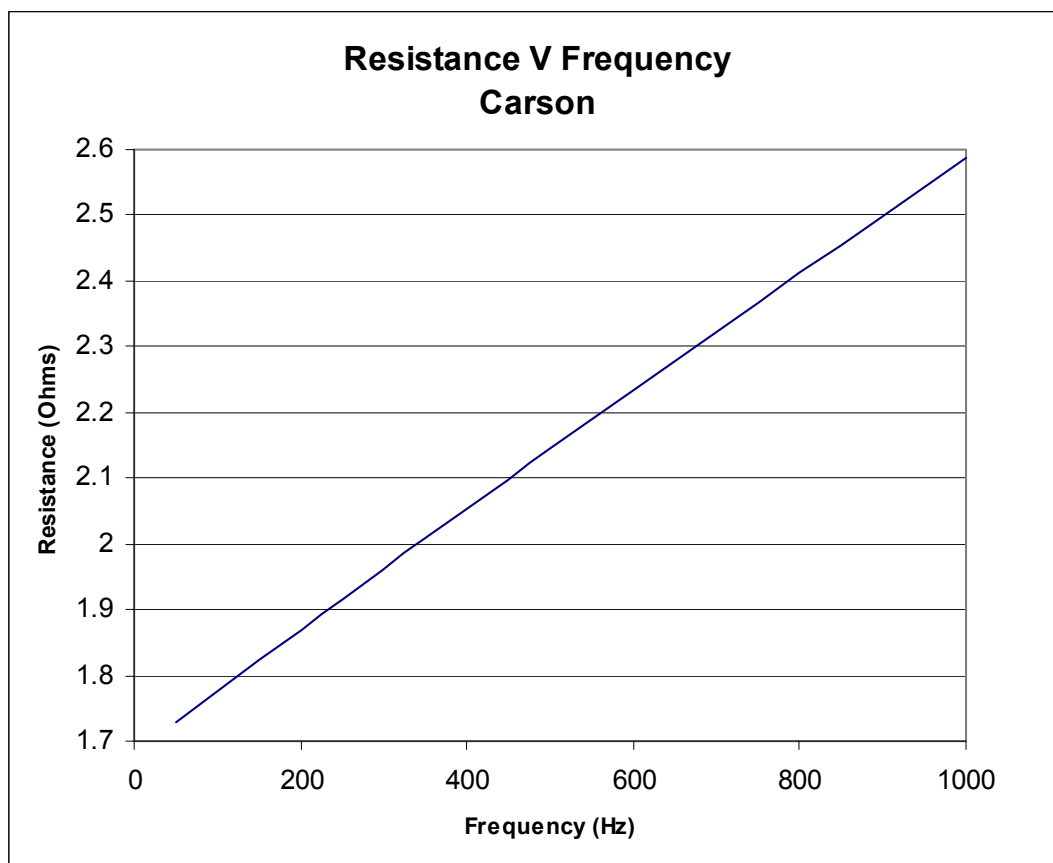
Figure 6.15 - Resistance against Frequency for Carson's Equation

6.3.3 Solid Conductor Model

The ATP model as depicted in Figure 6.9 has been used to compare the reactance and resistance values of a 1km section of line. Both line sections present a constant inductance throughout the frequency range of interest. The output for both line inductance and the resistance are tabulated and plotted below in Table 6.3, Figure 6.16 and Figure 6.17 below. Using the stranded conductor we have a higher reactance per unit length than the solid conductor. The model we have used does not include the effect of the steel conductor. The actual line impedance exists between the solid conductor and the stranded conductor model.

Table 6.3 - Stranded and Solid Conductor Impedances (Bergeron Model)

Frequency (Hz)	Stranded		Solid	
	Reactance (Ω)	Inductance (mH)	Reactance (Ω)	Inductance (mH)
50	0.811	2.582	0.575	1.831
100	1.622	2.582	1.151	1.831
200	3.244	2.582	2.301	1.831
400	6.489	2.582	4.603	1.831
800	12.979	2.582	9.206	1.832
1000	16.225	2.582	11.508	1.832
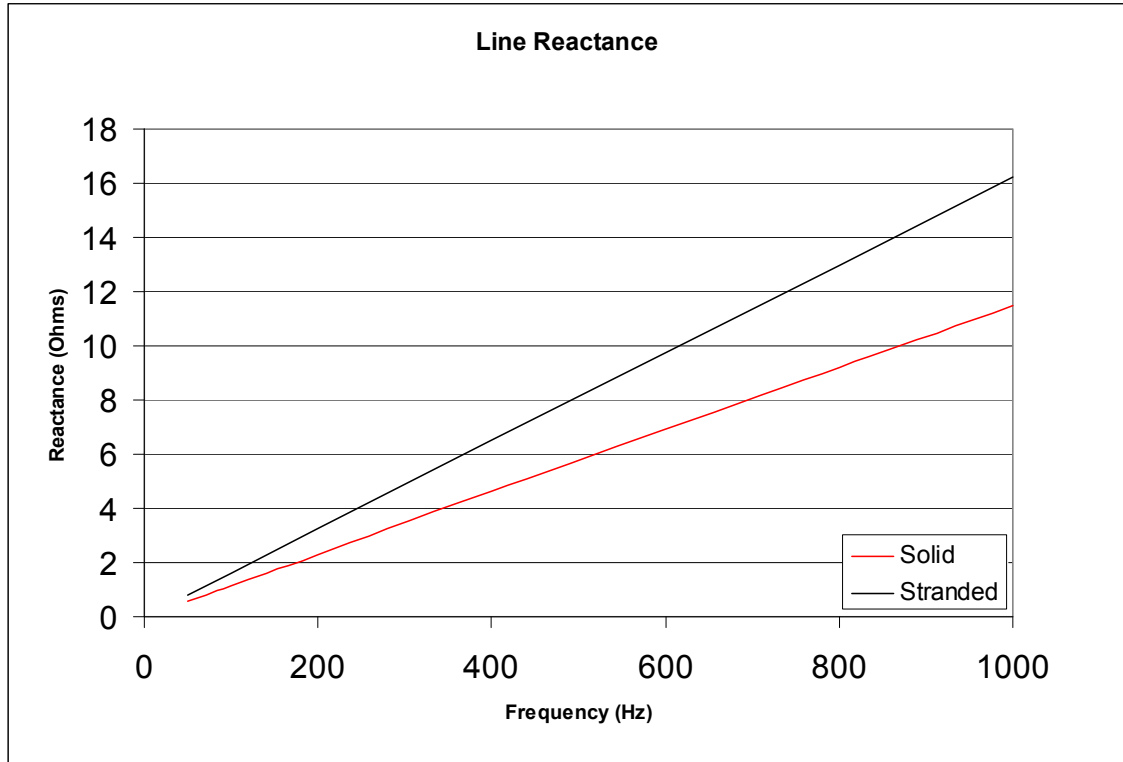
Figure 6.16 - Solid and Stranded Conductor Model Reactance

The conductor resistance for the stranded and solid conductor use two different starting points. 1.68Ω/km has been taken for the solid conductor as this value is published in the respective Australian standard for bare overhead conductor. The resistance for the three independent cores have been calculated as follows.

$$R \quad = \quad \frac{\rho l}{A}$$

Where ρ   =   Resistivity (for aluminium = 0.0283μΩ/m)

     l   =   Length

     A   =   Area in m^2

$$R \quad = \quad \frac{0.0283 \times 10^{-6} \times 1000}{\pi \times \left(\frac{1.25}{1000}\right)^2}$$

$$= 5.76\Omega/\text{km per strand}$$

In this application we have three strands and therefore we have 1/3 the calculated resistance 1.92Ω/km.
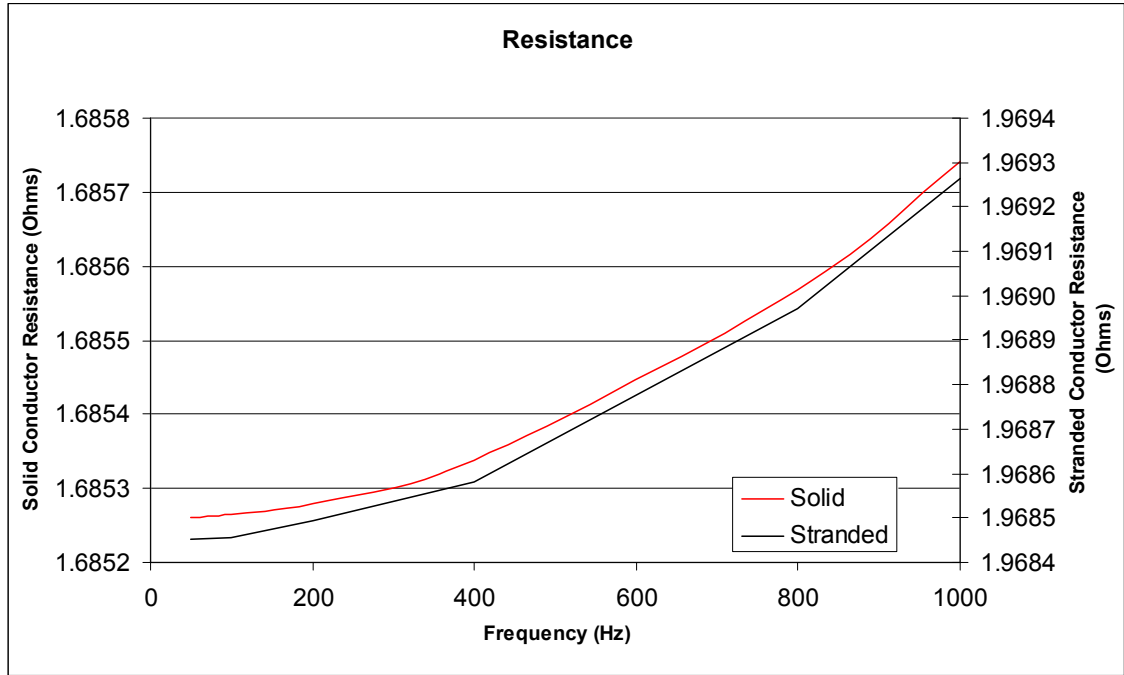
Figure 6.17 - Solid and Stranded Conductor Model Resistance

6.3.4 Steel Line Component

The 3/4/2.5 SCGZ line section was modelled in Femlab® in order to determine the ratio of current magnitudes between the Aluminium and Steel Strands throughout the frequency range of interest. The conductor was modelled in free air and the effect of the ground plane has been ignored. The results of the simulation are included in Figure 6.18. The results show that greater than 84% of the current travels through the aluminium strands despite the cross sectional area of the aluminium being only approximately 42% of the total area.
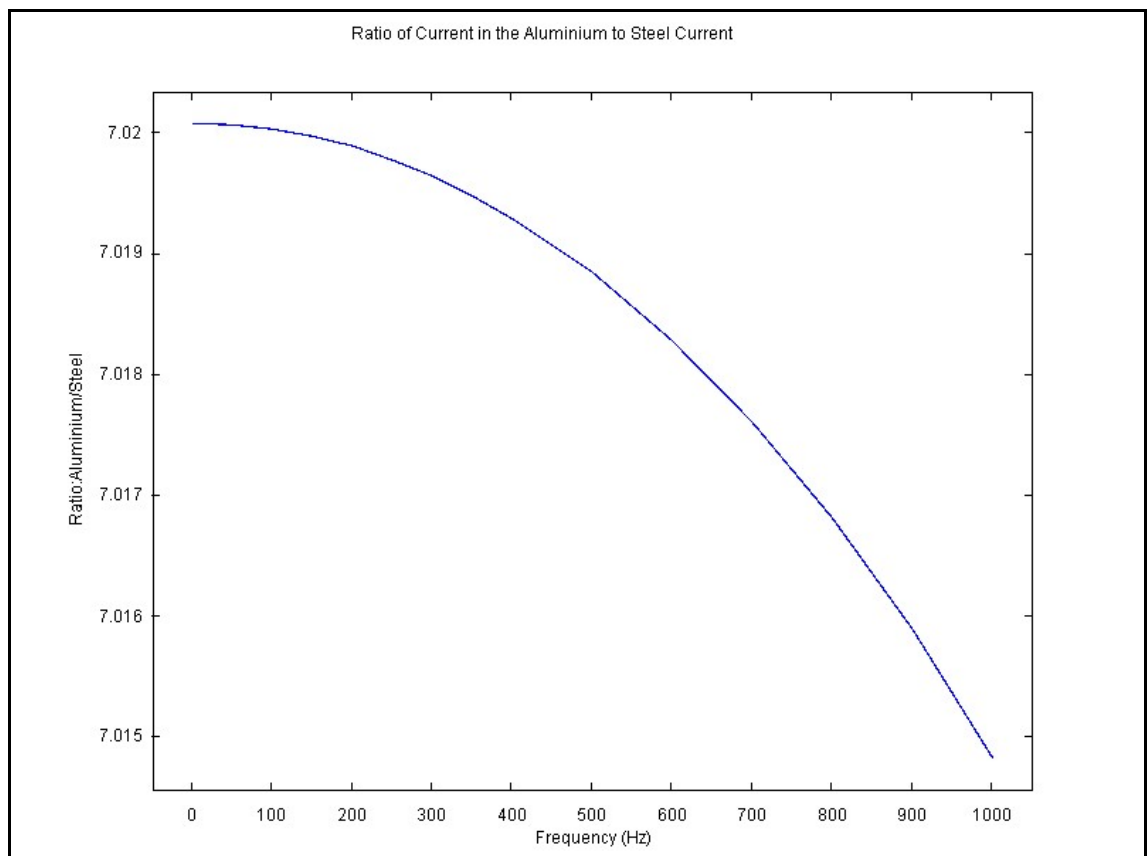
Figure 6.18 – Femlab® Conductor Model Aluminium to Steel Current Ratio

6.4 Summary

The general parameters that describe the performance of an overhead line have been investigated as part of this chapter. The line capacitance, inductance and resistance have been verified against third party techniques to aid in deciding on the appropriate line model that will be used for a SWER distribution model and specifically one that will be subjected to frequencies in the 50Hz to 1000Hz range.

The line capacitance has been verified using a method of images and a third party Femlab® application. The line capacitance in each case has matched the ATP output extremely accurately.

The line inductance was modelled in ATP in a similar manner to the line capacitance. By decreasing the line length to a value that was as short as practical the line inductance was able to be measured without creating sending end voltages that were high enough affect the results due to capacitive effects. Using the Bergeron line model the parameters are calculated by ATP at 50Hz and the parameters kept constant throughout the frequency range. The Bergeron method produced errors in the order of 11% at the upper frequency limit of 1000Hz. The Semylen method employs a correction factor for higher frequencies. In this case the higher end error was reduced when comparing to Carson's equation, however the 50Hz values presented large errors of 32%.

The resistance calculated from ATP does not follow the values calculated using Carson's equations for either the Bergeron or the Semlyen models. In an attempt to validate the model the resistance against skin depth has been used. Using skin depth the resistance of the conductors remains constant up to a point where the depth of penetration is less than the conductor radius. This occurred at 500Hz and 5000Hz for the 1.25mm and 3.73mm conductors respectively. The Bergeron model showed a slight increase at values below 1000Hz but provided a more reasonable approximation to the resistance calculated in Figure 6.12 and 6.13.

The stranded conductors were compared against a solid conductor. For the case of the stranded conductor it was found that the majority of the current (84%) was carried in the aluminium strands instead of the steel reinforcing. Omitting the steel was a solution as the application did not facilitate hybrid aluminium/steel conductors. Comparing the stranded conductors against the solid conductor in terms of inductive reactance gives an 18% increase in the inductive reactance per unit length at 1000Hz. When this reactance is included with the transformer reactance at 1000Hz from Table 5.4 we have in increase in the total inductive reactance of the system of 3.3% for a 15km line or 12% for a 150km line. The output of the system model is in Table 7.2 below, in this it is shown that the high frequency components still exist at high frequencies.

For this application it is believed that the Bergeron model provides an output that is physically sensible and will produce results that are indicative of what will occur on the primary system.

Chapter 7

Relay Performance

7.1 Overview

At this point in time two protection relays exist on the market for detecting high impedance faults The GE F60 and the Schweitzer Engineering Laboratories SEL451. Both relay have proprietary protection elements that are designed to detect, indicate and depending on the user configuration disconnect the power system.

7.2 GE F60

7.2.1 Overview

The F60 relay produced by GE-Multilin is one of two relays that is a commercially available product for detecting high impedance earth faults. The relay employs multiple algorithms which run in parallel in an attempt to detect high impedance faults with confidence.

With application of this relay to a Single Wire System (SWER) the elements of the high impedance monitor have been assessed as application critical or application non critical. Application critical elements are elements that have the potential to make a decision which is conveyed to the user. Application non critical elements are elements that are do not influence the relay performance.

Application non critical monitoring functions:

- Arc Burst Pattern Analysis Algorithm

- Even Harmonic Restraint Algorithm

- Voltage Supervision Algorithm

- Load Extraction Algorithm

- Load Analysis Algorithm

- Load Event Detector Algorithm

Application critical monitoring functions:

- Energy Algorithm

- Randomness Algorithm

- Expert Arc Detector Algorithm

- Spectral Analysis Algorithm

- Arcing-Suspected Identifier Algorithm

7.2.2 Application Non-Critical Functions

The **arc burst pattern analysis algorithm** is used to correlate the arcing information of a phase with that in the power system neutral. Application of the relay to single wire system with no phase connection eliminates the requirements of this algorithm.

The **Even harmonic restraint algorithm** measures the 2nd harmonic content in the phase currents and is used to inhibit starting of the high impedance element in the event of an inrush condition associated with energising of plant. The relay is not intended to be connected to a phase element so the operation of the element is inhibited by wiring and will not impact on the performance in this application.

Voltage supervision algorithm is not enabled by virtue of the fact that no voltage connection is intended to be made to the relay. The voltage supervision element monitors voltage dips on the power system that may be associated with faults on adjacent feeders. Assertion of this element will inhibit the high impedance function. The element can be inhibited by setting selection. As no VT connection is intended in the application testing is carried out without this bus supervision in operation.

Load extraction algorithm is used to remove the normal neutral current from the arcing current before application of the arc data to the arc burst algorithm. No details are provided about the operation of this element and how is determines the quiescent state to identify the load current in the neutral.

Load analysis algorithm attempts to define if a loss of load has occurred or and overcurrent asserted at the moment that an arc event develops. This load analysis will use the information to determine if the conductor is intact or likely to have disconnected downstream load. Disconnecting downstream load at the initiation of the arcing event is used as an indication that the conductor is downed (come in contact with ground).

Load Event Detector Algorithm is used to reset the expert arc detection algorithm based on five conditions from the instruction manual that are listed below.

- overcurrent condition

- precipitous loss of load

- high rate-of-change

- significant three-phase event

- breaker open condition.

Each of these conditions are indications that the power system is undergoing change and are used to inhibit the relays arc algorithm as the event is probably not an arcing event.

7.2.3 Application Critical Functions

Energy algorithm monitors the energy content in the odd, even and interharmonic components of the measured phase and neutral currents. The algorithm monitors each of the three components for a sudden, sustained increase and then reports this to the expert arc detection algorithm.

The **randomness algorithm** monitors the same odd, even and interharmonic components that the energy algorithm above monitors. Once a sustained increase has occurred the relay monitors the spectral energy components for an erratic behaviour indicative of an arcing condition.

The **expert arc detector algorithm** is used to consolidate the results from all of the individual phase and neutral arcing elements. This element identifies the arcing element that have asserted and the number of assertions from each element to determine the relay response.

The **spectral analysis algorithm** is used to increase the arcing suspected result by 3% in the event that comparison of the 5 second averaged non harmonic residual current data with a 1/frequency curve gives a positive result. This element is based on the arcing suspected element and not the arcing detected element. The project is aimed at positive detection and ideally will not rely on assertion of this element as part of the initial assessment. The spectral components from the models and the arc tests are shown in table 7.1 below. The interharmonics are not present in the modelled waveforms. Arc 2 has small interharmonic contents that do not follow the 1/f curve exactly, however they

are present. The section of the waveform analysed from arc 2 was that from 70ms to 110ms in Figure 3.7. The waveform at no time is constant between two cycles however 70ms to 110ms had the least variation. The cycle by cycle magnitude variation is believed to be the major cause of the interharmonic content.

The **arcing-suspected identifier algorithm** is used to account for repeated low level events that do not warrant an operator taking action. In events where repeated momentary contact with a line from a tree branch for example will not result in a sustained level of harmonic (or interharmonic) content. In these cases a reset timer is used to allow for cumulative events to be classified as a feeder or line segment for investigation.

7.2.4 F60 Configuration for Testing

The GE Relay Settings employed for the study are detailed in Table 7.1 and are explained below.

Table 7.1 – GE F60 Settings for Testing

Setting Name	Setting Value
Signal Source	SRC 2 (SRC 2)
Arcing Sensitivity	10
Arcing Detected Reset Time	2.5 sec
Phase Event Count	30
Ground Event Count	30
Event Count Time	15 min
OC Protection Coord Timeout	10 s
Phase OC Min Pickup	10.0 pu
Neutral OC Min Pickup	10.0 pu
Phase Rate of Change	150-999 A/2cycle
Neutral Rate of Change	150-999 A/2cycle
Loss of Load Threshold	15%
3-Phase Event Threshold	25 A
Voltage Supv Threshold	0%
Voltage Supv Delay	60 cycles
Even Harmonic Restraint	50%

Signal Source - This setting defines the Current and Voltage transformer module that includes the DSP card for monitoring of high impedance faults. In the application here it has been allocated to Source 2.

Arcing Sensitivity - has been set to the most sensitive setting that is available in the relay. To ensure trouble free operation the set the setting will be installed on its most sensitive and reduced if it is found that background signals that exist on the feeder cause unwanted operation.

Arcing Detected Reset Time – This setting does not impact on the operation of the relays detection algorithm. The setting defines the time that needs to elapse after an arcing event has been written to the sequence of event recorder before a subsequent event is written as an independent event. This setting has been set to 0 so that each time the relay declares an arc event it is traceable in the fault record.

Phase Event Count – The arcing suspected alarm for phase elements can be made more sensitive by decreasing the Phase Event Count. The relay manufacturer allows the user to adjust the number of belief in arcing counts before an indication is given. The phase element is not used in this application. The manufacturer default setting of 30 has been maintained in this application.

Ground Event Count - The arcing suspected alarm for neutral elements can be made more sensitive by decreasing the Ground Event Count. The relay manufacturer allows the user to adjust the number of belief in arcing counts before an indication is given. The phase element is not used in this application. The manufacturer default setting of 30 has been maintained in this application

OC Protection Coord Time – This is the guaranteed minimum time that the high impedance protection will wait before issuing a trip or an alarm indication. This setting is intended to ensure that conventional protection elements like phase overcurrent, earth fault and sensitive earth fault have time to operate. Ergon Energy Employs Sensitive Earth Fault Protection on its distribution feeders with 8A, 8 second operating characteristics. On SWER feeders definite maximum time settings are employed for low level faults with long clearing times. It is believed that 8A, 8 seconds is a practical maximum operating time for feeder protection. The minimum available OC Protection Coord Time setting is 10 seconds. The minimum setting of 10 seconds has been applied in this case.

Phase OC Min Pickup – The phase overcurrent minimum pickup defines the phase current that once exceeded will inhibit operation of the high impedance arc detection algorithm. For testing purposes this setting has been set to the maximum value of 10pu. This corresponds to10A when injecting in the relays 1A input or 50A when injecting in the 5A input. For normal operation this setting would be set to a value not less than the user defined IDMT (Inverse Definite Minimum Time) over current pickup.

Neutral OC Min Pickup - The Neutral overcurrent minimum pickup defines the Neutral current that once exceeded will inhibit operation of the high impedance arc detection algorithm. For testing purposes this setting has been set to the maximum value

of 10pu. This corresponds to 10A when injecting in the relays 1A input or 50A when injecting in the 5A input. For normal operation this setting would be set to a value not less than the user defined IDMT (Inverse Definite Minimum Time) neutral over current pickup.

Phase Rate of Change – The phase rate of change is used to distinguish between switching events and high impedance arcing events. The phase element is not wired for SWER systems. Therefore this setting has been left at the recommended manufacturer setting of 150A primary.

Neutral Rate of Change – When the rate of change of current over a two cycle period is in excess of the Neutral Rate of Change setting the relay will inhibit the high impedance arcing protection. The high rate of change setting is selected to distinguish the difference between a switching event and a high impedance arcing event. The manufacture recommends that this setting is left at the default of 150A/2cyc. Testing will be carried out to determine the maximum setting that can be employed without nuisance operation and indications.

Loss of Load Threshold – This setting is used to determine a downed conductor by monitoring the phase currents. When a phase current decreases by the percentage defined in this setting for two successive two cycle intervals the relay will declare a loss of load event. The percentage decrease is based on the average measured phase current prior to the fault. This element makes the assumption that the load has decreased as a result of the network failure. This would generally be indicative of a line break. For SWER networks the power system current transformer is not intended to be connected to a relay phase input. For this reason the default setting to 10% has been maintained.

3 Phase Event Threshold – The relay declares a three phase event when the power system line currents increase by the 3 Phase Event Threshold. The manufacturer default (and recommended setting) is 25A. The relay for SWER applications has not access to three phase signal sources. This effectively disables the setting, the manufacturers setting will be left at its default value of 35A for this application.

Voltage Supv Threshold – Voltage supervision is associated with the relays Loss of Load Algorithm. When a piece of plant is subject to a fault, the corresponding reduction in system voltage has the potential to reduce the current measured on the unfaulted feeders fed from the same busbar. The Voltage Supv Threshold is used to inhibit the loss of load alarm in these instances. As the relay is not wired so that the Loss of Load

Alarm can operate, the Voltage Supervision Threshold has been set to 0 so that it is effectively disabled.

Voltage Supv Delay – Voltage Supv Delay is not used in this case as the voltage supervision threshold above has been disabled.

Even Harmonic Restraint – Harmonic restraint is a traditional technique used to make protection relays insensitive to the overcurrent that is associated with the energisation of transformers. For the initial testing the setting will be set to 50% of the RMS current. This means that when the measured even harmonic components exceed the Calculated RMS current we will inhibit the high impedance protection. In this arrangement the phase currents are not intended to being monitored and the setting should not impact on the monitored waveform.

7.2.5   GE F60 Relay Response

The GE relay had two types of waveforms created and replayed in an attempt to have positive identification of a high impedance power system fault. The models only varied in line length, the first being 15km and the second being 150km. The choice of line lengths was based on a practical minimum and a line of sufficient length to allow an observable resonance or ringing to be created. As the model determined the arcing flash points stochastically multiple model outputs were made for each selected line length.

The system model was run and sampled at 50kHz to ensure that time step was less than the propagation time of the distributed parameter line that was being modelled. This would allow line lengths as short as 1km to be modelled as required. A healthy power system was created by placing a resistive load at the end of the feeder for 30 second prior to the arcing event. The arcing model was then switched so as it was in parallel with the existing load.

Before playback the modelled waveforms were re-sampled to 10kHz as this is the maximum frequency that the Doble F6 power system simulator and Transwin3 software would operate with.

In all cases the relay failed to indicate a power system event was present. The relays arcing confidence indicator was observed during the replayed faults. With the fault being run multiple times the arcing confidence indicator only reached a level of 8% indicating that the relays signature based detection algorithm was not convinced that there was a legitimate event.

7.2.6   Analysis of Measured Values

An FFT of the developed models and laboratory test for arc 2 has been carried out. The developed arc models comprise of fundamental plus predominantly odd harmonics there after. The 15km Line and the Arc 2 have arc harmonic content that is a similar percentage of the fundamental. This similarity agrees with the analysis of the SEL relay in section 7.32 below where the 15km line would appear to be easier to detect due to the rapid cumulative error summation. The 150km line harmonic content up to the 15th harmonic is generally a few percent higher that the actual arc (ARC2) and the 15km line. The results are summarised in Table 7.2 and Figure 7.1

Table 7.2 - FFT of Arc and Arc Model

| Frequency (Hz)	DFT Peak Magnitude (A)		
	15km Line	150km Line	Arc2
25	0.001	0.001	0.214
50	14.282	3.368	12.389
75	0.000	0.000	0.137
100	0.018	0.010	0.117
125	0.000	0.000	0.075
150	1.069	0.420	0.979
175	0.000	0.000	0.061
200	0.003	0.001	0.029
225	0.000	0.000	0.035
250	0.385	0.173	0.290
275	0.000	0.000	0.038
300	0.001	0.001	0.025
325	0.000	0.000	0.026
350	0.192	0.102	0.214
375	0.000	0.000	0.016
400	0.002	0.001	0.016
425	0.000	0.000	0.023
450	0.119	0.081	0.141
475	0.000	0.000	0.007
500	0.001	0.001	0.015
525	0.000	0.000	0.020
550	0.008	0.102	0.106
575	0.000	0.000	0.005
600	0.010	0.002	0.009
625	0.000	0.000	0.016
650	0.057	0.035	0.068
675	0.000	0.000	0.002
700	0.010	0.000	0.005
725	0.000	0.000	0.013
750	0.043	0.007	0.048
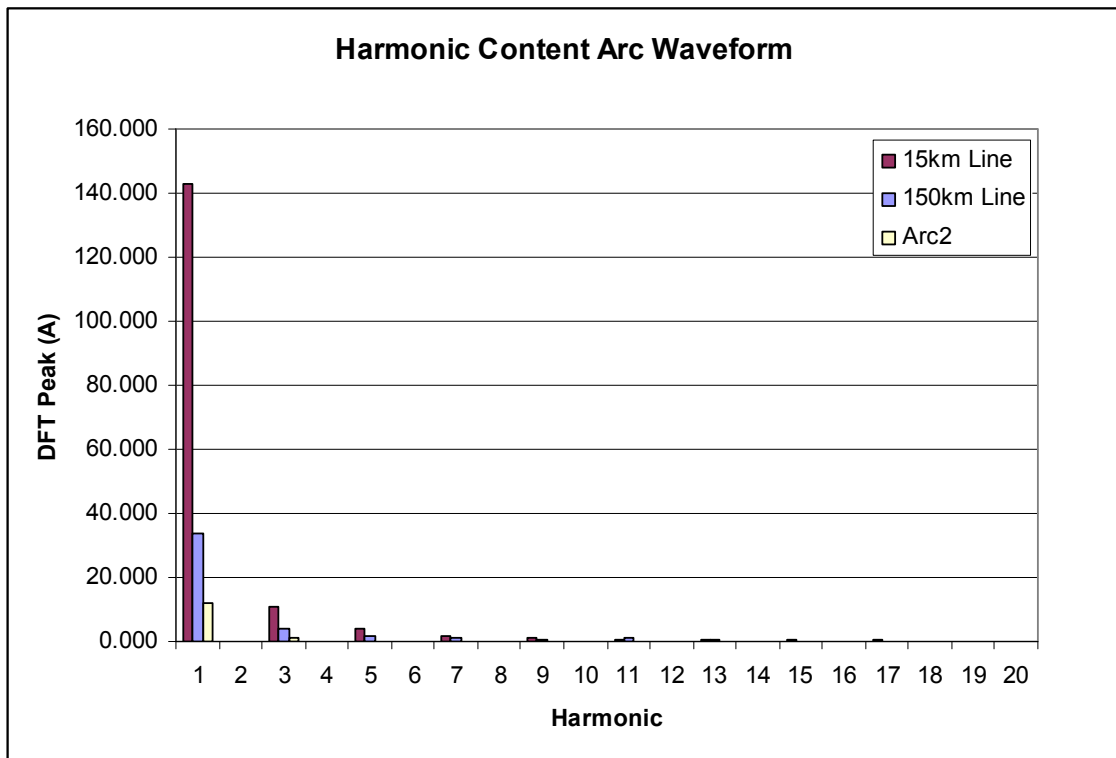
Figure 7.1 - ARC waveform harmonic content

7.3   Schweitzer Engineering Laboratories SEL451

7.3.1   Overview

Schweitzer has included a High Impedance Detection Algorithm in their SEL451 Relay. The element is described in Hou's (2007) Detection of High Impedance Faults is Power Distribution Systems . The relay uses a sum of difference currents to determine if a fault is present on the system. The difference current is calculated by subtracting the sampled phase current value now with one corresponding to once cycle ago. The calculated differences are stored in a cumulative counter and compare against the trended sum of difference currents.

7.3.2   Analysis of Measured Values

The longest available arc waveform from the arc testing results in section 3.3.3 has been analysed to determine if the Sum of Difference Currents existed throughout the arc period. The system primary current and the absolute value of the difference filter from the Arc2 waveform is shown in Figure 7.2. In the testing the arc was fully established after 20ms. The large transition of the one cycle difference current before 20ms is due to the inception of the fault and having no prior current. Inspection of the arc after this 20ms establishment period shows an output of the difference filter. Varying levels of

output from the difference filter occurs throughout the 20 to 170ms period due to minor variations in the waveform cycle by cycle.
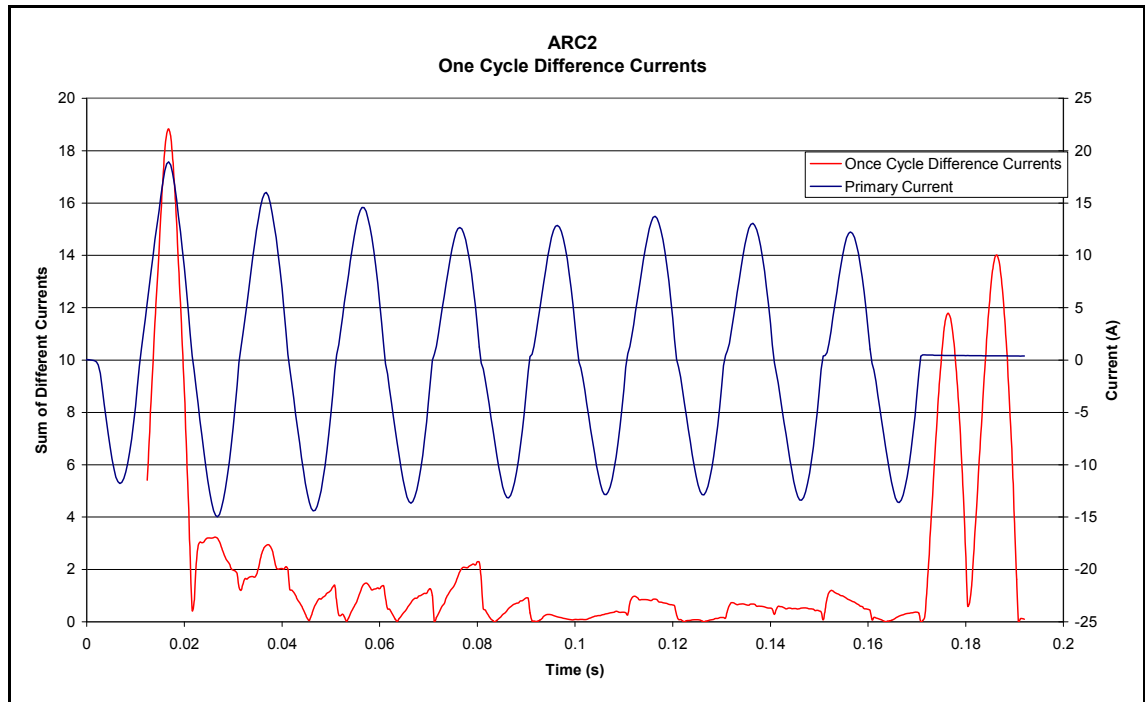
Figure 7.2 - ARC 2 Primary Current and One Cycle Difference Filter

The same output from the difference filter in Figure 7.2 is shown in Figure 7.3 along with the cumulative summation. The cumulative summation over several cycles is used to detect arcing faults. As the relay uses prefault loading conditions to modify the pickup it is not possible to show the actual threshold of detection on the same graph.
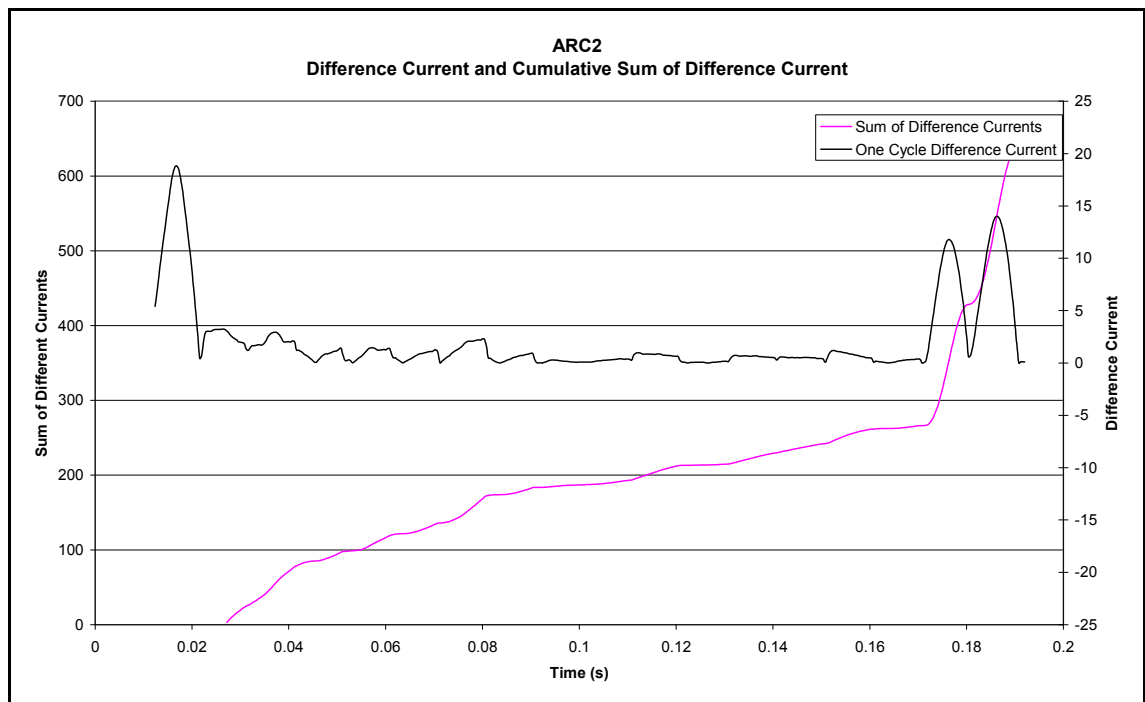
Figure 7.3 - ARC 2 One Cycle Difference Filter and Cumulative Summation

Below in Figure 7.4 and Figure 7.5 is a similar assessment of the model output. Prior to the fault inception the difference filter output is 0 as there is a comparison being made against an identical load cycle that occurred in the past. At fault inception two pulses of the difference filter occur due to the change in load current. After time 130ms the difference filter calculation is started and is continuously proving an output for the duration of the fault current. 130ms was selected as the starting time so that the large transitions that occur due to system switching are ignored. The omitted peaks are those in the initial part of the trace of one cycle difference currents shown in Figure 7.4. In Figure 7.5 we start a cumulative summation of the difference currents after the fault inception at 130ms. The increasing cumulative summation indicates that a measurable quantity is present; the effectiveness of the high impedance element to detect this is determined by the prefault system noise.
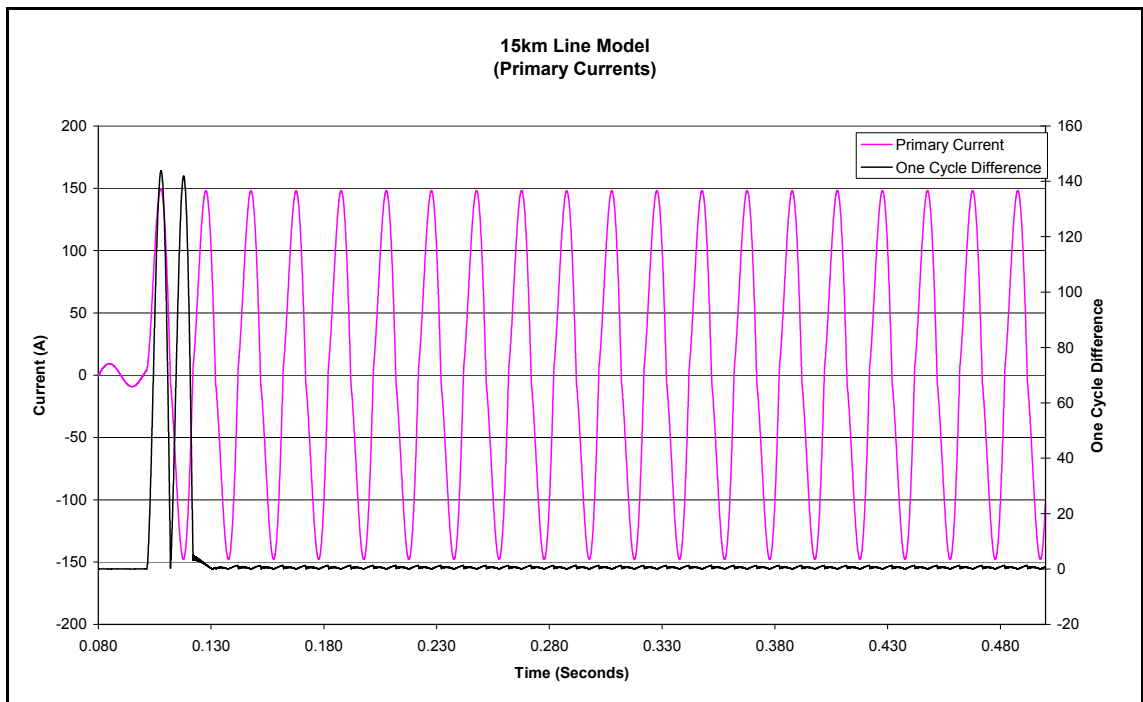
Figure 7.4- 15km Line Model Primary Current and Once Cycle Difference Filter
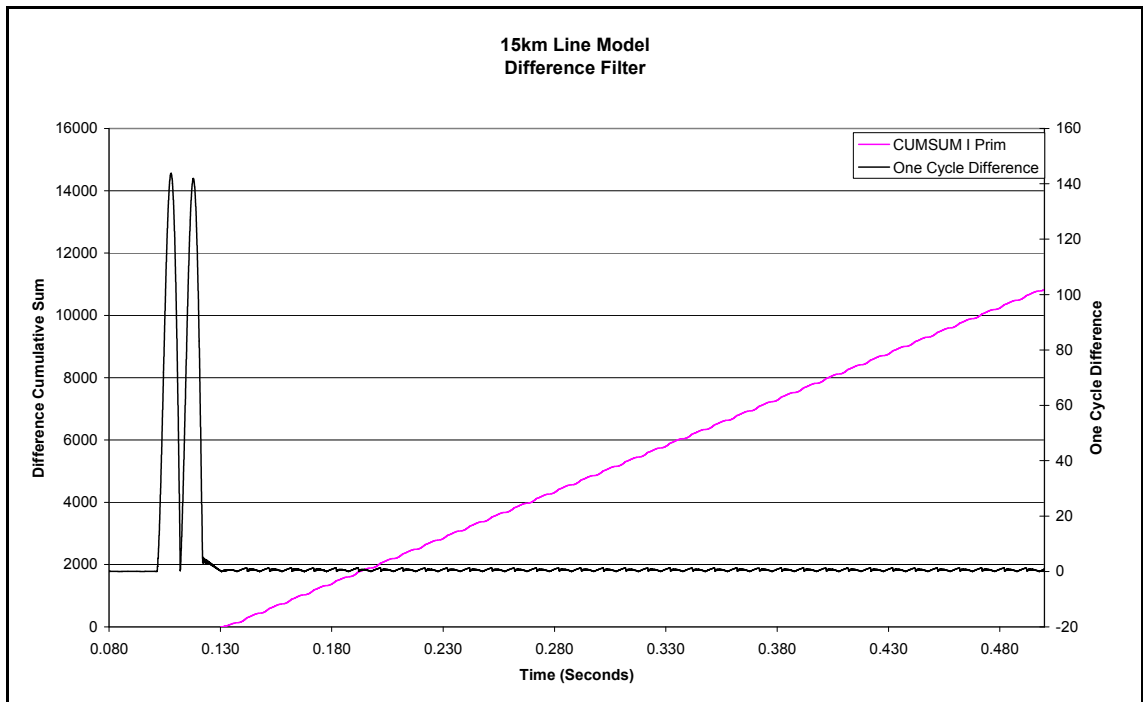
Figure 7.5 - 15km Line Model One Cycle Difference Filter and Cumulative Summation

A similar test was carried out using a 150km line model. The results of this evaluation are shown in Figure 7.6 and Figure 7.7. The current waveform distortion is higher for the fault. In Figure 7.7 the cumulative summation is in the order of 800 at 240ms which is of the same order of the measured Arc2 waveform which was 300 at a similar time after fault inception. The 15km line model however exhibits a large cumulative summation in the order of 4000 at the 240ms time mark. This fact is encouraging by virtue of the fact that the system modelled has a lower attenuation.
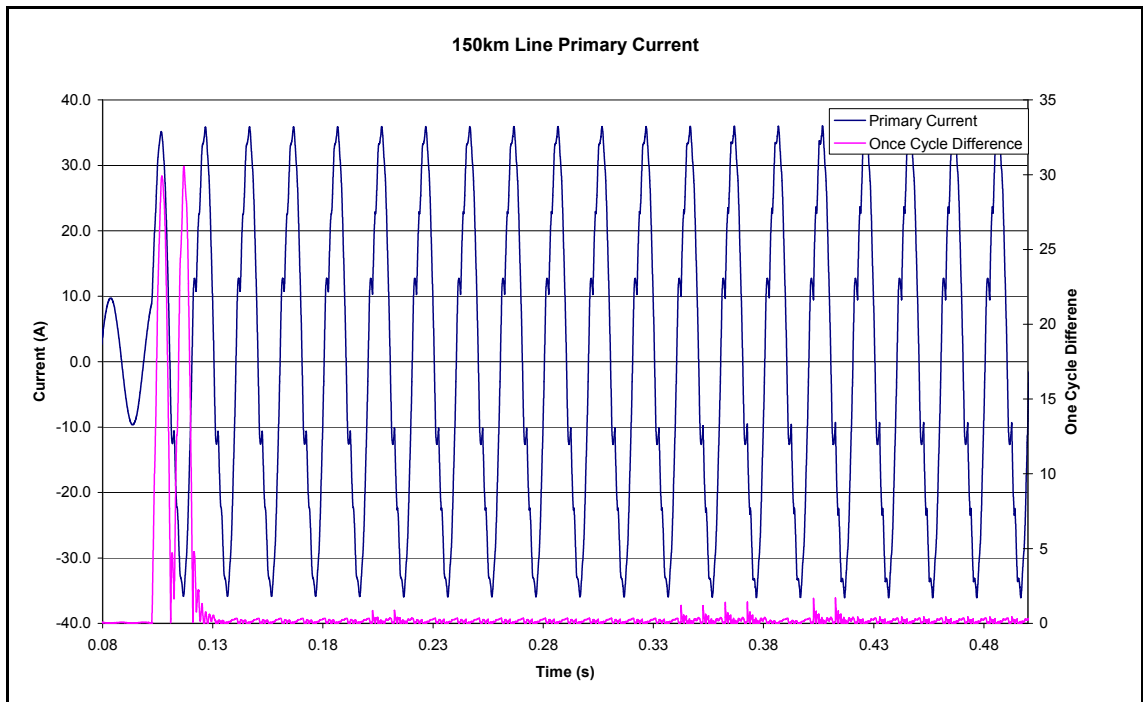
Figure 7.6 - 150km Line Model Primary Current and One Cycle Difference Filter

Figure 7.7 - 150kM Line Model One Cycle Difference Filter and Cumulative Summation

A similar once cycle difference plot and cumulative summation has been calculated on the output of the current transformer, this is shown in Figure 7.8. The current transformer output has been multiplied by the CT ratio (10:1) prior to calculation of the difference and cumulative summation. This has been done to allow direction

comparison between the CT input (Figure 7.7) and output (Figure 7.8). In both cases the cumulative summation finishes at a value between 3000A and 3500A indicating that the CT performance has no significant impact on the measured primary signals.
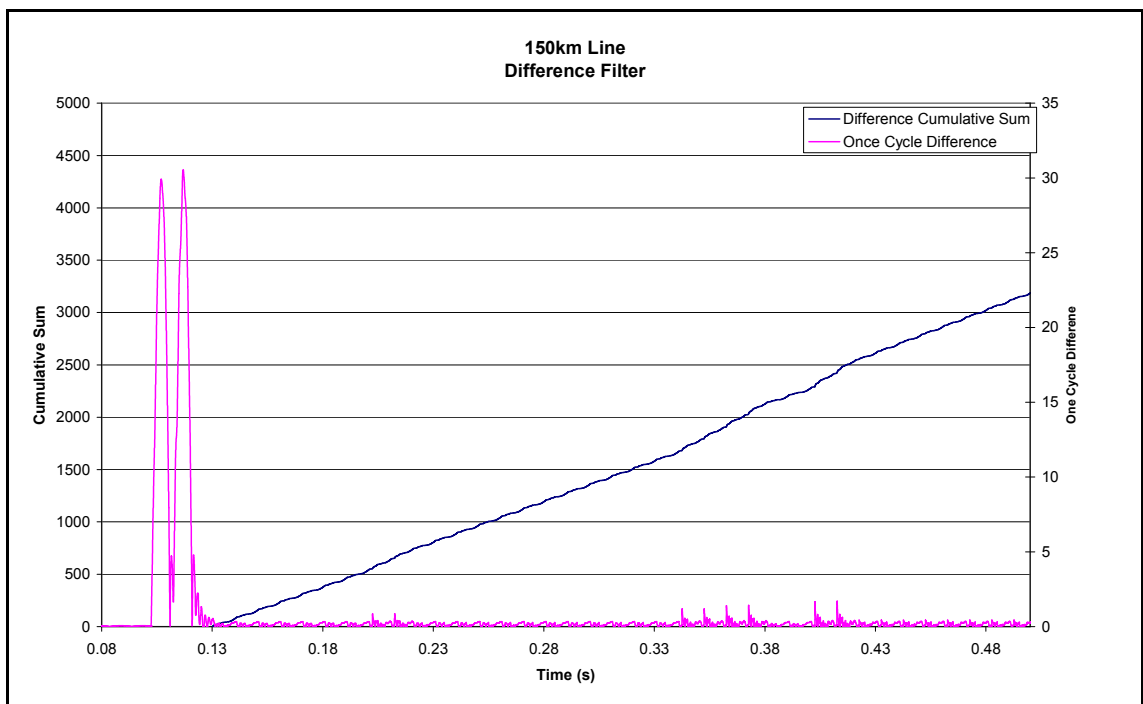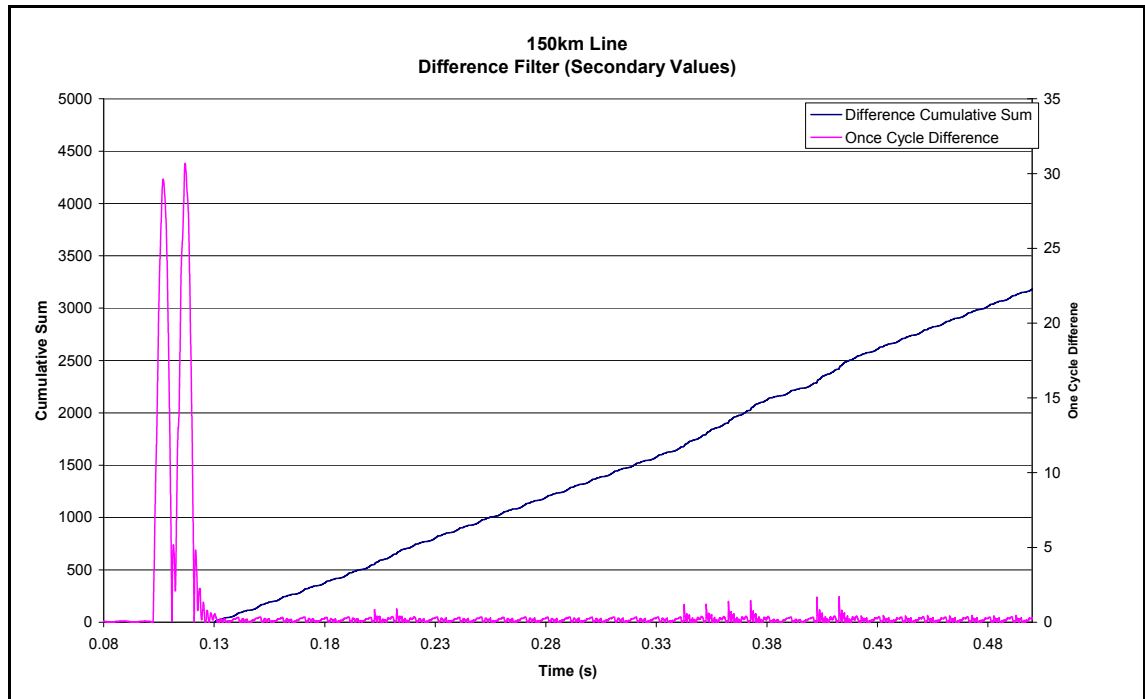

Figure 7.9 - 150km Line Model One Cycle Difference Filter and Cumulative Summation (CT Output)

7.4   Discussion

Testing of the created COMTRADE files with commercially available hardware has been carried out on the GE Multilin F60. The relay did not respond to the waveforms created this is expected to be due to one of three aspects user configurable restraints, algorithm constraints or hardware constraints. The user configurable restraints are those outlined and addressed in 7.2.4, using guidance from the manual these restrains have been addressed and set beyond both those expected in practice and those identified from the model outputs. Algorithm constrains are those implemented by the manufacturer and due to commercial sensitivity are not explained in detail by the manufacturer. In assessing relay operation the algorithm constraints are tested holistically by injecting a test waveform and assessing the relay output. The output of each of the relay elements that are used provide the overall arc and high impedance detection are not available to the user and fault finding or user assessment is not able to be undertaken. Hardware limitations are not always published by the manufacturer, care must be taken to ensure that the resolution of the current transformer inputs is sufficient to ensure that the high

frequency components are measured correctly. 16bit Analogue to Digital (A/D) converters are becoming common and are used in the 300 series SEL relays. Using this as a guide and having an A/D current input limit of 225A secondary (measured from a previous fault) the resolution is calculated by:

$$I_{RES} = \frac{2 \times 225}{2^{16}}$$

$$= 3.433mA$$

The CT inputs have a resolution of 3.433mA on a 5A nominal CT. This resolution equates to 0.069% of nominal. With a 50/5 CT that was evaluated in Chapter 4 we have a primary resolution of 0.0345A. This resolution is higher than that of the 15km line measurements above.

The GE Multilin F60 relay samples the power system at 64 samples per cycle. 64 samples per cycle will allow a sampling of signals up to 1600Hz (allowing no over sampling). The signals that have been created and studied have been up to 1000Hz with magnitudes decreasing as the frequency increases, values at 150Hz have been as high as 2% of the CT ratio reducing to 0.086% at 1000Hz. This inversely proportional characteristic makes the requirements of monitoring the frequency components greater than 1000Hz less critical as the system attenuation has a large effect.

Chapter 8

Conclusion

8.1 Project Summary

The project was aimed at creating waveforms so that testing independent of the relay manufacturer could be undertaken. To this end waveforms have been created that approximate what is expected in practice.

An opportunity was taken to replay the waveforms to a commercially available protection relay, the GE-F60. The waveforms created were not in a form that the GE-F60 protection relay recognised as such the relay did not respond with an arcing alarm.

The theoretical analysis of the SEL451 relay appears to be more in line with the waveforms observed from the simulation. Testing of the SEL relay with the waveforms created will provide a reference to determine if the arc model requires further modification.

Waveforms created for playback to the protection relay were all in a COMTRADE format. The COMTRADE file type was able to be exported from the TOP Plot waveform viewer. The file did not meet the COMTRADE standard directly and using a text editor each file the units were modified in the COMTRADE header file.

8.2 Further Work

Many areas for further work exist in the study of high impedance earth faults. Work in this area is available to equipment manufacturers and end users, with a collaborative approach likely to provide the best outcome. End users require the techniques to be implemented in tested hardware for safe implementation on a power system, while manufactures and researchers require access to system data and events to validate the approaches implemented.

8.2.1 Impact of Arc Medium

This study has been about the detection of arc events. The methodology has relied on the fact that there is a voltage expressed across a quasi insulator and that prior to this insulating medium conducting an elevated voltage has occurred. This voltage for the

most part has been termed breakdown. Whilst testing as part of this work has proven that the breakdown voltage occurs for free air arcs a more comprehensive assessment should be undertaken to identify if this is true of materials that are likely come in contact with the an energised part of the power system.

An approach has been made to the Ergon Energy's high voltage test facility at Banyo to identify if testing of common materials can be undertaken. A meeting with the resource facilitator was carried out in mid October 2010 to determine what resources and expertise are available to provide material analysis. Testing of contact between the power system and granite, loamy (sandy) soils and identified problem materials is expected to be carried out to determine the performance of the relays when subject to a system event involving one. This is expected to be a long term process that will allow a catalogue of items and their electrical performance to be quantified.

8.2.2 SEL451 Investigation

The positive outcome of the Once Cycle Difference Filter calculations in section 7.3.2 warrants further investigation with the Schweitzer Engineering Laboratories SEL-451 relay. The created waveforms indicate that operation should occur with relays employing this algorithm. Investigation of the relay performance on power systems that have non linear loads is required to determine if the relay is sensitive enough to detect arcing fault once the relay increases its thresholds to account for signals present on a typical power system feeder. There appears from the SEL-451 manual to be no method to monitor the actual dynamic threshold that the relay is applying to the difference current filter. This facility would allow the user to understand the potential performance of the SEL relay prior to the inception of a high impedance fault.

8.2.3 Comprehensive Monitoring

Historically protection relays were configured to only detect and act upon fundamental components of a waveform during a power system event. There were some cases as with transformer differential protection which were designed to restrain harmonic components up to the 5th. This allowed for sampling frequencies as low as 500Hz using the Nyquist theorem. In practice this has not been used as the sampling frequency for protection relays.

Protection relay manufacturers have generally provided relay with sampling between 12 and 16 times per power frequency cycle. This sampling frequency allows end users to recreate waveforms with frequencies up to 400Hz on a 50Hz nominal power system.

Some manufacturers, especially those who are offering high impedance algorithms have increased the sampling frequency of the waveform recording facilities to 64 samples per cycle or better. With a finite amount of storage in the protection devices the higher sampling frequency results in waveforms of significantly shorter duration than those sampled at 16 samples per cycle.

This improvement in sampling frequency allows the arc waveform at the time the circuit breaker operates to be analysed in greater depth than could be done in the past. For devices like the GE-F60 and the SEL-451 that adjust detection thresholds of the protection elements based on the history of the power system consideration of extending the length of the recorded waveforms should undertaken. This will allow the user to record the history that the decision was based and allow for better post fault analyses.

In the interim all configurable fault recorders should be set to sampling rates that allow signals of 1000Hz or higher to be analysed.

8.2.4   Cataloguing of System Events

Australian users of relays that have high impedance facilities require co-ordination to enable file sharing post high impedance fault events. Currently known users of this in Australia are awaiting a true high impedance fault with correct detection. The information regarding high impedance faults should be catalogued internally within Ergon, defining the location of the fault, the environmental conditions at the time of the fault and records from relays leading up the fault.

Appendix A – Project Specification

Project Specification

**High Impedance Earth Fault for High Voltage Single Wire Earth Return (SWER)
Distribution Networks**

1. Identify the spectral components that would be generated at the location where a high impedance arcing fault occurs.

2. Identify the response of a SWER system to spectral components generated by an arcing fault.

3. Quantify the frequency response of current transformers typically used for protection.

4. Develop a system model that can be used to investigate arcing faults.

5. Create a test signal / suite of test signals that can be used. The signal is to be compatible with available test sets and will be in Comtrade 1999 or .PL4 format.

Time and Data and Hardware Permitting

1. Where the frequency response of the selected current transformer is not sufficient to pass the required spectral components. Investigate to determine if a filter could be designed to allow the pass band of identified current transformers to be compatible with the desired signal.

2. Where access to identified relay types is available the developed waveforms shall be replayed.

3. Installation of a limited number of protective relays is currently being undertaken on three phase networks in areas that are know to suffer from high impedance faults. Should a fault of this nature occur within the project timeframe use extracted events to determine if model validation can be achieved.

Appendix B- Carson's Correction Factors

Calculation of Carson's Correction Factors for the resistance and inductance of a single wire earth return line.

$\text{ORIGIN} := 1$ $f := 50, 100 .. 1000$ $\rho := 200$ $S := 2 \cdot 12.667$ $\phi := 0$

$i := 1 .. 20$ $bi := 3 .. 20$ $ci := bi$

$\omega(f) := 2\pi \cdot f$

$$a(f) := 4\pi \cdot \sqrt{5} \cdot 10^{-4} \cdot S \cdot \sqrt{\frac{f}{\rho}}$$

$$b_1 := \frac{\sqrt{2}}{6} \qquad b_2 := \frac{1}{16} \qquad b_{bi} := b_{bi-2} \cdot \frac{\text{sign}_{bi}}{bi \cdot (bi + 2)}$$

$$c_2 := 1.3659315 \qquad c_{ci} := c_{ci-2} + \frac{1}{ci} + \frac{1}{ci + 2}$$

$$d := \frac{\pi}{4} \cdot b$$

$$\Delta R(f) := 4\cdot\omega(f)\cdot 10^{-4}\cdot\left[\begin{array}{l}\dfrac{\pi}{8} - b_1\cdot a(f)\cdot\cos(\phi) + b_2\cdot\left[\left(c_2 - \ln(a(f))\right)\cdot a(f)^2\cos(2\cdot\phi) + \phi\cdot a(f)^2\sin(2\phi)\right] + b_3\cdot a(f)^3\cdot\cos(3\cdot\phi) - d_4\cdot a(f)^4\cos(4\cdot\phi)\ ... \\[2mm] + -b_5\cdot a(f)^5\cdot\cos(5\phi) + b_6\cdot\left[\left(c_6 - \ln(a(f))\right)\cdot a(f)^6\cos(6\cdot\phi) + \phi\cdot a(f)^6\sin(6\phi)\right] + b_7\cdot a(f)^7\cdot\cos(7\cdot\phi) - d_8\cdot a(f)^8\cos(8\cdot\phi)\ ... \\[2mm] + -b_9\cdot a(f)^9\cdot\cos(9\phi) + b_{10}\cdot\left[\left(c_{10} - \ln(a(f))\right)\cdot a(f)^{10}\cos(10\cdot\phi) + \phi\cdot a(f)^{10}\sin(10\phi)\right] + b_{11}\cdot a(f)^{11}\cdot\cos(11\cdot\phi) - d_{12}\cdot a(f)^{12}\cos(12\cdot\phi)\ ... \\[2mm] + -b_{13}\cdot a(f)^{13}\cdot\cos(13\phi) + b_{14}\cdot\left[\left(c_{14} - \ln(a(f))\right)\cdot a(f)^{14}\cos(14\cdot\phi) + \phi\cdot a(f)^{14}\sin(14\phi)\right] + b_{15}\cdot a(f)^{15}\cdot\cos(15\cdot\phi) - d_{16}\cdot a(f)^{16}\cos(16\cdot\phi)\ ... \\[2mm] + -b_{17}\cdot a(f)^{17}\cdot\cos(17\phi) + b_{18}\cdot\left[\left(c_{18} - \ln(a(f))\right)\cdot a(f)^{18}\cos(18\cdot\phi) + \phi\cdot a(f)^{18}\sin(18\phi)\right] + b_{19}\cdot a(f)^{19}\cdot\cos(19\cdot\phi) - d_{20}\cdot a(f)^{20}\cos(20\cdot\phi)\end{array}\right]$$

$$\Delta X(f) := 4\cdot\omega(f)\cdot 10^{-4}\cdot\left[\begin{array}{l}\dfrac{1}{2}\cdot(0.6159315 - \ln(a(f))) + b_1\cdot a(f)\cdot\cos(\phi) - d_2\cdot a(f)^2\cdot\cos(2\cdot\phi) + b_3\cdot a(f)^3\cdot\cos(3\cdot\phi) - b_4\cdot\left[\left(c_4 - \ln(a(f))\right)\cdot a(f)^4\cos(4\cdot\phi) + \phi\cdot a(f)^4\sin(4\phi)\right]\ ... \\[2mm] + b_5\cdot a(f)^5\cdot\cos(5\cdot\phi) - d_6\cdot a(f)^6\cdot\cos(6\cdot\phi) + b_7\cdot a(f)^7\cdot\cos(7\cdot\phi) - b_8\cdot\left[\left(c_8 - \ln(a(f))\right)\cdot a(f)^8\cos(8\cdot\phi) + \phi\cdot a(f)^8\sin(8\phi)\right]\ ... \\[2mm] + b_9\cdot a(f)^9\cdot\cos(9\phi) - d_{10}\cdot a(f)^{10}\cdot\cos(10\cdot\phi) + b_{11}\cdot a(f)^{11}\cdot\cos(11\cdot\phi) - b_{12}\left[\left(c_{12} - \ln(a(f))\right)\cdot a(f)^{12}\cos(12\cdot\phi) + \phi\cdot a(f)^{12}\sin(12\phi)\right]\ ... \\[2mm] + b_{13}\cdot a(f)^{13}\cdot\cos(13\phi) - d_{14}\cdot a(f)^{14}\cdot\cos(14\cdot\phi) + b_{15}\cdot a(f)^{15}\cdot\cos(15\cdot\phi) - b_{16}\left[\left(c_{16} - \ln(a(f))\right)\cdot a(f)^{16}\cos(16\cdot\phi) + \phi\cdot a(f)^{16}\sin(16\phi)\right]\ ... \\[2mm] + b_{17}\cdot a(f)^{17}\cdot\cos(17\phi) - d_{18}\cdot a(f)^{18}\cdot\cos(18\cdot\phi) + b_{19}\cdot a(f)^{19}\cdot\cos(19\cdot\phi) - b_{20}\left[\left(c_{20} - \ln(a(f))\right)\cdot a(f)^{20}\cos(20\cdot\phi) + \phi\cdot a(f)^{20}\sin(20\phi)\right]\end{array}\right]$$

Appendix C – ATP SATURA Input Data

```
BEGIN NEW DATA CASE
$OPEN, UNIT=3 FILE=C:\ATP\10P35.PCH
C
C ******************************************************************************
C
C     ATP DATA FILE - C:\ATP\UNI\CTMAG1.DAT
C    CT MAG CURVE 10P35F20 on 100/5 Mag Curve on 50/5
C
C ******************************************************************************
C
C     MAGNETIC-SATURATION ROUTINE                          (P 101)
C
SATURATION
C
C     MISCELLANEOUS DATA                                   (P 102)
C
C  FREQ.  VBASE.  PBASE. IPUNCH. KTHIRD.
    50.0  0.0175 8.75E-5       1       1
C
C    (I , V)  POINTS                                       (P 102)
C
C     I_RMS(PU).       V_RMS(PU).
         0.02559          0.115
         0.04449          0.241
         0.05649          0.338
         0.06806          0.441
         0.08315          0.577
         0.09561          0.684
         0.10567          0.757
         0.11980          0.826
         0.12220          0.857
         0.13644          0.921
         0.15467          0.977
         0.18213          1.022
         0.41957          1.093
         1.04798          1.139
          9999
BLANK CARD TERMINATING ALL SATURATION CASES
C
$CLOSE, UNIT=3 STATUS=KEEP
BEGIN NEW DATA CASE
BLANK TERMINATION-OF-RUN CARD
```

References

Tending, J et al. 1996, 'PSRC Working Group D15 1996, High Impedance Fault Detection Technology', viewed 7 June 2010 <http://grouper.ieee.org/groups/td/dist/documents/highz.pdf>

Daqing, H 2007, 'Detection of high-impedance faults in power distribution systems' Power Systems Conference: Advanced Metering, Protection, Control, Communication, and Distributed Resources, 2007. PSC 2007 pp85-95

Samesima, M.I. 1991 'Frequency Response Analysis and Modelling of Measuring Current Transformers under distorted current and voltage supply', IEEE Transactions on Power Delivery, pp1762-1768.

Cataliotti, A. et al 'Frequency response of Measurement Current Transformers', Instrumentation and Measurement Technology Conference Proceedings, pp1254-1258

Ojanguren, I n.p., 'Working Group B5.94, High Impedance Faults' < http://www.e-cigre.org/Search/download.asp?ID=402.pdf>

M. Kezunovic, et al. 1994 'Experimental Evaluation of EMTP-Based current transformer models for protective relay studies', IEEE Transactions on Power Delivery, pp405-413.

Folkers, R 1999, 'Determine Current Transformer Suitability using EMTP Models', viewed 15 May 2010, <https://www.selinc.com/search/SearchPage.aspx?searchtext=Determine%20Current%20Transformer%20Suitability%20using%20EMTP%20Models>

Taylor, J.R. 1987 'Mistake Creek North S.W.E.R. Scheme December 1987 Tests, and Initial Protection Overview', Capricornia Electricity Board Report

GE Industrial Systems 2008, 'F60 Feeder Protection – UR Series Instruction Manual F60 Revision:5.6'

Goldberg, S et al. 1989 'A computer Model of the Secondary Arc in Single Phase Operation of Transmission Lines' IEEE Transactions of Power Delivery, Vol 4, No. 1, January 1989

Ergon Energy Risk Management Guideline, P89T01R01, viewed 16 May 2010 < http://intranet/Docs/P89ManageFinancialResources/P89TPublished/P89T01R01.doc>

Adimaik, M 2010, 'High Impedance Fault Detection on Rural Electric Distribution Systems', 2010 IEEE Rural Electric Power Conference pp B3 – B3-8

Rogers, W n.d. 'Modelling of Free-Air Arcs' viewed 10 May 2010, < http://www.eeug.org/files/secret/Publications/arc_rogers.pdf>

'Alternative Transient Program Rule Book' viewed 5 May 2010 < http://www.eeug.org/files/secret/ATP_RuleBook/>

Hasman, T. 1997 'Reflection and Transmission of Travelling Waves on Power Transformers', IEEE Transactions on Power Delivery Issue 4 Volume 12, pp 1684 - 1689

Marti, J.R, et al. 1993 'Transmission Line Models for Steady-State and Transient Analysis' IEEE Transactions on Power Delivery Issue 4 Volume 15, pp1318-1319

Standards Australia, 'Instrument Transformers Part 1: Current transformers (IEC 60044-1 Ed1.2 (2003) MOD) AS60044.1-2007' viewed 14 June 2010 < http://www.saiglobal.com/online/autologin.asp>

Standards Australia, 'AS1675 – 1986 : Current transformers – Measurement and protection' viewed 14 June 2010

< http://www.saiglobal.com/online/autologin.asp>

Standards Australia, 'AS3607 – Conductors- Bare overhead, aluminium and aluminium alloy- Steel reinforced', viewed 12 August 2010

< http://www.saiglobal.com/online/autologin.asp>

Schweitzer Engineering Laboratories, 2010, 'SEL-451-5 Protection, Automation, and Control System Instruction Manual' version 20102026

ANSI/IEEE, 'IEEE Standard Requirements for Instrument Transformers," IEEE Std C57.13-2008 (Revision of IEEE Std C57.13-1993) viewed 7 July 2010

<
http://ieeexplore.ieee.org.ezproxy.usq.edu.au/stamp/stamp.jsp?tp=&arnumber=45816 34>